UNITED STATES DEPARTMENT OF THE INTERIOR

GEOLOGICAL SURVEY

PRELIMINARY REPORT ON AFTERSHOCK SEQUENCE FOR EARTHQUAKE OF JANUARY 31, 1986 NEAR PAINESVILLE, OHIO

(TIME PERIOD: 2/1/86–2/10/86)

edited by

R. D. Borcherdt
U.S. Geological Survey

sponsored by

Electric Power Research Institute
U.S. Geological Survey

OPEN-FILE REPORT 86–181

CONTENTS

ABSTRACT

A ten-station array of broad-band digital instrumentation (GEOS) was deployed to record the aftershock sequence of the moderate ($m_b \sim 4.9$) earthquake that occurred on January 31, 1986 (16:46:43 UT) near Painesville, Ohio. The occurrence of the event has raised questions concerning possible contributory factors to the occurrence of the event and questions concerning the character of earthquake-induced high-frequency ground motions in the area. To aid in the timely resolution of the implications of some of these questions, this preliminary report provides copies of the ground motion time-histories and corresponding spectra for the six aftershocks and two events, thought to be quarry blasts, recorded as of February 10, 1986. Recording station locations and epicenter locations based on two preliminary estimates of local seismic velocity structure are provided.

INTRODUCTION

The moderate earthquake ($m_b \sim 4.9$) that occurred near Painesville, Ohio (41.650°N, 81.162°W; J. Dewey, pers. comm., 1986) on January 31, 1986 (16:46:43 GMT) was felt over a broad region including eleven states, the District of Columbia, and parts of Ontario, Canada. Isoseismals for the event as inferred by field investigation (M. Hooper, pers. comm., 1986) were centered in the general area of the small communities of Chardon, Mentor, and Hambden, Ohio. The largest observed intensities were in the VI-VII range with only minor building damage (M. Hooper, pers. comm., 1986). Fifteen people were reported to have experienced minor injuries.

Considerable scientific and engineering interest in the event resulted in a team of five seismologists being dispatched from Menlo Park, California on the evening of January 31 to install ten digital event recorders (GEOS) in the epicentral area (USGS: R.D. Borcherdt, C. Dietel, J. Gibbs, G. Sembera; EPRI: J. King). Seven of these stations were installed subsequent to arrival on February 1 (6:00 a.m.; −8°C) and the remaining three stations were installed on February 2, 1986. This preliminary report provides the data recorded as of February 10, 1986 for six aftershocks and two events thought to be quarry blasts. Station locations, time histories, Fourier amplitude spectra, and epicentral locations of the aftershocks based on two different preliminary velocity models are provided.

On February 10, 1986 the number of stations deployed in the area was reduced to five. As of this writing, these stations are planned for removal during the week of March 23, 1986. Any data recorded at these stations subsequent to February 10, 1986 will be reported in subsequent, more thorough reports.

INSTRUMENTATION

Data presented in this report were recorded, using General Earthquake Observation Systems (GEOS). A detailed description of the systems is provided by Borcherdt *et al.*, 1985. A brief summary is provided of general recording and playback system characteristics of interest for this report. Recording system parameters chosen for this experiment are provided.

Recording System

The GEOS recording system, deployed to record the aftershock sequence, was developed by the U.S. Geological Survey for use in a wide variety of active and passive seismic experiments. The digital data acquisition system operates under control of a central microcomputer which permits simple adaptation of the system in the field to a variety of experiments including near-source high-frequency studies of strong motion aftershock sequences, crustal structure, teleseismic earth structure, earth tidal strains, and free oscillations. Versatility in system application is achieved by isolation of the appropriate data acquisition functions on hardware modules controlled with a single microprocessor via a general computer bus. CMOS hardware components are utilized to reduce quiescent power consumption to less than two watts for use of the system as either a portable recorder in remote locations or in an observatory setting with inexpensive backup power sources. The GEOS together with two sets of three-component sensors (force-balance accelerometer, velocity transducer) and ferrite WWVB antenna as often used for aftershock studies is shown in Figure 1 (see Borcherdt *et al.*, 1985 for hardware modules comprising the system).

The signal conditioning module for the GEOS is configured with six input channels, selectable under software control, to permit acquisition of seismic signals ranging in amplitude from a few nanometers of seismic background noise to 2 g in acceleration for

ground motions near large events. The analog-to-digital conversion module is equipped with a 16-bit CMOS analog-to-digital converter which affords 96 dB of linear dynamic range or signal resolution; this, together with two sets of sensors, implies an effective system dynamic range of about 180 dB. A data buffer with direct memory access capabilities allows for maximum throughput rates of 1200 sps. With sampling rates selectable under software control as any integral quotient of 1200, broad and variable system bandwidth ranging from ($10^{-5} - 6 \times 10^{2}$ Hz) is achieved for use of recorders with a wide variety of sensor types.

Modern high-density (1600–6400 bpi) compact tape cartridges offer large data storage capacities (1.25–33 Mbyte) in ANSI standard format to facilitate data accessibility via minicomputer systems. Read capabilities of cartridge tape recorders is utilized to allow recording parameters and system operational software to be changed automatically. Read capability also allows systems equipped with modems to transmit data via telecommunications to a central data processing laboratory.

Microprocessor control of time-standard provides capability to synchronize internal clock via internal receivers (such as WWVB and satellite), external master clock, or conventional digital clocks. Microprocessor control of internal receivers permits systems on command to determine time corrections with respect to external standard. This capability permits especially accurate correction for conventional drift of internal clocks.

Convenient system set-up and flexibility to modify the system in the field for a wide variety of applications is achieved using a 32-character alphanumeric display under control of the microcomputer. English-language messages to the operator executed in an interactive mode, reduce operator field set-up errors. A complete record of recording system parameters is recorded on each tape together with calibration signals for both the sensor and the recorders. These records assure rapid and accurate interpretation via computer of signals, both in the field and in the laboratory.

Flexibility to modify the system to incorporate future improvements in technology is achieved using a structured software architecture and modular hardware components. Incorporation of new hardware modules is accomplished in a straightforward manner by replacing appropriate module and corresponding segments of controlling software.

The system response designed for strong-motion and aftershock applications of the GEOS was intended to allow large-amplitude near-source signals of 1–10 Hz as detected by a force-balance accelerometer (FBA) to be recorded on scale, while at the same time permitting much smaller-amplitude high-frequency signals (50–100 Hz) as might be detected on FBA's or velocity transducers to be recorded with high signal resolution. The amplitude response of the recording system, together with that for two types of sensors frequently used for aftershock studies in the near-source region of large earthquakes, is shown in Figure 2.

Data Playback System

The read and write capabilities of the mass-storage module, together with the D/A conversion module, permits the GEOS to be used as an analog as well as digital (via RS–232) playback system in the field. Visual inspection of digitally recorded data is useful for determining instrument performance, evaluation of recording parameters, evaluation of environmental factors (*e.g.*, local noise sources, etc.). RS–232 capabilities of data playback unit and ANSI-standard tape cartridges permit playback of digital time series on minicomputer systems in the field or laboratory. Digital playback of data is generally performed using an ANSI-standard serpentine tape reader as a peripheral to minicomputer systems in the laboratory. Deployment of minicomputer digital playback systems in the field is generally most feasible for large-scale high-data volume experiments.

For these experiments only analog playback capability was utilized in the field. Analog playbacks on light-sensitive paper were utilized in the field to identify seismic events, trigger parameters, and evaluate instrument performance. Digital playback of the data was conducted with a Tanberg serpentine tape drive attached to the PDP 11/70 at the National Strong Motion Data Center in Menlo Park, using a variety of software packages, developed in large part by G. Maxwell, E. Cranswick, and C. Mueller.

SITE SELECTION AND INSTRUMENT CONFIGURATIONS

Locations for the stations deployed in the 10-station array are shown in Figure 3 together with the location of the main shock. Objectives in choice of the locations included event location, source parameter determination, attenuation of high-frequency ground

motion along a linear north-south array, and effects of local site conditions at stations 001 and 002.

Due to the suspected low seismicity and expected small magnitudes for aftershocks, attempts were made to locate the stations at sites with anticipated low seismic background noise levels in areas (with the exception of station 001) where the effects of local soil conditions were expected to be minimized. To reduce the effect of the adverse environmental conditions ($-15°$C; snow and ice) on the recording equipment, each unit was located in an unheated shelter (small tool sheds or abandoned animal shelters some distance from local sources of cultural noise were chosen).

Stations 001, 002, 003, 004, 005, 006, and 007 were installed in the time period 1400–1800 hours EST on February 1, 1986. Stations 008, 009, and 011 were installed on February 2, 1986. Station 005 was moved to location 055 on February 4, 1986 at 1800 hours EST.

In anticipation of recording only small events, some of which had signal levels just above seismic background noise levels, the GEOS recorders with the exception of station 005 and 055 were operated as high-gain, three-channel recorders, using only L-22 (2 Hz) three-component velocity transducers. Station 005 (055) in the expected epicentral region was operated as a six-channel recorder with both three-component force-balance accelerometers (FBA-13; USGS case) and similar three-component velocity transducers to permit on-scale recordings of any larger events. The channels used to record the output of the L–22 seismometers were operated at relatively high gain of 48 and 54 dB initially and later reduced to 42 and 48 dB gain. The output of the FBA channels were recorded at 12 dB gain. Sampling rates for the three-component stations with velocity transducers were chosen at 400 sps/channel with a resultant Nyquist frequency of 200 Hz. No anti-aliasing filters were utilized for these stations because of the anticipated low background noise level near the Nyquist. Sampling rates of 200 sps/channel and anti-aliasing filters of 50 and 100 Hz were utilized for the stations recording six-component data.

Timing at each of the stations was obtained using the automatic capability of the recorders to synchronize to WWVB. Timing corrections at 12-hour intervals with an accuracy of generally less than 5 ms are automatically recorded and used to correct the internal clock for each recorder, which has a temperature stability specification of

$\pm 1 \times 10^{-6}$ – 20°C to +70°C.

The recorders were operated in trigger mode with activation to record sensor outputs on digital cartridge tape for the various seismic events being determined from a variety of various trigger parameters programmed into the systems, depending on characteristics of local background noise at the sites. In general, the trigger parameters were set to ensure that essentially all seismic events with peak amplitudes more than a factor of five above background noise would be recorded. Subsequent comparison of recorded events with those apparent on visible recorders (C. Langer, pers. comm., 1986, and H. Seeber, pers. comm., 1986) confirms that all events identified on visible recorders were detected and recorded on at least the three stations closest to the epicenters.

Surprisingly few instrument malfunctions, considering the cold environmental conditions, have been encountered to date. Station 004 experienced a varmit with active molars resulting in a semi-severed seismometer cable on February 3, 1986. Intermittent behavior of station 005 from February 1 through February 4 was attributed to a poor shelter with a leaky roof and no endwall. System performance stabilized upon moving this system to location 055 within a new barn (unheated). Two short interruptions in station operation at stations 006 and 007 were corrected on February 3 and 4 with replacement of defective automobile batteries. Some difficulties in reading two of the tapes from station 004 have been encountered in Menlo Park, even though no difficulties were encountered in reading the same tapes in the field. At this point, it appears the difficulty is attributable to deterioration of magnetic flux on the affected tapes due either to shipping environment or playback procedures.

AFTERSHOCK TIME HISTORIES AND SPECTRA

Time histories recorded at each of the stations for the six aftershocks and two suspected quarry blasts detected in the time period February 1 through February 10, 1986 are presented as Figures A–1 to A–37 (Appendix A). The three-component time histories are identified by universal time and station number. Six seconds of time history in units of ground velocity (cm/s) are plotted for each station with additional six-second intervals plotted for the more distant stations. The time scale for each event expressed in universal

time permits accurate absolute timing of various phases from the figures presented. The time scale is the same for each figure, permitting straightforward comparisons of frequency content. (The time histories are plotted using a basic software package developed by C. Mueller, with modifications for format implemented by G. Glassmoyer.)

The amplitude scale presented for each time history was determined using the gain factors and sensor coil constants recorded automatically by GEOS near the time of event detection. With the instrument response taken into account the time histories as presented can be interpreted in terms of ground velocity. Exceptions are the peak amplitudes on trace H=0 (Fig. A–8), three traces (Fig. A–18), and traces H=0, H=90 (Fig. A–19) for which the peak signal amplitudes for the S waves and one P wave exceeded full-scale resolution level at the gain level of 54 dB used to record these traces. It should be noted that the high sampling rates of 400 sps used to record the velocity time histories (200 sps for stations 005 and 055), resulted in accurate resolution of the peak amplitudes, many of which occur at relatively high frequencies. Lower sampling rates (*e.g.*, 100 sps) with anti-aliasing filters set near 30 Hz would be expected to yield time histories for the nearest stations having smaller peak amplitudes.

To summarize the relative frequency content of the recorded signals, Fourier amplitude spectra were computed for 10.24 seconds of each of the time histories. The resulting amplitude spectra, shown in Figures B–1 to B–37 (Appendix B) were computed using a software package developed by C. Mueller for a time interval, commencing approximately 2 seconds prior to onset of the P wave, with a 10 percent cosine taper applied to correct for leakage. The amplitude spectra were smoothed with a 0.25 Hz Hanning window and plotted for the interval 0.5 Hz to 200 Hz (Nyquist). The spectra for several of the stations closer to the epicenter (*e.g.*, 003, 055, 006, and 002) show that the recorded time histories are relatively rich in frequency content in the high-frequency interval (30–70 Hz). Interpretation of the spectra in terms of source parameters, attenuation, and local site conditions is planned for subsequent reports.

PRELIMINARY VELOCITY MODELS AND AFTERSHOCK LOCATIONS

This summary covers aftershocks recorded between 1 February 19:45 GMT (1

February 14:45 EST) and 10 February 20:07 GMT (12 February 15:07 EST). During this period, six aftershocks occurred that were detected by three or more GEOS stations. Visual examination of time histories for all triggers that occurred within 20 seconds of each other at two stations only did not reveal any seismic events other than those that were recorded at three or more stations. The occurrence times of the six aftershocks and the number of stations detecting each one are listed in Table 1a. Table 1a also lists coda duration magnitudes determined from smoked-paper records obtained by Lamont–Doherty Geological Observatory (J. Armbruster and L. Seeber, pers. comm., 1986).

In addition to the aftershocks, two events believed to be quarry blasts were recorded at three stations (Table 1b). These events occurred on a weekday during working hours. Preliminary locations for the events near a sand and gravel pit about 5.5 km north-northeast of station 006, and the substantially different nature of the time histories (see Figs. A32–37) suggest that the events are quarry blasts. Additional confirmation with quarry owners is being pursued.

Station locations, determined from 7.5–minute series topographic maps, were independently checked by a second interpreter and are believed to be accurate to within 60 meters. Station locations are listed in Table 2 and plotted together with the location of the main shock in Figure 3. Expansion of the digital traces on a graphics terminal permitted picking of P and S arrival times to within 0.02 seconds by two independent observers. The automatic clock corrections provided every 12 hours and recorded on the GEOS tapes indicate the clock errors for the GEOS recordings are within ± 5 ms.

Two preliminary velocity models were used to locate the events using the computer program HYPOINVERSE (Table 3). The first model is essentially a half-space with a P wave velocity of 5.5 km/s and and S wave velocity of 3.27 km/s. The second model contains five sedimentary layers overlying Precambrian basement at a depth of 2.1 km. The interfaces included in the flat layered model are based on a compilation of information from wells drilled as far as the top of the Precambrian basement (Cleveland Electric Illuminating Company, 1982). An average of down-hole and cross-hole velocity logs was used to determine the P velocity in the upper 0.5 km. The P velocity in the Precambrian basement is based on regional earthquake travel-time studies (Nuttli *et al.*, 1969). Average

P and S velocities for the other sedimentary layers were estimated from a geologic cross section using a handbook of physical constants. The boundary between the Precambrian basement and the lower crust was chosen arbitrarily at 20 km depth and has no influence on the derived locations. The two velocity models should be considered as preliminary. With the exception of the near-surface P velocities, they are not based on *in-situ* measurements in the area, and they do not take into account dip of the Precambrian interface from about 6000 feet at the shore of Lake Erie to about 7000 feet in the epicentral region.

In addition to the GEOS recording locations shown in Figure 3, C. Langer (pers. comm., 1986) provided preliminary recording locations for 10 smoked-paper recorders deployed in the area on February 2, 1986. He also provided preliminary P and S times for the five aftershocks recorded at these stations as of February 10, 1986. The station locations provided by C. Langer are referred to subsequently using a three-letter code to distinguish them from the GEOS locations identified by a three-digit code.

Locations for the six aftershocks and two quarry blasts are summarized on Figure 4. The aftershock locations also are shown at an expanded scale in Figure 5. The event locations shown in Figures 4 and 5 have been derived using the layered velocity model summarized in Table 1a. Within the accuracy of the location for the main shock ($\pm$ 4 km; 90% confidence interval, J. Dewey, pers. comm., 1986) the aftershock locations are in the epicentral region of the main shock. Procedures utilized to locate the events based on the preliminary velocity models are discussed subsequently.

Four of the aftershocks (2 February 03:22, 3 February 19:47, 5 February 06:34, and 6 February 18:36) triggered four or more GEOS recorders with an appropriate station distribution to permit location of the events based only on P arrival times. For each of these events, the two velocity models yield epicenter locations that differ by at most 0.2km. Compared to the uniform crust, the layered crust gives depths as much as 0.85 km shallower and with somewhat smaller estimated errors. The maximum value of ERZ for the layered model was 2.65 km. The epicenters for these four events, located with the layered crustal model (Table 1b) and P arrival times only, are within 0.44 km of 41°38.85′N and 81°9.51′W, and at depths between 4.0 km to 6.5 km.

The preferred locations (Figure 5) for these four events were derived using the layered

model (Table 1b) and both P and S arrival times as determined from the GEOS recordings of the events. Output of HYPOINVERSE for this set of locations is presented in Appendix C. The epicenters based on both the P and S arrival times are displaced at most 80 meters from those determined on the basis of P information alone. Incorporation of S arrivals changed the depths by a maximum of 80 meters, with two depths becoming shallower and two becoming deeper.

For the last two events (7 February 15:20 and 10 February 20:06), the distribution of the digital stations for which digital tapes were available as of this writing was not considered adequate for determining locations, as illustrated by large uncertainties in preliminary locations based only on these data. The uncertainties were reduced significantly (as measured by ERZ, GAP) upon incorporation of the P arrival data provided by C. Langer. Although the uncertainties in the epicentral locations (ERH) are comparable to those for the other four events, the uncertainty in depth (ERZ) is large for the two events (5.21 and 6.33 km, respectively), suggesting that these events are not as well located as the four other events (see Appendix C). The epicenters for these two events are within 0.42 km of the average location for the epicenters of the four better-located events. Locations for these events are also summarized in Table 4.

Approximate locations for the two events throught to be quarry blasts (Table 1b) as determined from two sets of P and S times and one S time are shown on Figure 4 and tabulated in Appendix C.

In summary, the epicenters of the six aftershocks are reasonably tightly constrained, with the depths for the four better-located events ranging between 4.0 and 6.2 km. The locations of the epicenters are not particularly sensitive to the velocity model, but further work to improve the velocity model would better constrain inferred depths.

ACKNOWLEDGMENTS

The data set reported in this investigation represents the combined efforts of several individuals, as indicated in part by the distributed authorship of the various sections. The rapid release of this data set was facilitated by efficient processing and analysis software, major portions of which were developed by G. Maxwell, E. Cranswick, and C. Mueller. The

determination of preliminary event locations was facilitated with software and hardware implemented with contributions from J. Fletcher, H. Bundock, L. Baker, F. Klein, and L. Haar. C. Stepp (Electric Power Research Institute) and J. Filson (U.S. Geological Survey) expertly initiated and coordinated the investigation in its early stages. C. Langer (USGS, Golden, CO) provided preliminary event locations in the field and made his initial travel time and event locations available for location of some of the smaller events. J. Armbruster and L. Seeber (Columbia Univ., NY) kindly provided preliminary estimates of coda magnitude.

REFERENCES

Borcherdt, R. D., Fletcher, J. B., Jensen, E. G., Maxwell, G. L., VanSchaack, J. R., Warrick, R. E., Cranswick, E., Johnston, M. J. S., and McClearn, R., 1985, A General Earthquake Observation System (GEOS): *Seismological Society of America Bulletin*, v. 75, p. 1783–1823.

Cleveland Electric Illuminating Company, 1982, The Perry Nuclear Power Plant Units I and II: *Final Safety Analysis Report*, Cleveland, Ohio.

Nuttli, O. W., Stauter, W., and Kisslinger, C., 1969, Travel time tables for earthquakes in the central United States: *Earthquake Notes*, v. 40, p. 19-28.

Table 1a. Occurrence time and magnitude
for aftershocks recorded 2/2–10/86

Date 1986	Time (UT)	Hours after Main Shock	Number of Stations	Magnitude (coda)*
2 Feb.	32:03:22	34.6	5	0.5
3 Feb.	34:19:47	75.0	8	2.1
5 Feb.	36:06:34	109.8	4	−0.5
6 Feb.	37:18:36	145.8	8	2.5
7 Feb.	38:15:20	166.6	4	1.0
10 Feb.	41:20:06	243.3	3	0.7

*Coda magnitude determined by J. Armbruster from visual records (smoked paper).

Table 1b. Occurrence times for apparent quarry blasts.

Date 1986	Time (UT)	Time (EST)	Day of Week	Stations Recording Event
5 Feb.	15:39	10:39	Wednesday	003, 055, 006
5 Feb.	17:57	12:39	Wednesday	003, 055, 006

TABLE 2 - RECORDING STATION LOCATIONS

DIGITAL (GEOS) STATION LOCATIONS

NAME	---LAT----	----LON----
001	41. 48.27N	81. 8.52W
002	41. 43.75N	81. 9.47W
003	41. 39.45N	81. 10.07W
004	41. 36.85N	81. 17.55W
005	41. 35.64N	81. 8.19W
055	41. 37.10N	81. 7.18W
006	41. 37.75N	81. 3.77W
007	41. 32.40N	81. 4.26W
008	41. 32.38N	81. 12.93W
009	41. 24.81N	81. 11.91W
011	41. 9.20N	81. 4.42W

VISIBLE (SMOKED PAPER) RECORDER LOCATIONS *

NAME	---LAT----	----LON----
HAR	41. 36.67N	80. 59.62W
FOT	41. 38.90N	80. 59.69W
MON	41. 35.52N	81. 2.39W
COT	41. 34.73N	81. 5.93W
WSH	41. 37.61N	81. 13.30W
LOX	41. 44.58N	81. 2.60W
BUR	41. 39.24N	81. 4.94W
CAL	41. 41.21N	81. 8.89W
HAM	41. 36.18N	81. 8.48W
CUY	41. 33.56N	81. 10.15W
ERJ	41. 39.44N	81. 5.00W

* Courtesy C. Langer (pers. commun., 1986)

Table 3. Preliminary models used to locate events listed in Tables 1a and 1b.

Depth (km)	Thickness (km)	P Velocity (km/s)	S Velocity (km/s)	Vp/Vs
A. Uniform Crust				
0.0	40.0	5.50	3.27	1.68
40.0	99.0	8.10	4.55	1.78

Depth (km)	Thickness (km)	P Velocity (km/s)	S Velocity (km/s)	Vp/Vs	Description*
B. Layered Crust					
0.0	0.05	1.80	0.60	3.00	Glacial till
0.05	0.45	3.00	1.60	1.88	Devonian shale
0.50	0.50	4.20	2.36	1.78	Silurian dolomite
1.00	0.75	4.50	2.53	1.78	Ordovician limestone and dolomite
1.75	0.35	4.75	2.67	1.78	Cambrian sandstone and dolomite
2.10	17.90	6.15	3.68	1.67	Precambrian granite
20.00	25.00	6.70	3.87	1.73	Lower crust
40.00	99.00	8.15	4.65	1.75	Mantle

*Cleveland Electric Illuminating Co. (1982)

TABLE 4 -- Origin time and locations for seismic events near Painesville, Ohio for time period 2/1/86 through 2/10/86

Aftershocks:

YR	MO	DA	ORIGIN	LAT N	LON W	DEPTH	RMS	ERH	ERZ	GAP
86-	2-	2	322 48.57	41 38.76	81 9.50	5.12	0.01	1.16	0.78	150
86-	2-	3	1947 19.65	41 38.92	81 9.43	5.81	0.03	0.88	0.76	116
86-	2-	5	634 2.40	41 38.96	81 9.68	4.05	0.02	0.88	1.31	134
86-	2-	6	1836 22.26	41 38.68	81 9.33	6.06	0.03	0.82	0.80	121
86-	2-	7	1520 20.19	41 38.97	81 9.42	4.66	0.03	0.92	5.21	115
86-	2-10	20	6 13.59	41 39.07	81 9.31	3.38	0.04	0.81	6.31	115

Quarry blasts:

YR	MO	DA	ORIGIN	LAT N	LON W	DEPTH	RMS	ERH	ERZ	GAP
86-	2-	5	1539 6.22	41 40.57	81 0.66	2.16	0.21	5.13	0.00	319
86-	2-	5	1757 3.39	41 39.92	80 59.65	2.71	0.03	4.89	27.56	329

Figure 1. Side and front panel view of the General Earthquake Observation System (GEOS) together with a WWVB antenna and two sets of three-component sensors commonly used to provide more than 180 dB of linear, dynamic range. System operation for routine applications requires only initiation of power. Full capability to reconfigure system in the field is facilitated by simple operator response to english language prompts via keyboard.

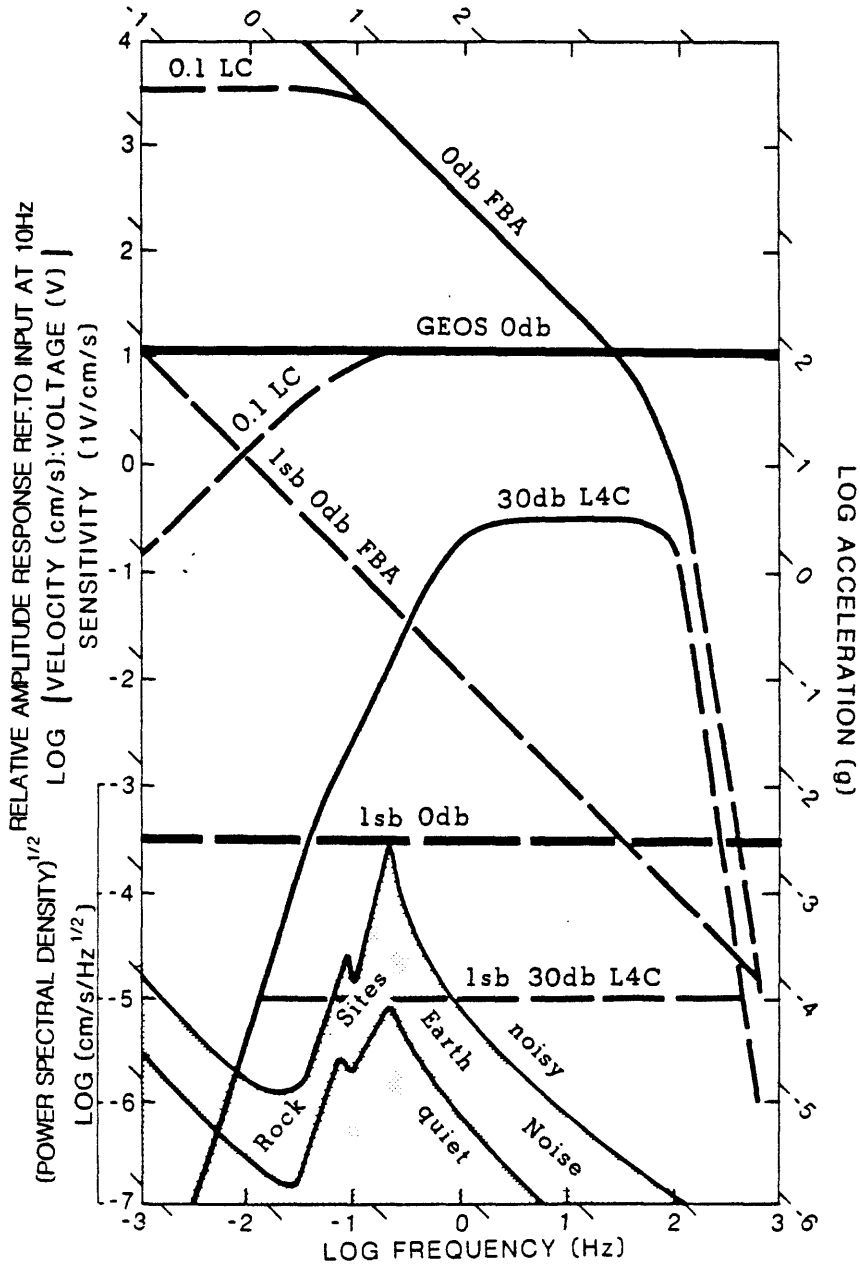

Figure 2. The unit-impulse response designed for the GEOS recorder, spectra for Earth noise (Aki and Richards, 1980), and complete system response with two types of sensors (force-balance accelerometer at 0 dB gain and L4–C velocity transducer at 30 dB gain). Two sets of sensors and linear dynamic range of 96 dB (16-bit) offers the capability to record without gain change 10 Hz signals on scale with amplitudes ranging from 20 angstroms in displacements to 2 g in acceleration.

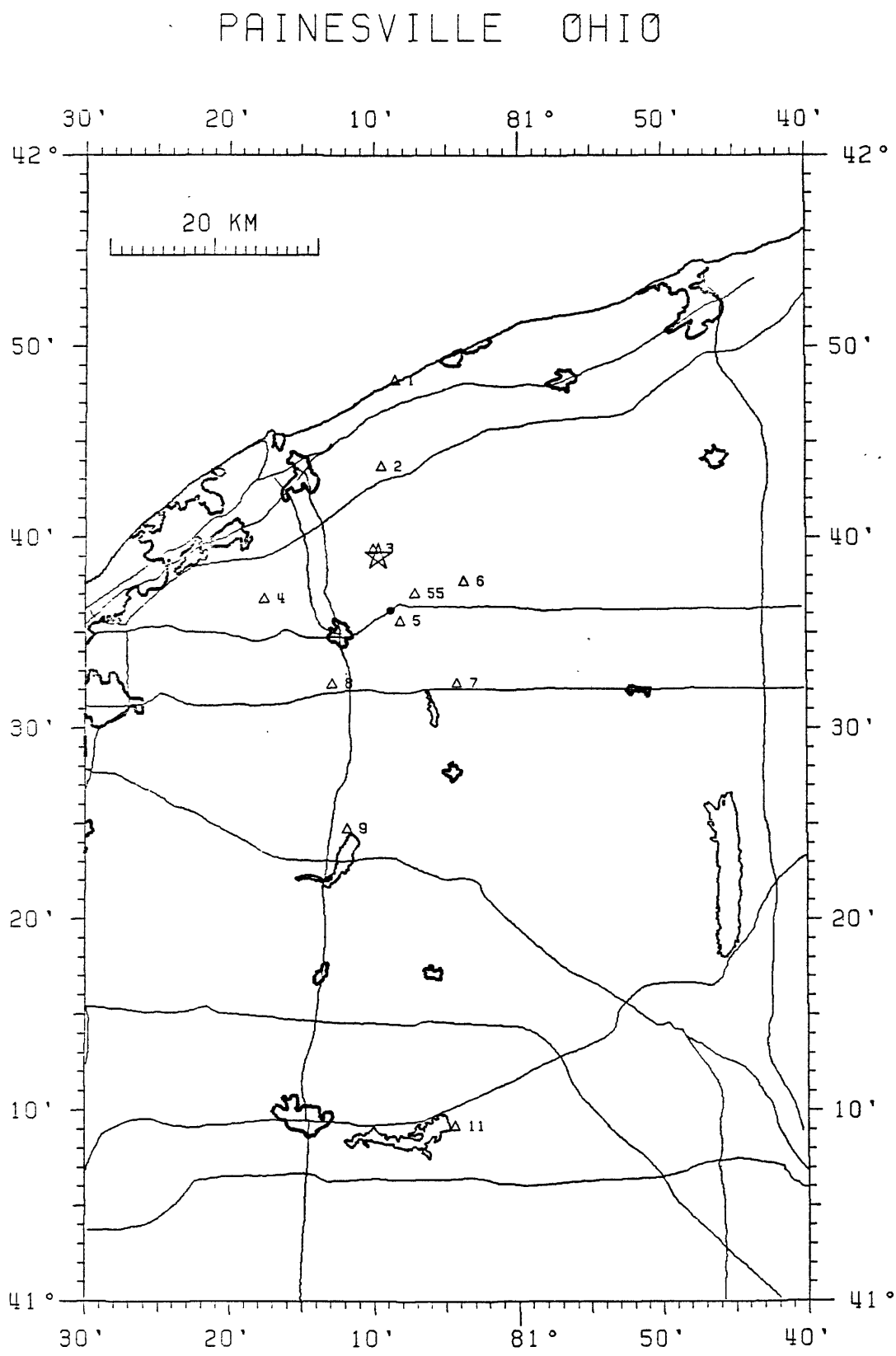

Figure 3. Locations of sites occupied by GEOS recorders and location of main shock on January 31, 1986 (J. Dewey, pers. comm., 1986). Major highways, city and community boundaries, and lake boundaries also are shown.

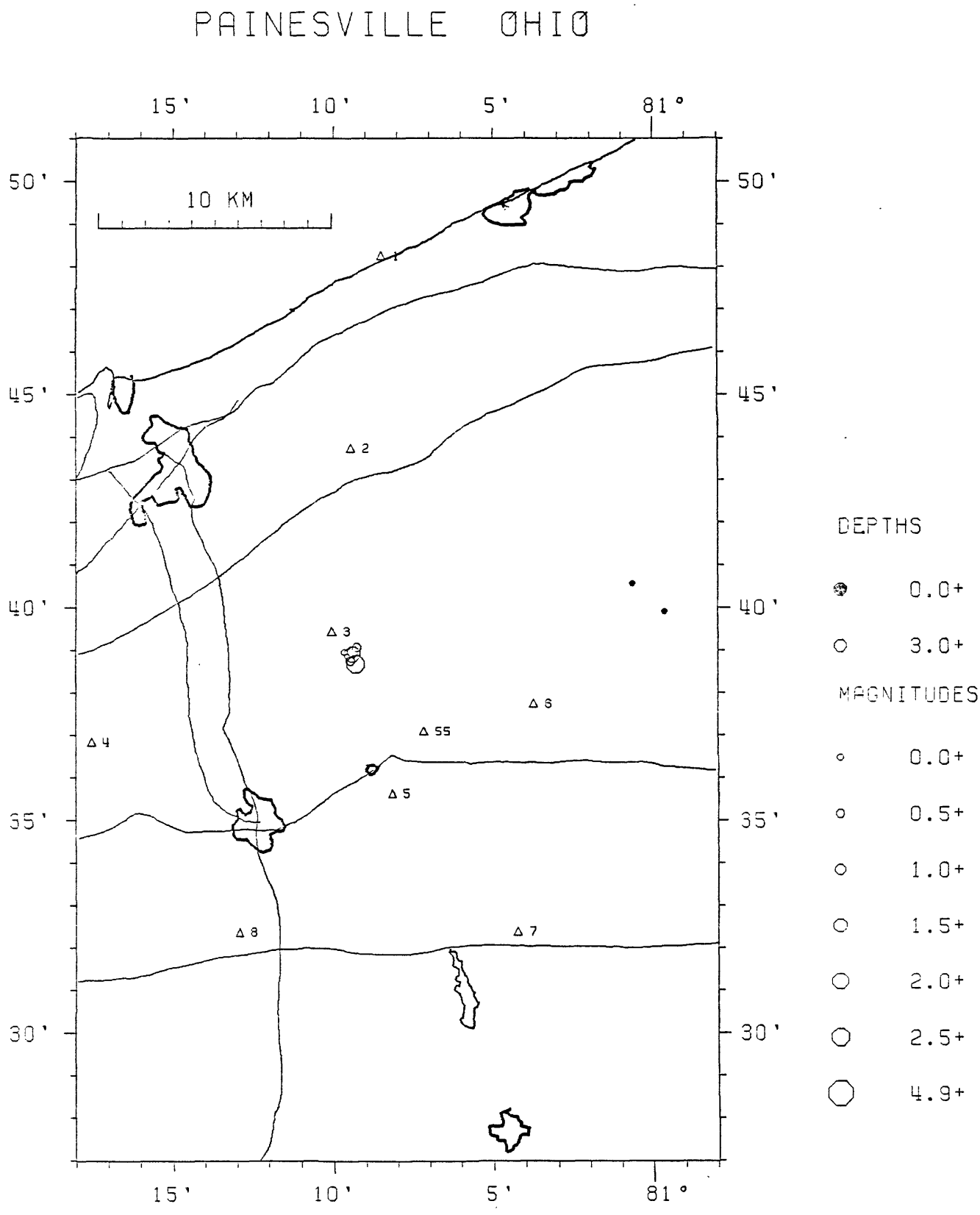

Figure 4. Epicenter locations designated according to estimated coda magnitudes (J. Armbruster, pers. commun., 1986). See Figure 3 for locations of stations 9 and 11. Depths for the events are summarized in Table 4.

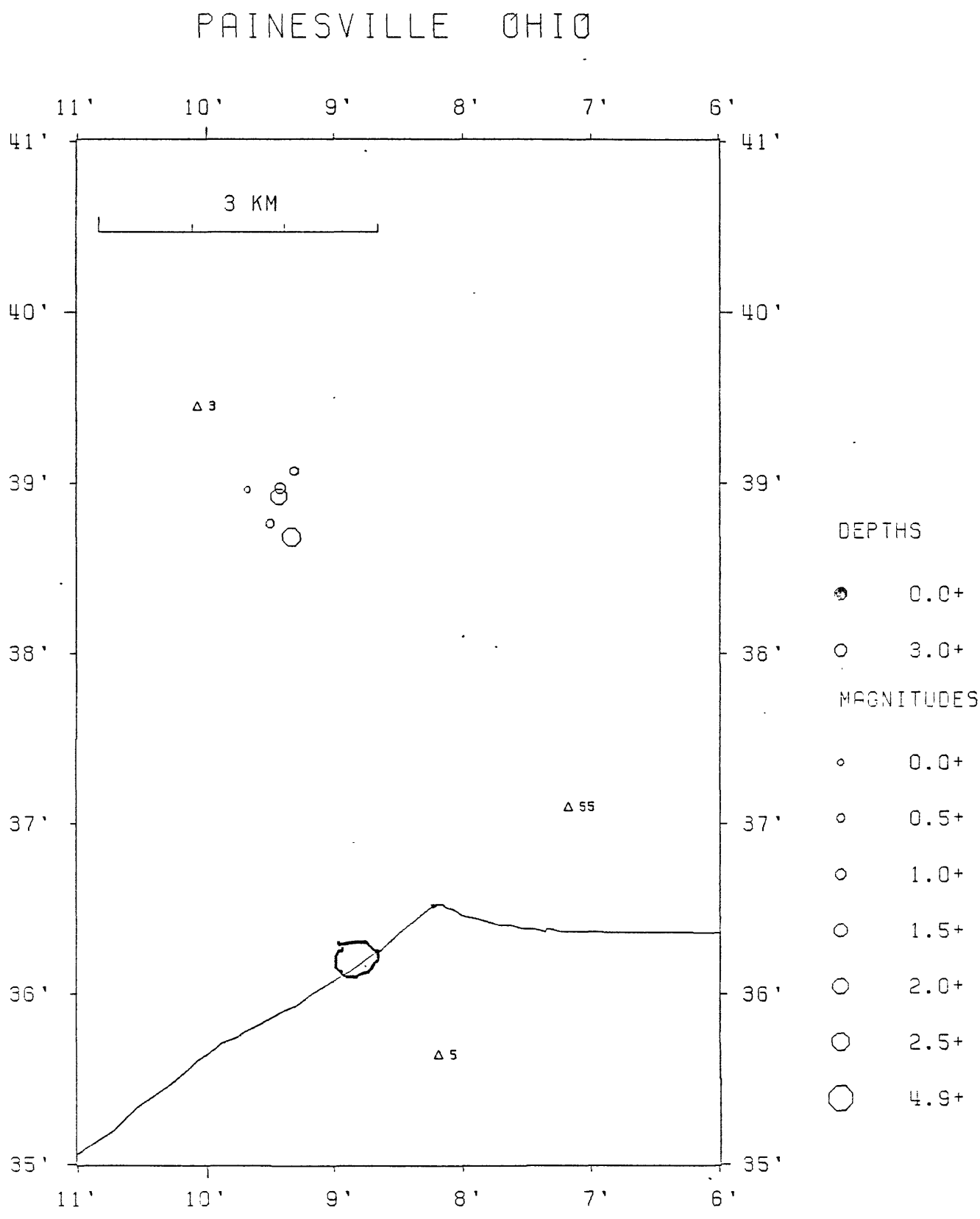

Figure 5. Epicenter locations plotted at a scale expanded with respect to that shown on Figure 4. Depths for the events are given in Table 4.

APPENDIX A

TIME HISTORIES FOR SEISMIC EVENTS RECORDED ON DIGITAL STATIONS NEAR PAINESVILLE, OHIO DURING THE PERIOD FEB. 1, 1986 THROUGH FEB. 10, 1986

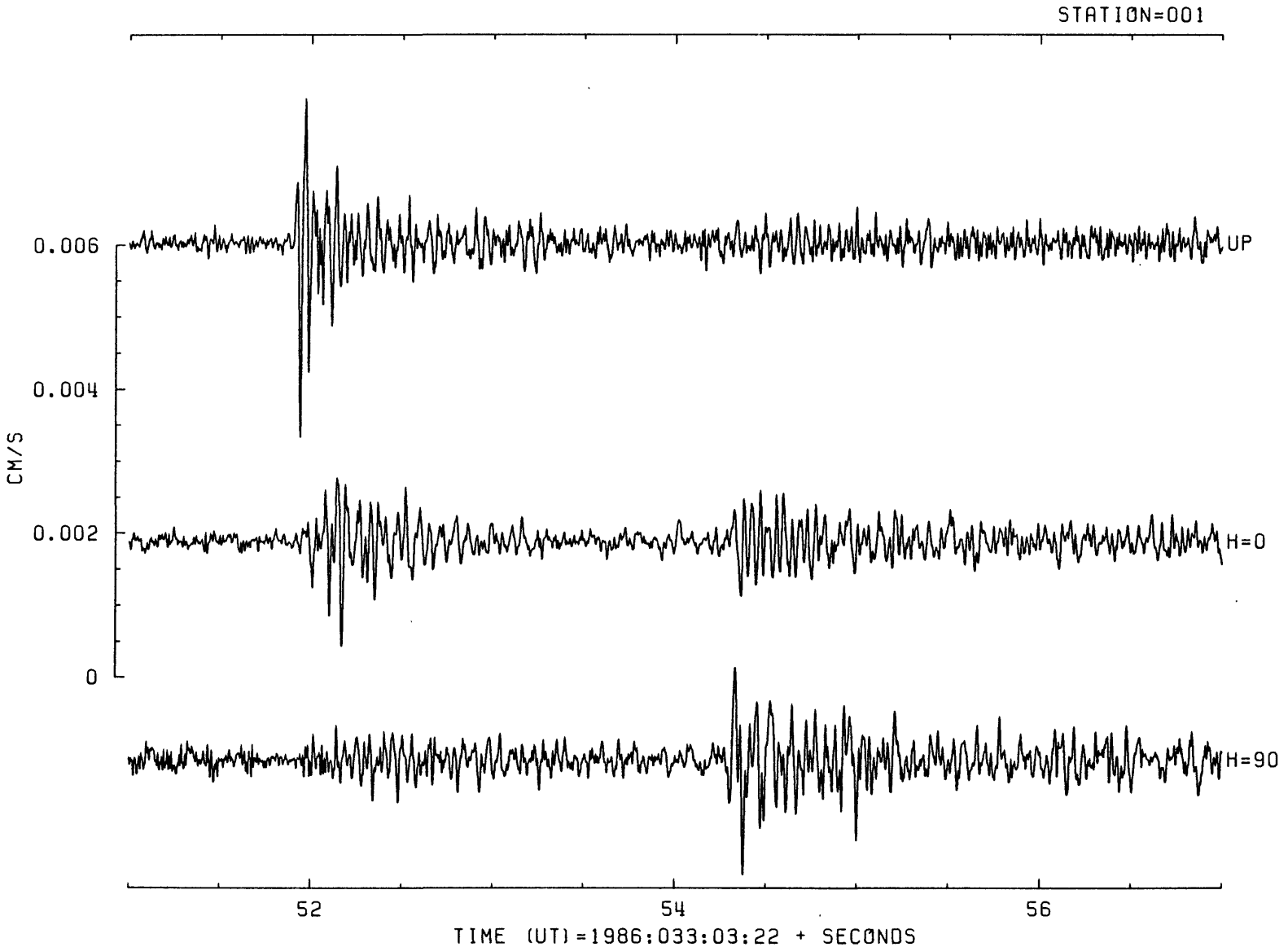

FIGURE A-1: Three component velocity recording of event 033:03:22 at station 001.

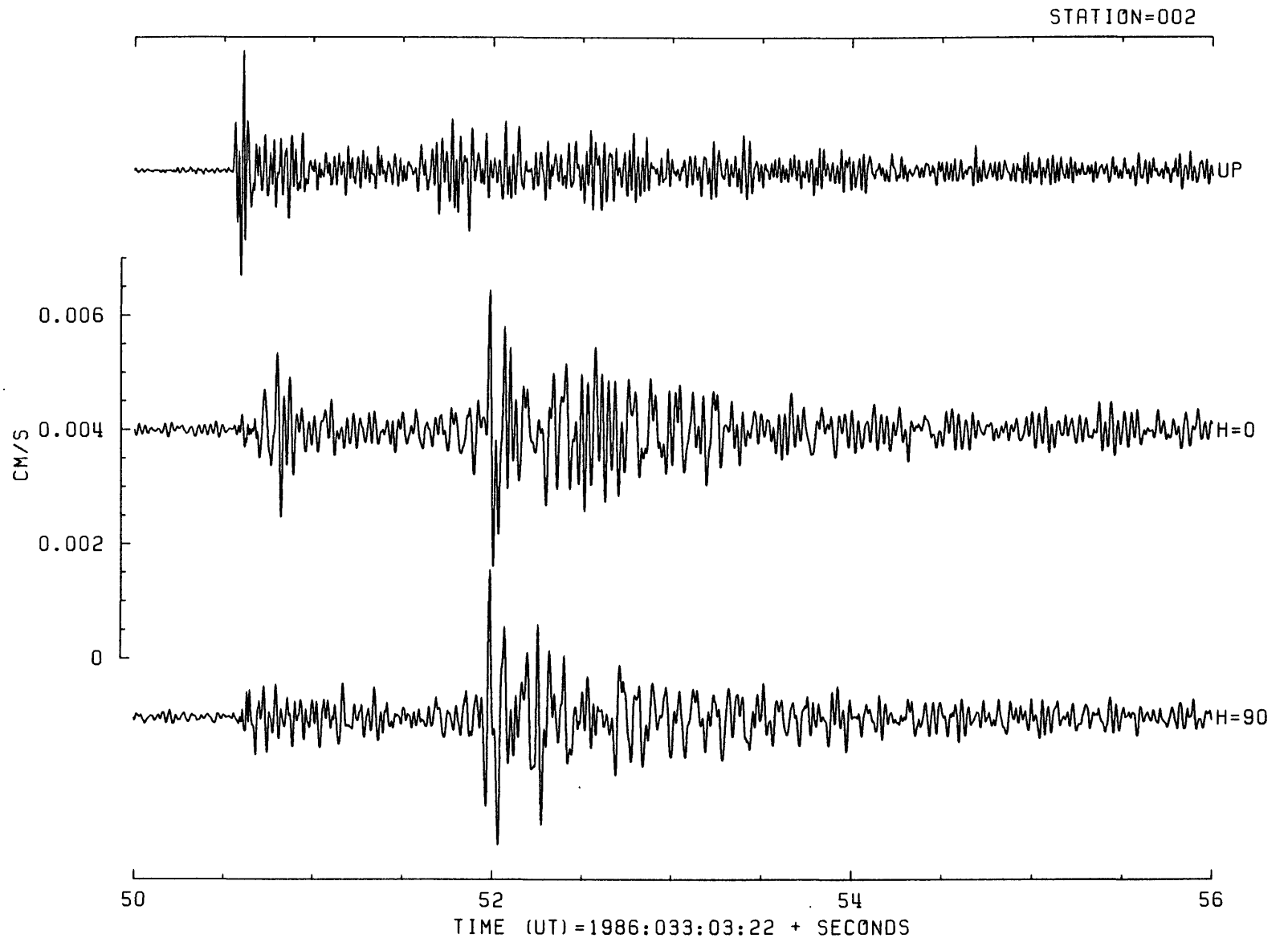

FIGURE A-2: Three component velocity recording of event 033:03:22 at station 002.

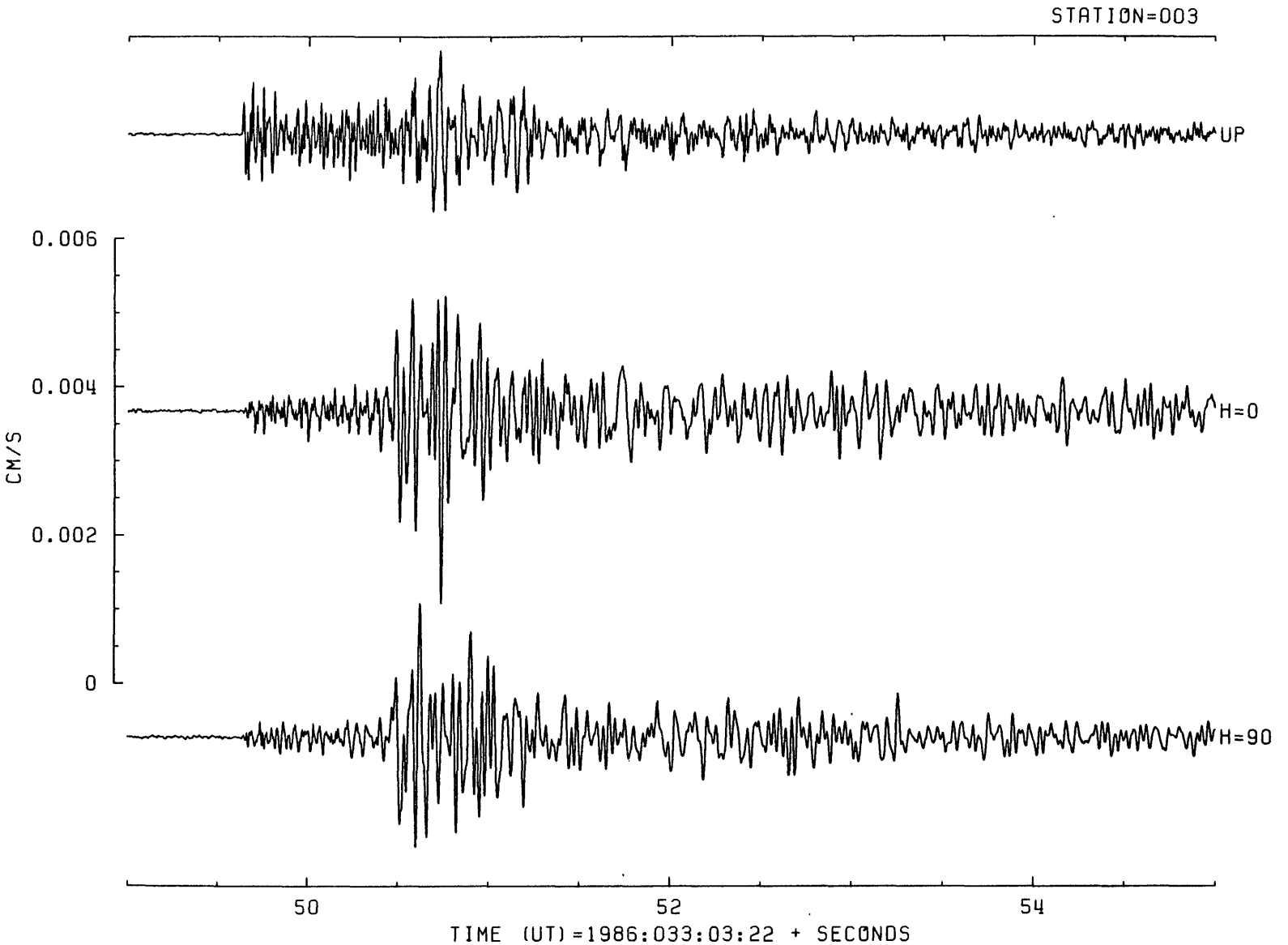

FIGURE A-3: Three component velocity recording of event 033:03:22 at station 003.

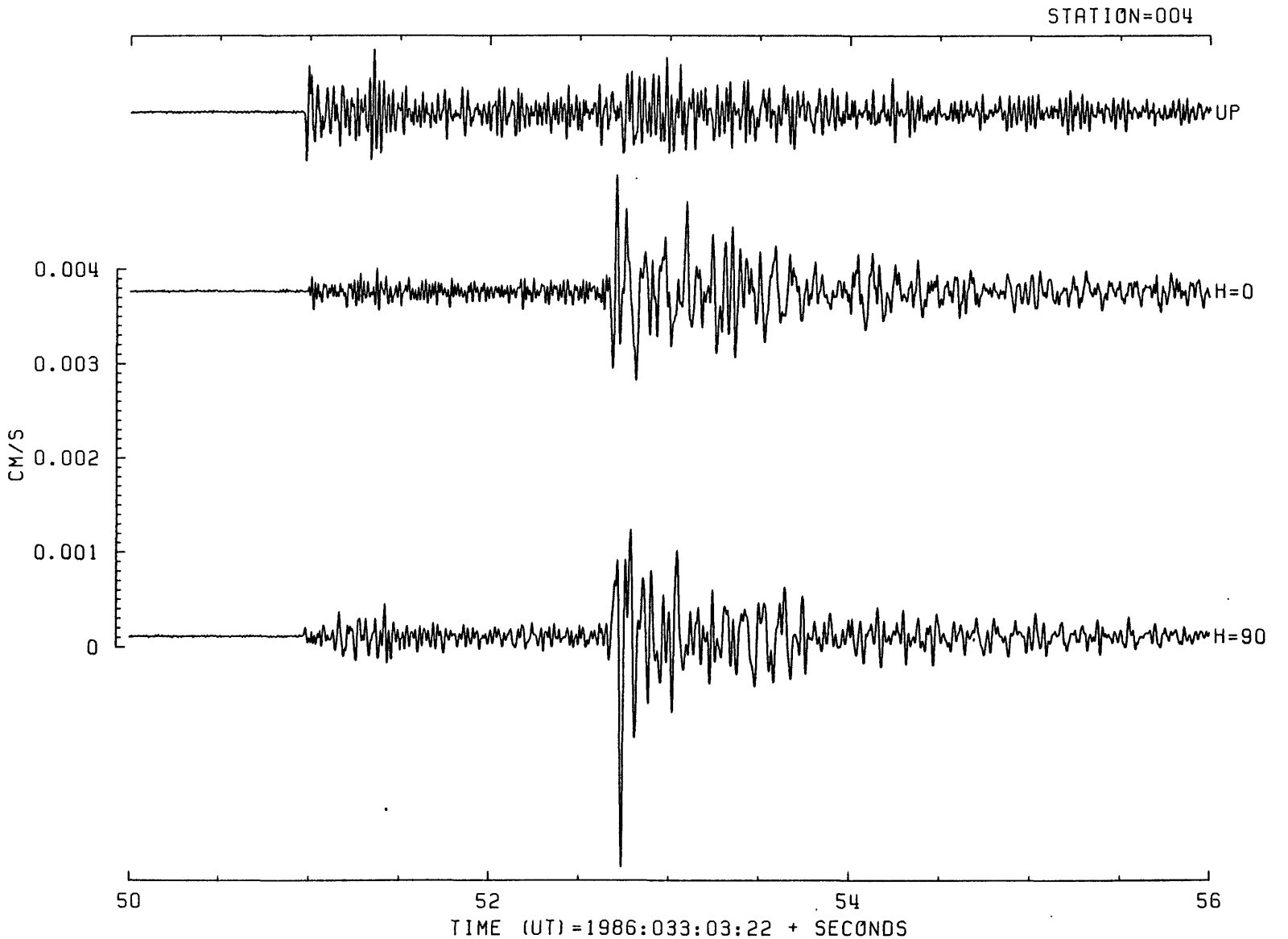

FIGURE A-4: Three component velocity recording of event 033:03:22 at station 004.

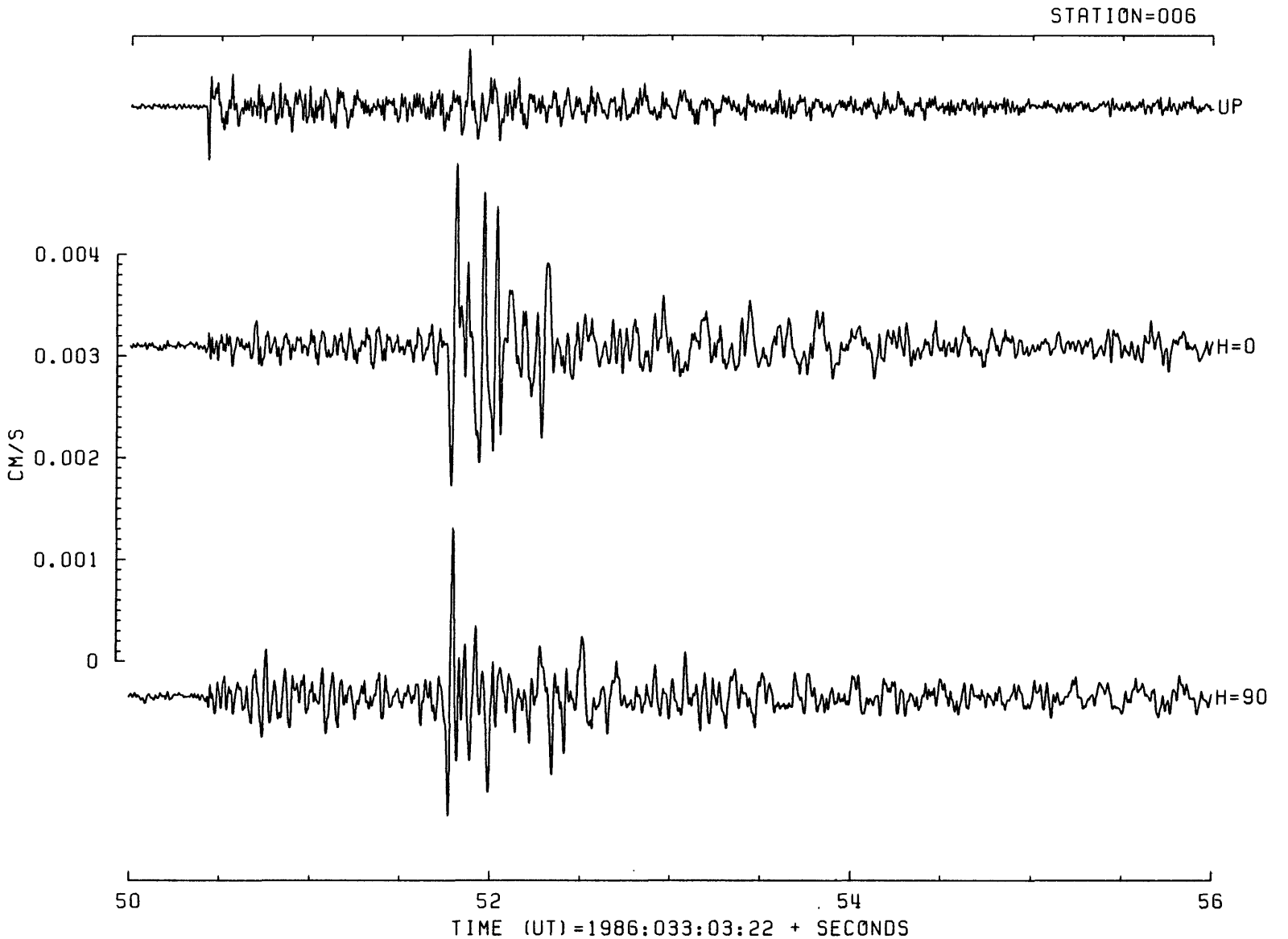

FIGURE A-5: Three component velocity recording of event 033:03:22 at station 006.

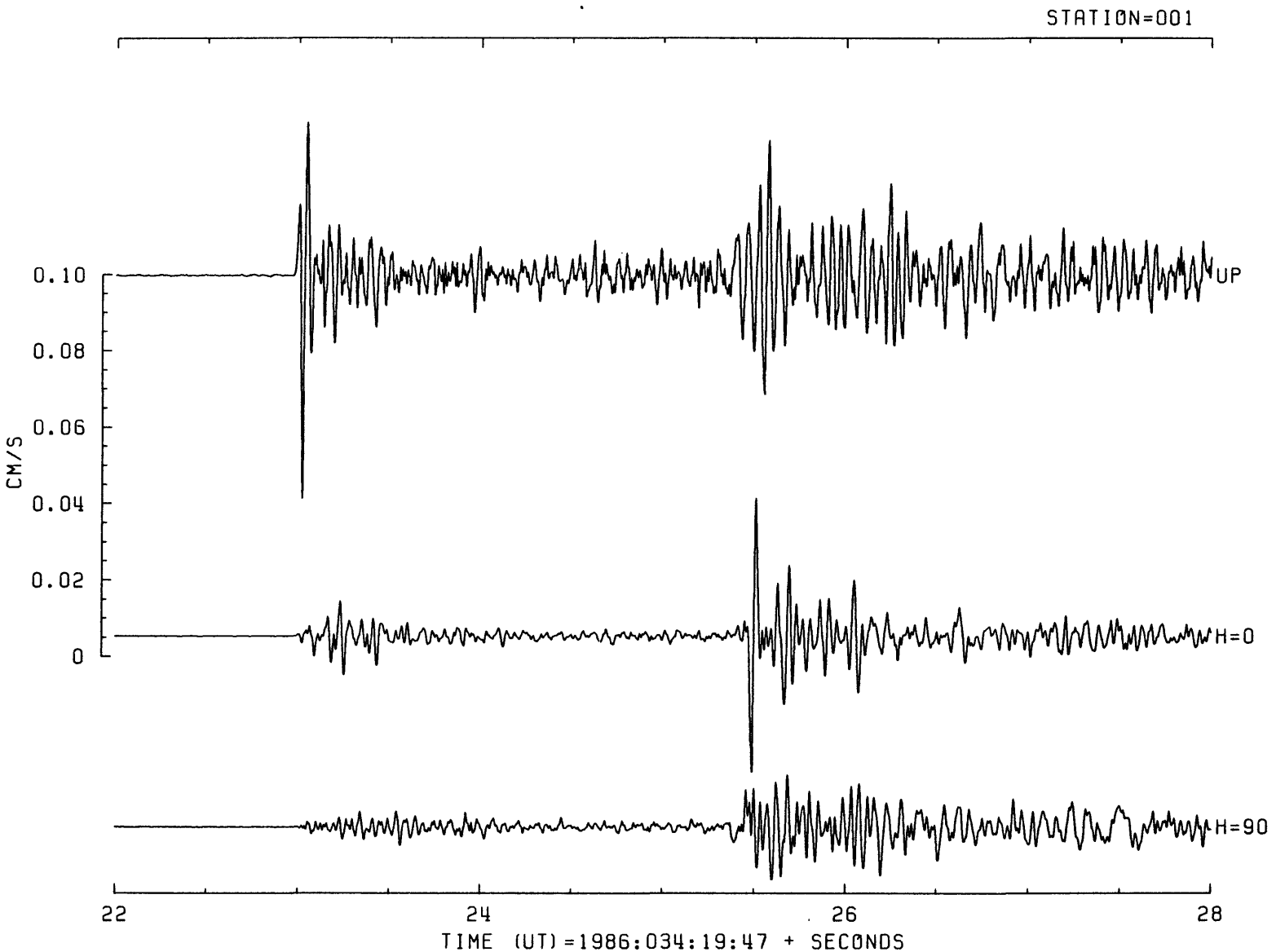

FIGURE A-6: Three component velocity recording of event 034:19:47 at station 001.

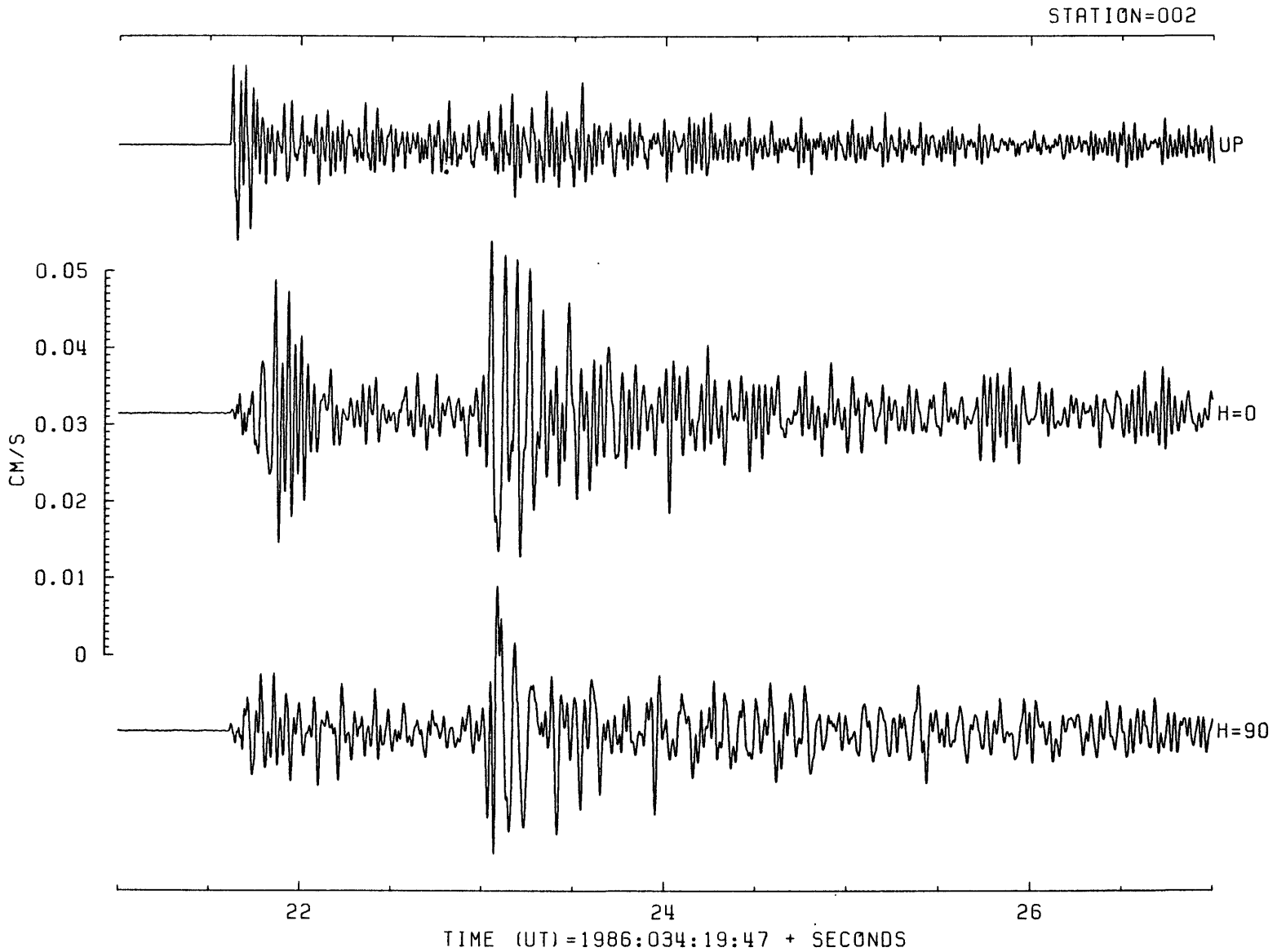

FIGURE A-7: Three component velocity recording of event 034:19:47 at station 002.

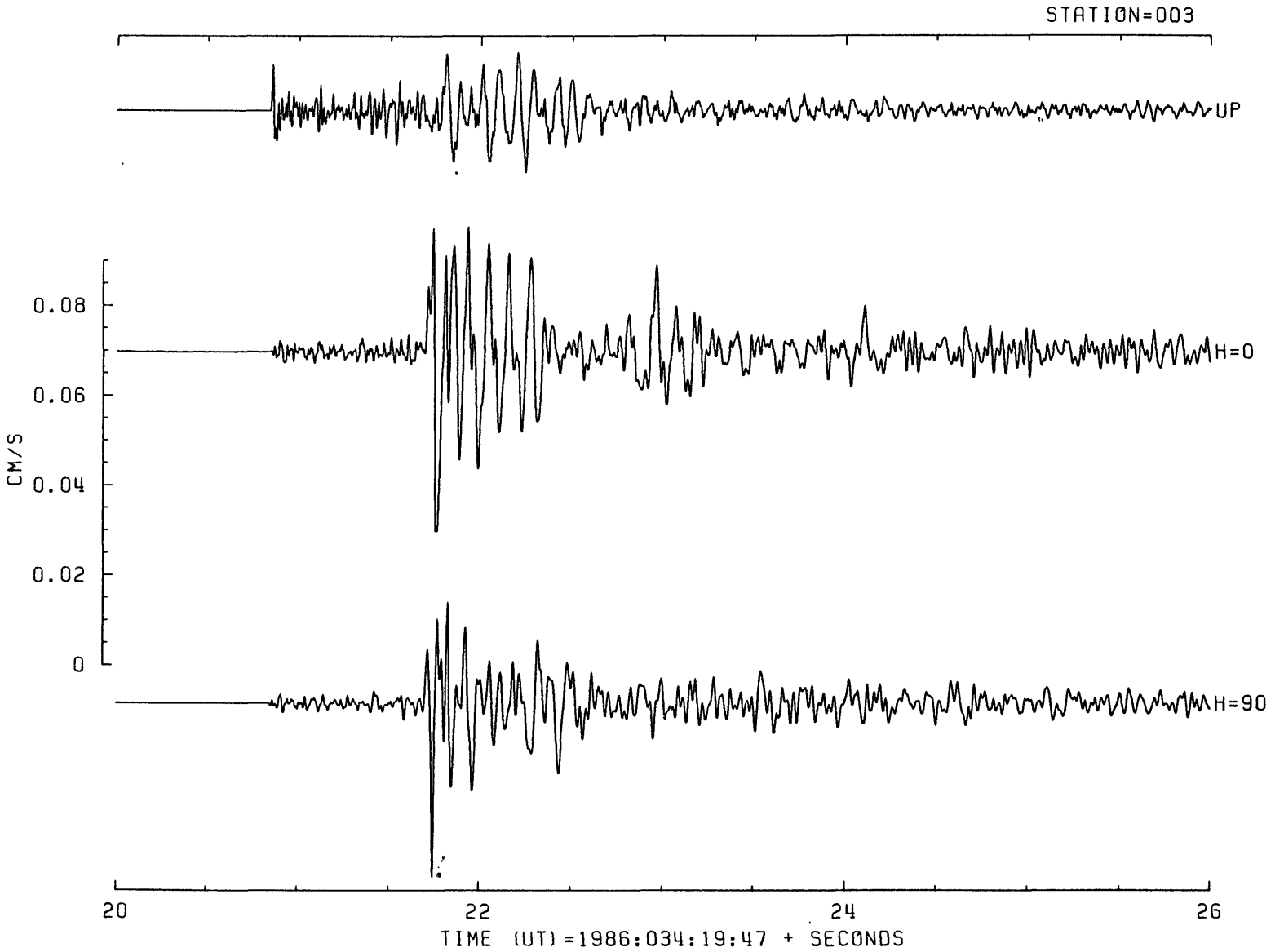

FIGURE A-8: Three component velocity recording of event 034:19:47 at station 003.

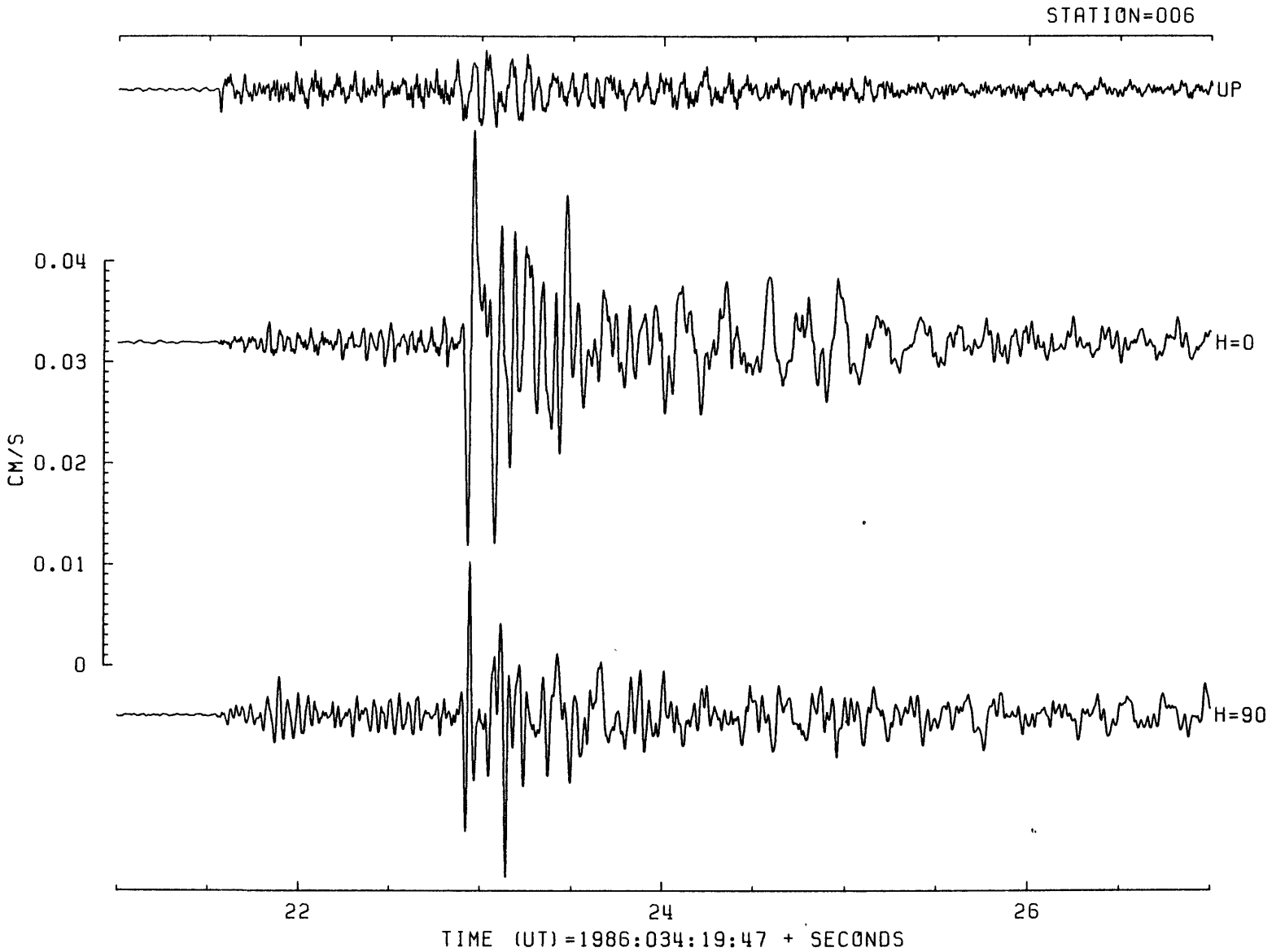

FIGURE A-9: Three component velocity recording of event 034:19:47 at station 006.

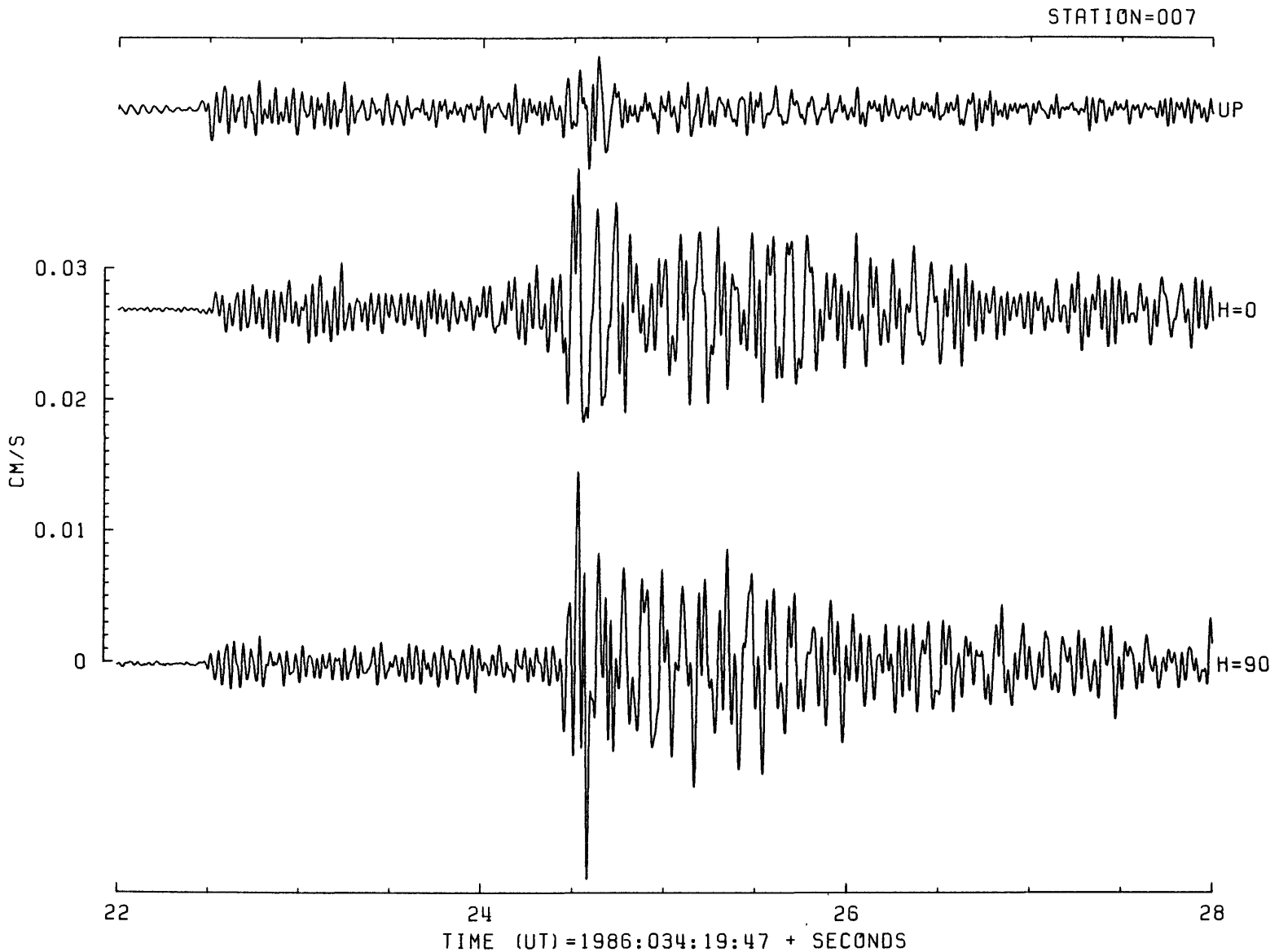

FIGURE A-10: Three component velocity recording of event 034:19:47 at station 007.

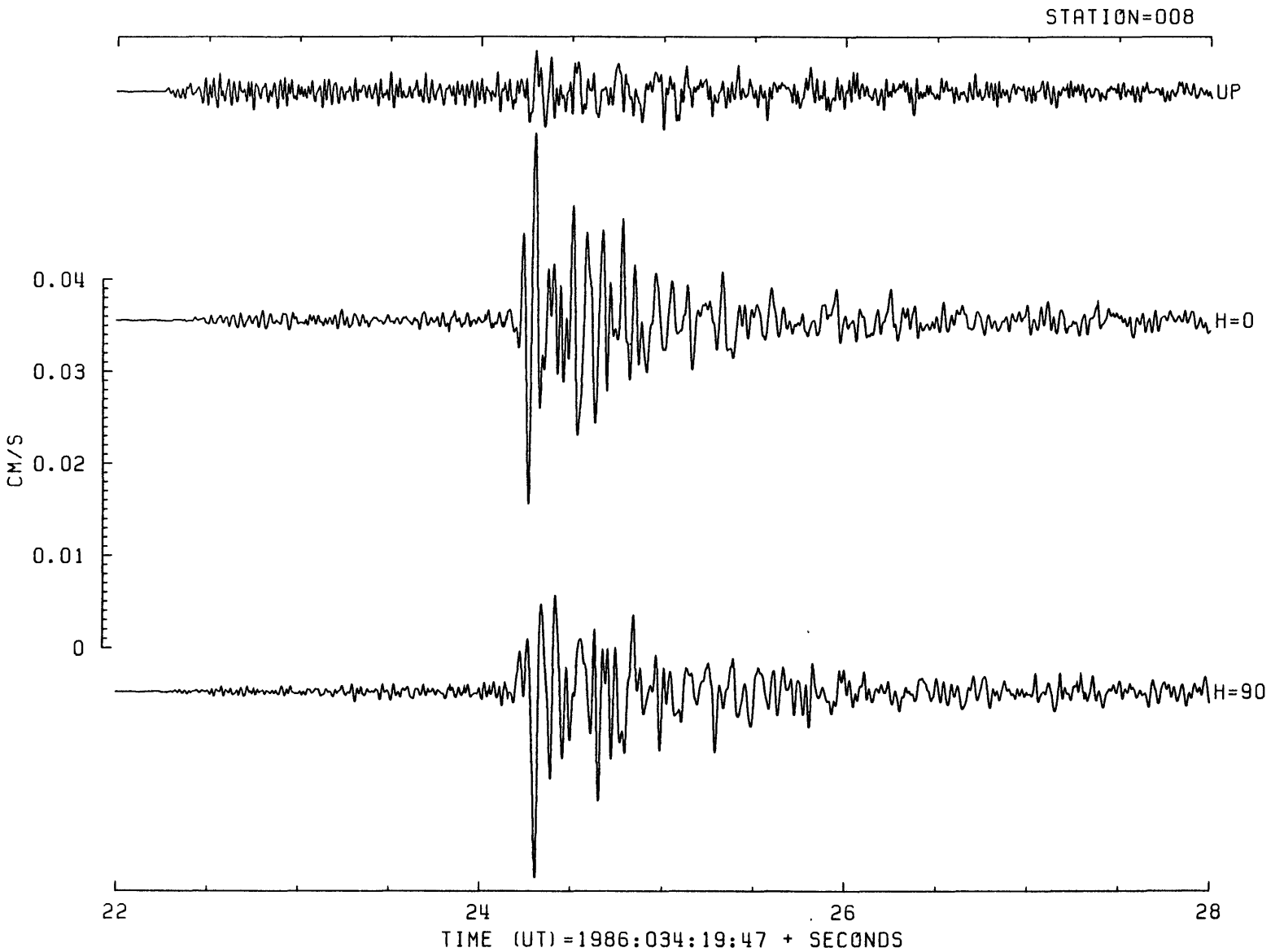

FIGURE A-11: Three component velocity recording of event 034:19:47 at station 008.

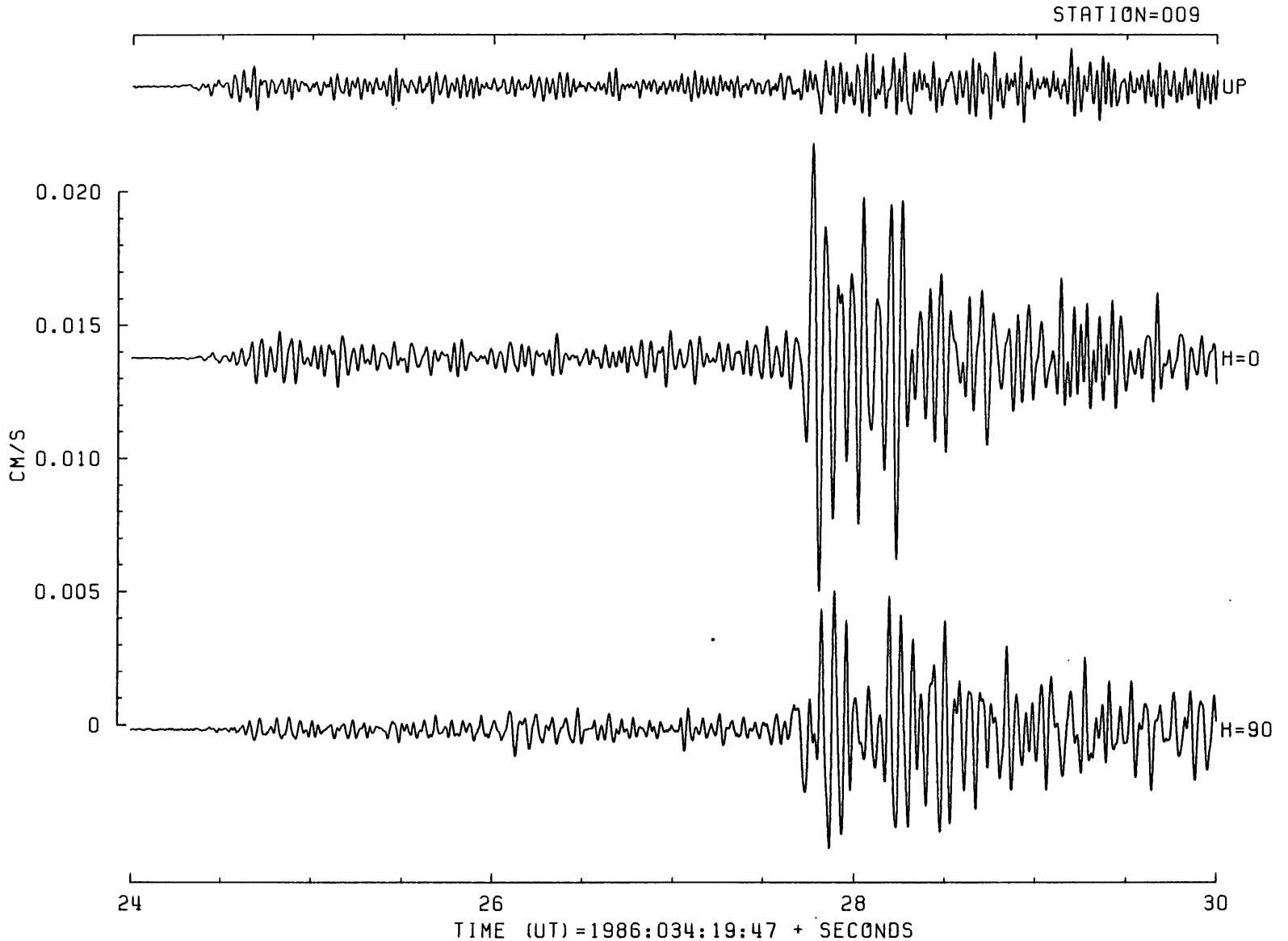

FIGURE A-12a: Three component velocity recording of event 034:19:47 at station 009.

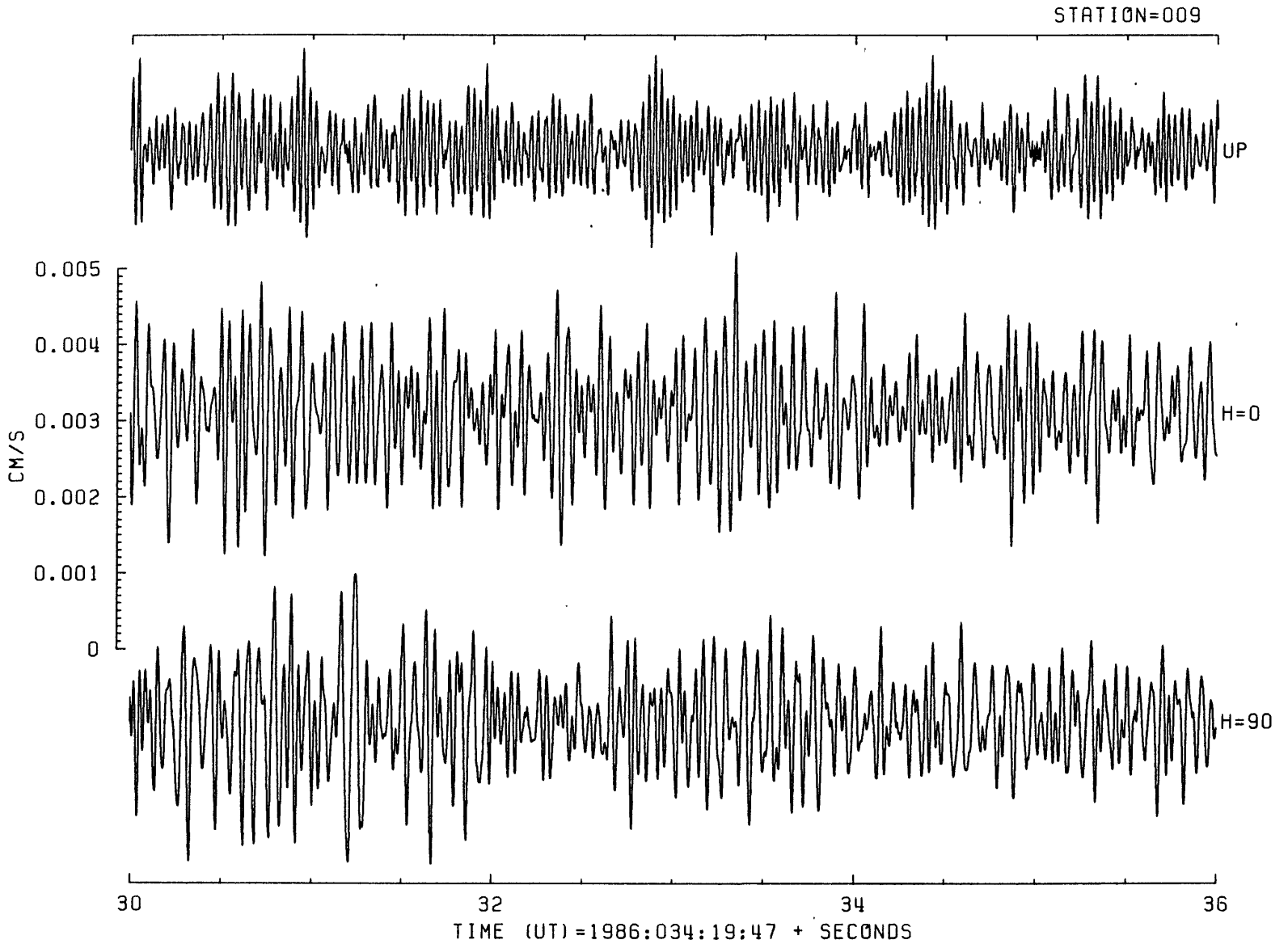

FIGURE A-12b: Three component velocity recording of event 034:19:47 at station 009.

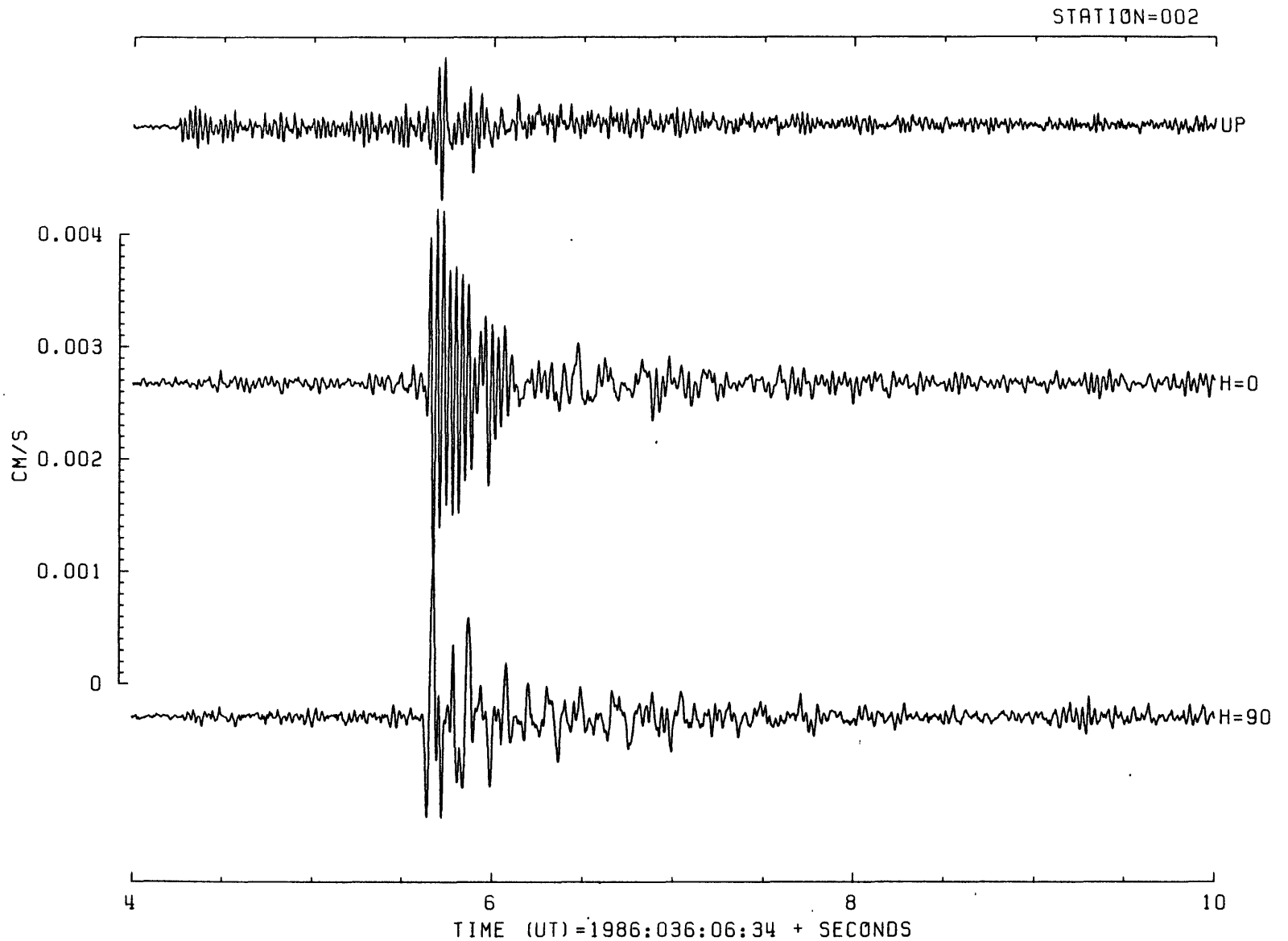

FIGURE A-13: Three component velocity recording of event 036:06:34 at station 002.

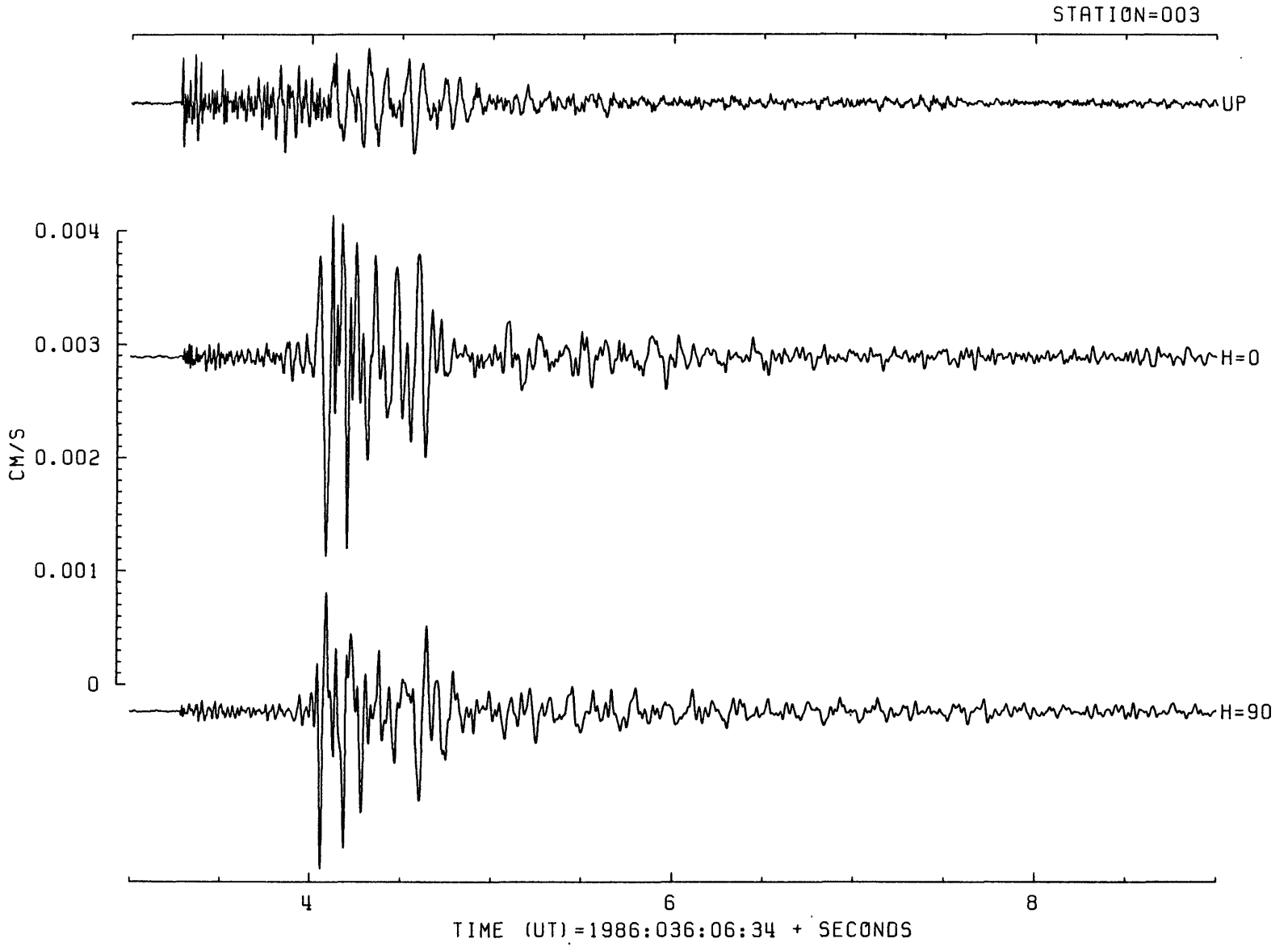

FIGURE A-14: Three component velocity recording of event 036:06:34 at station 003.

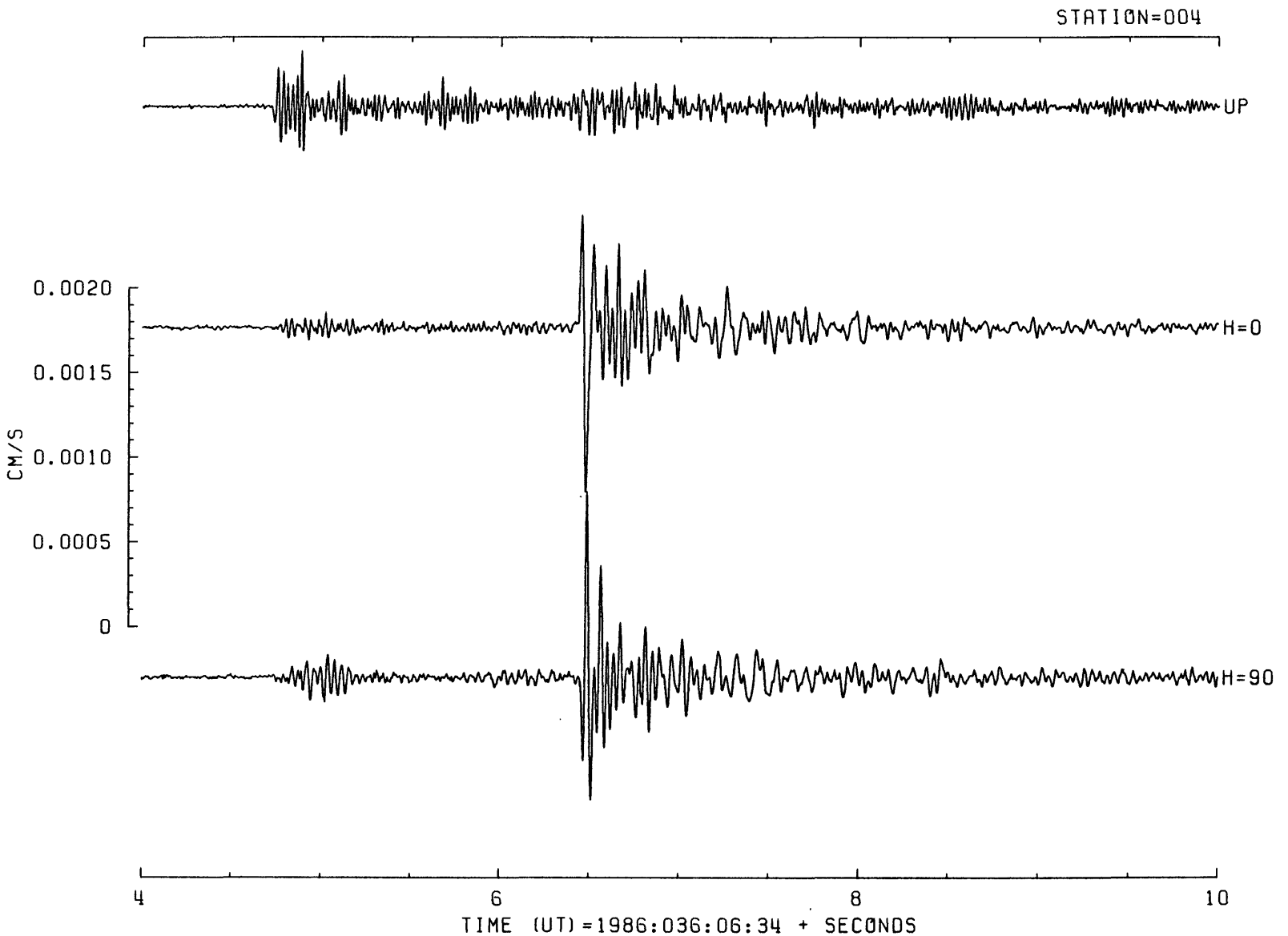

FIGURE A-15: Three component velocity recording of event 036:06:34 at station 004.

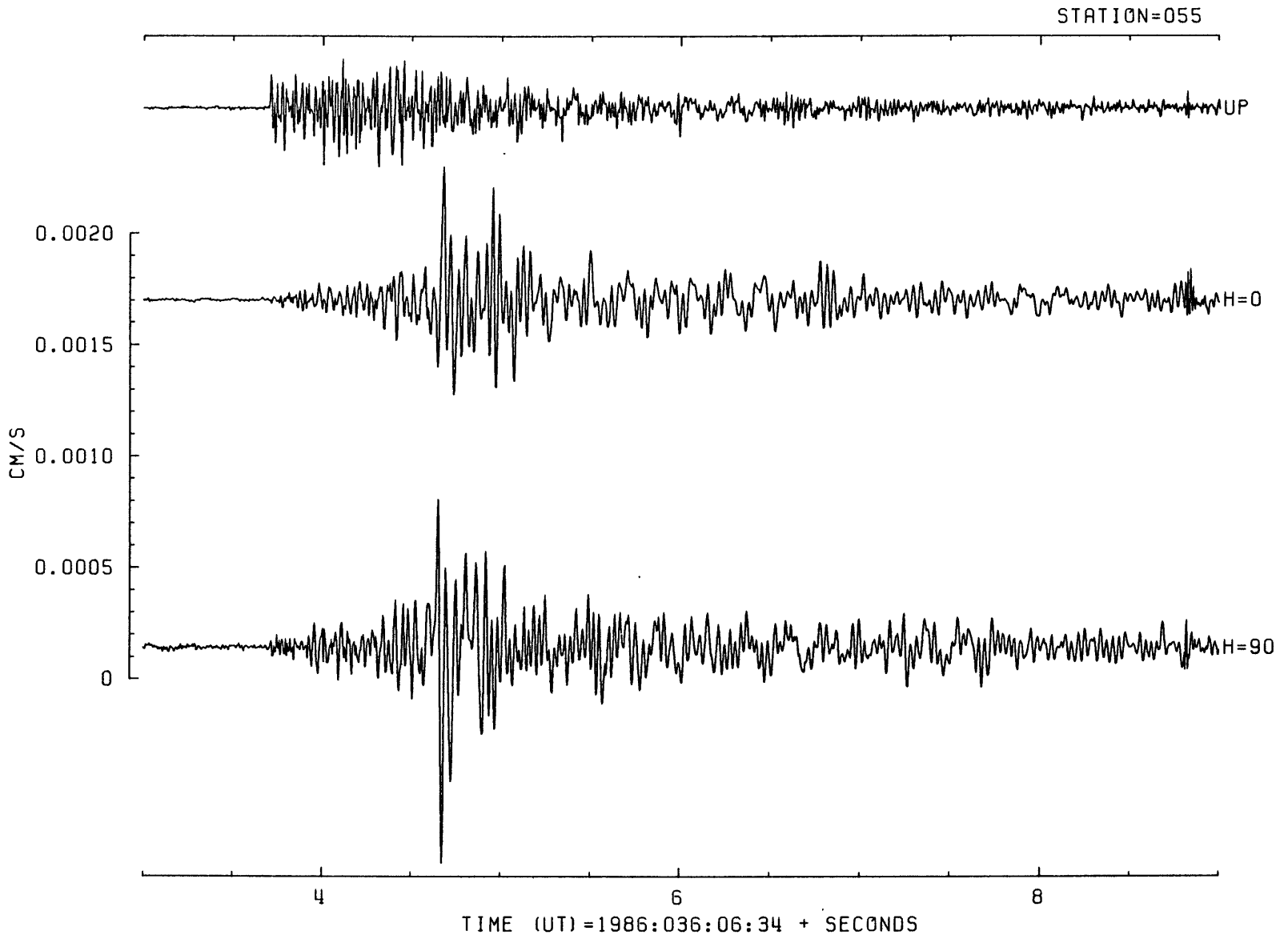

FIGURE A-16: Three component velocity recording of event 036:06:34 at station 055.

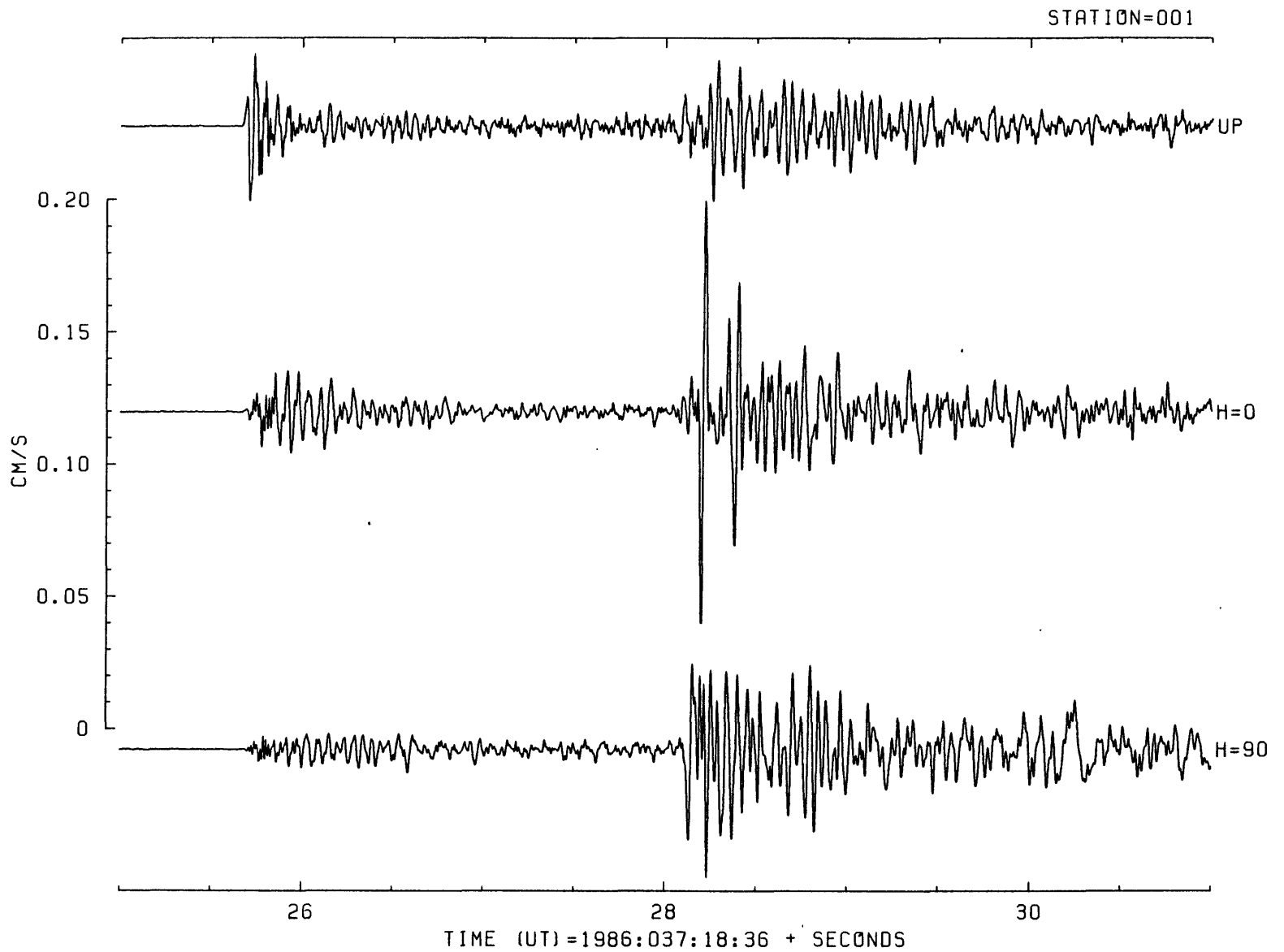

FIGURE A-17: Three component velocity recording of event 036:18:36 at station 001.

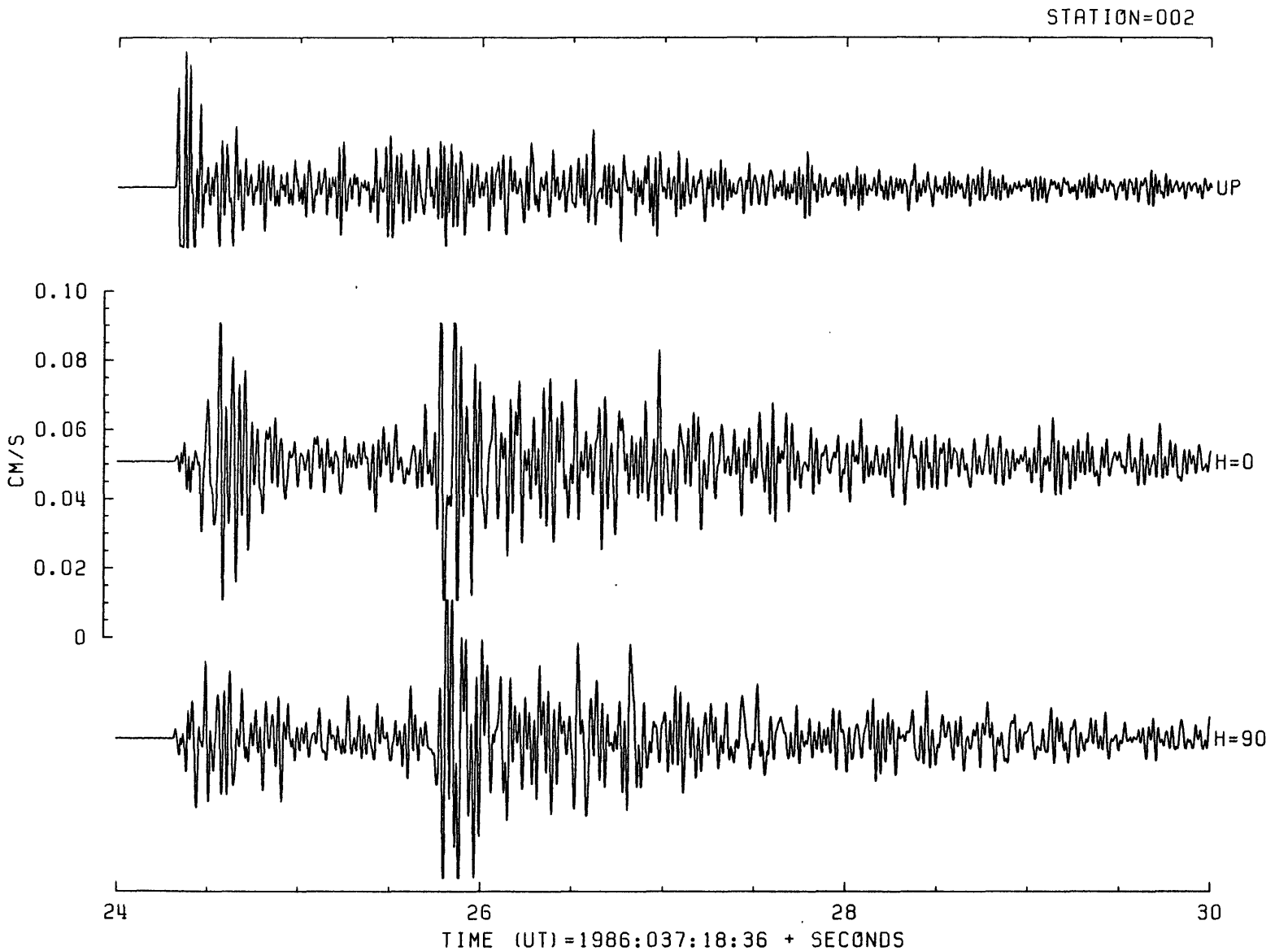

FIGURE A-18: Three component velocity recording of event 036:18:36 at station 002.

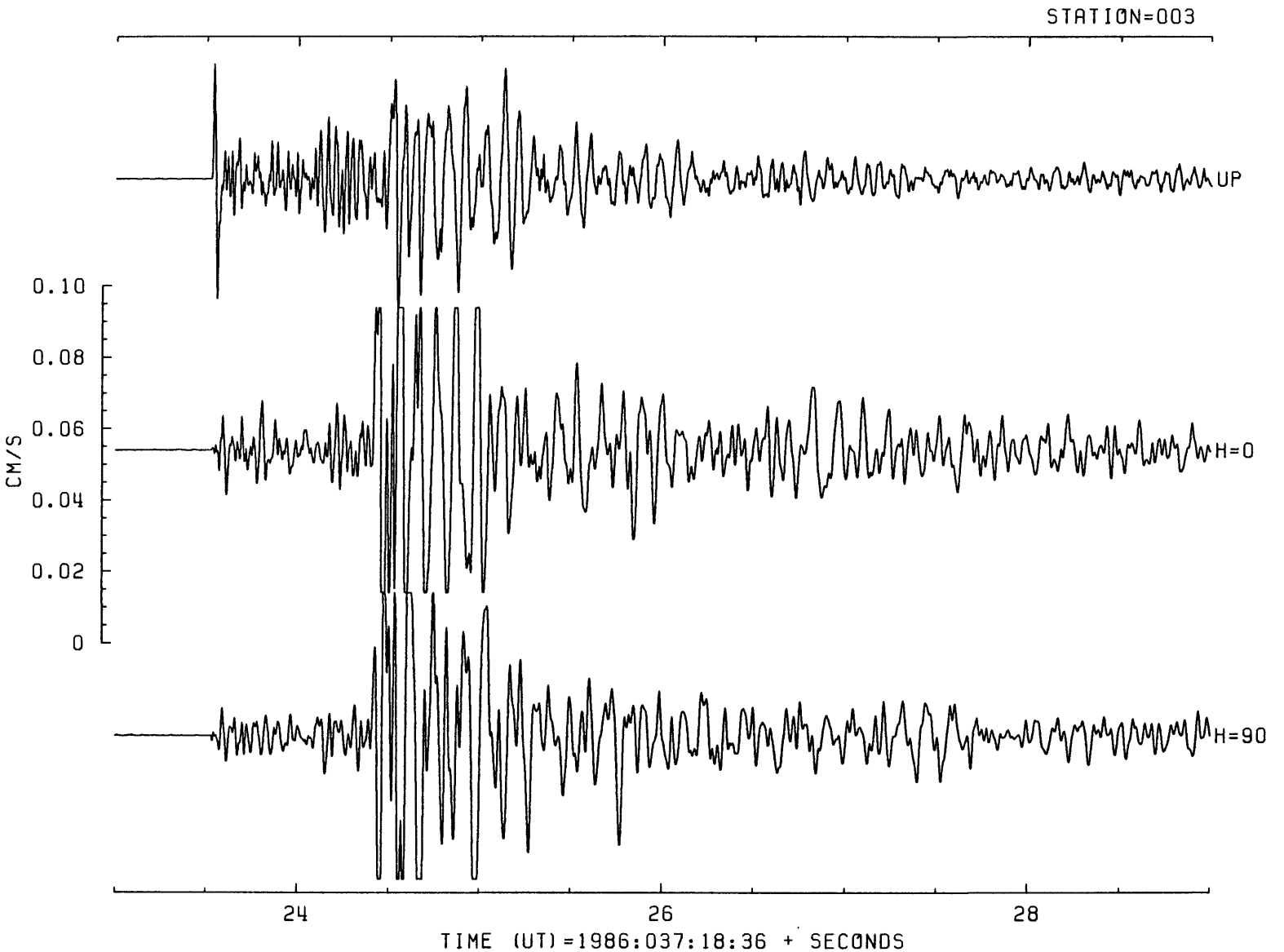

FIGURE A-19: Three component velocity recording of event 036:18:36 at station 003.

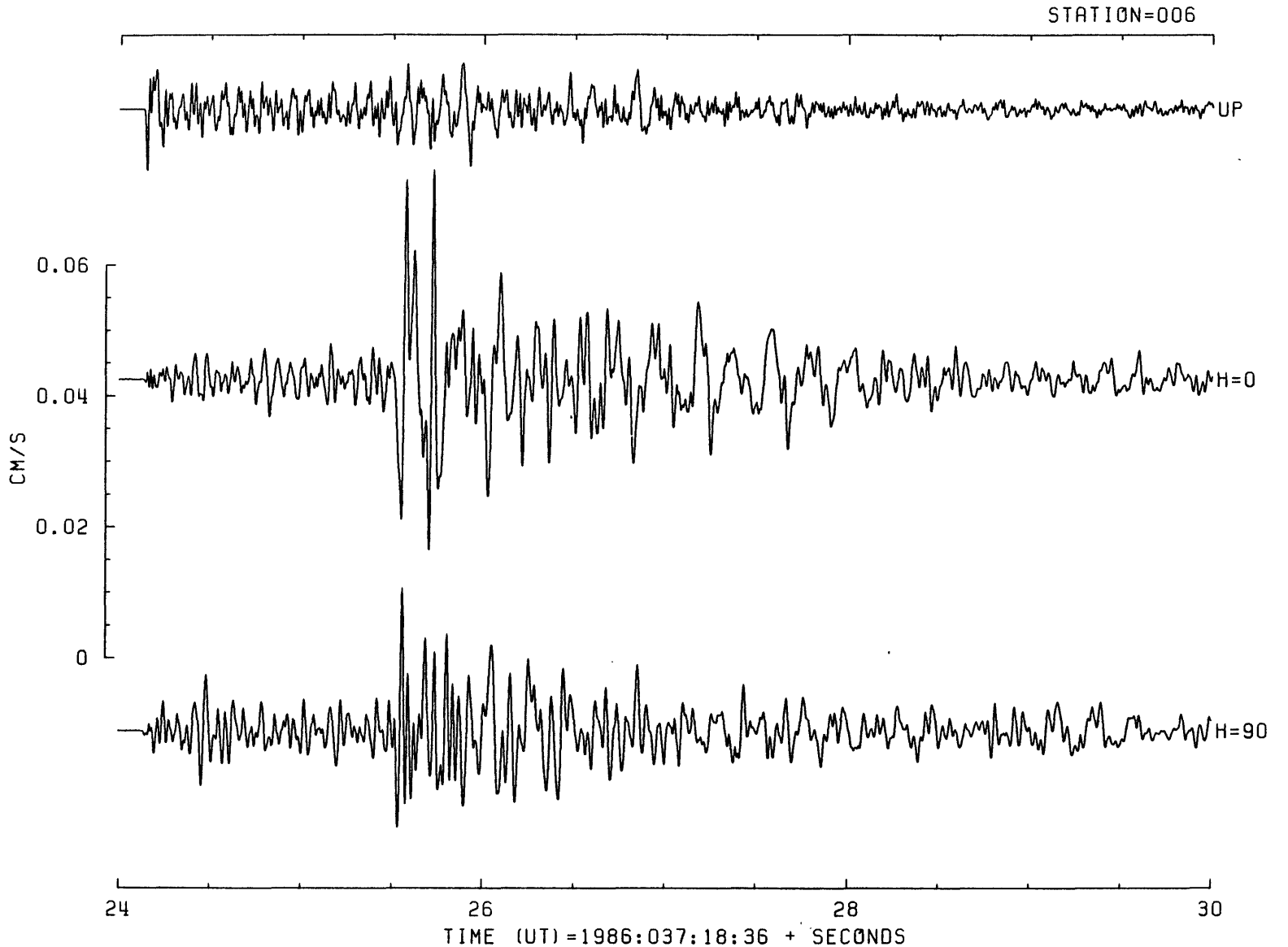

FIGURE A-20: Three component velocity recording of event 036:18:36 at station 006.

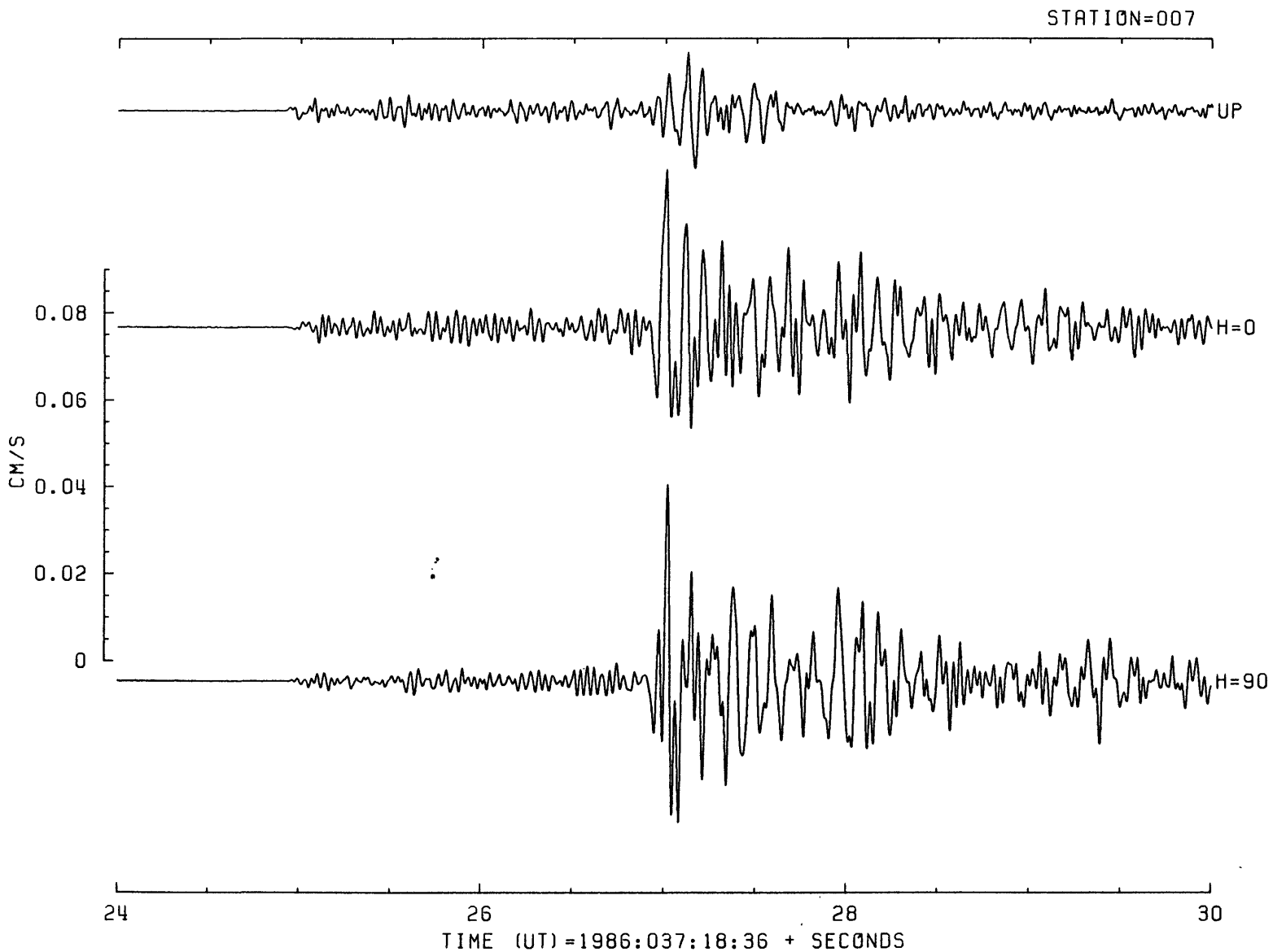

FIGURE A-21: Three component velocity recording of event 036:18:36 at station 007.

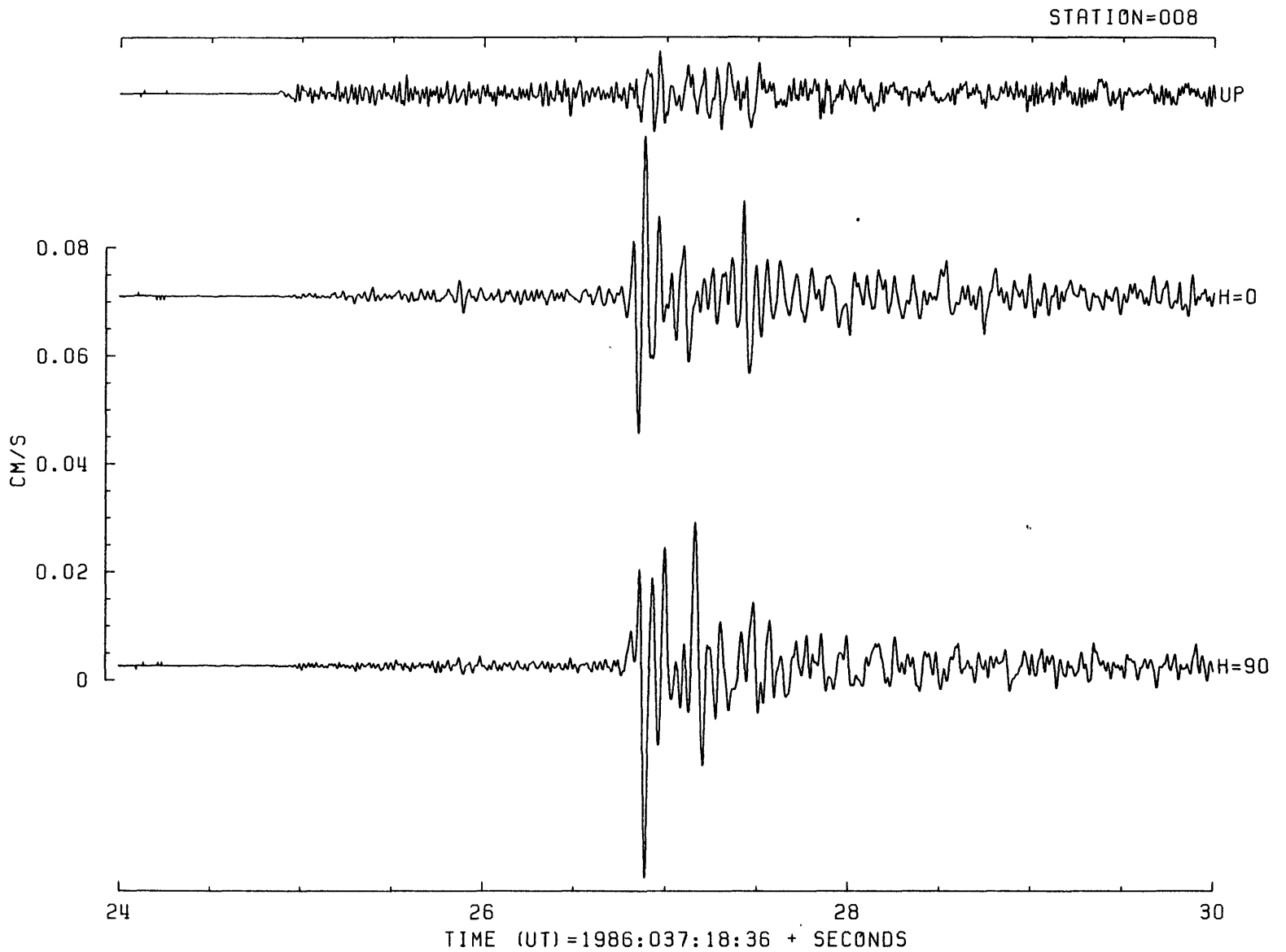

FIGURE A-22: Three component velocity recording of event 036:18:36 at station 008.

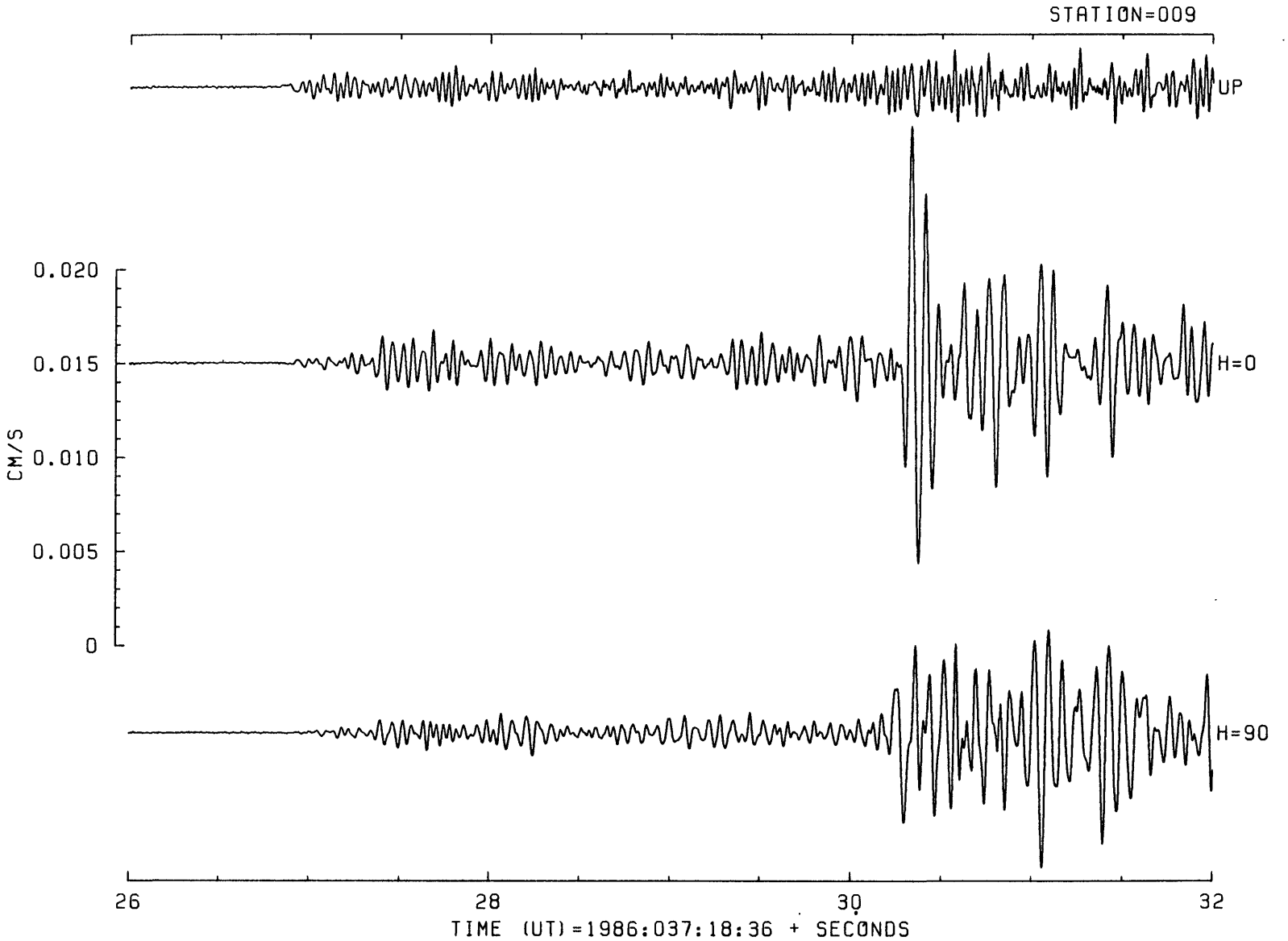

FIGURE A-23a: Three component velocity recording of event 036:18:36 at station 009.

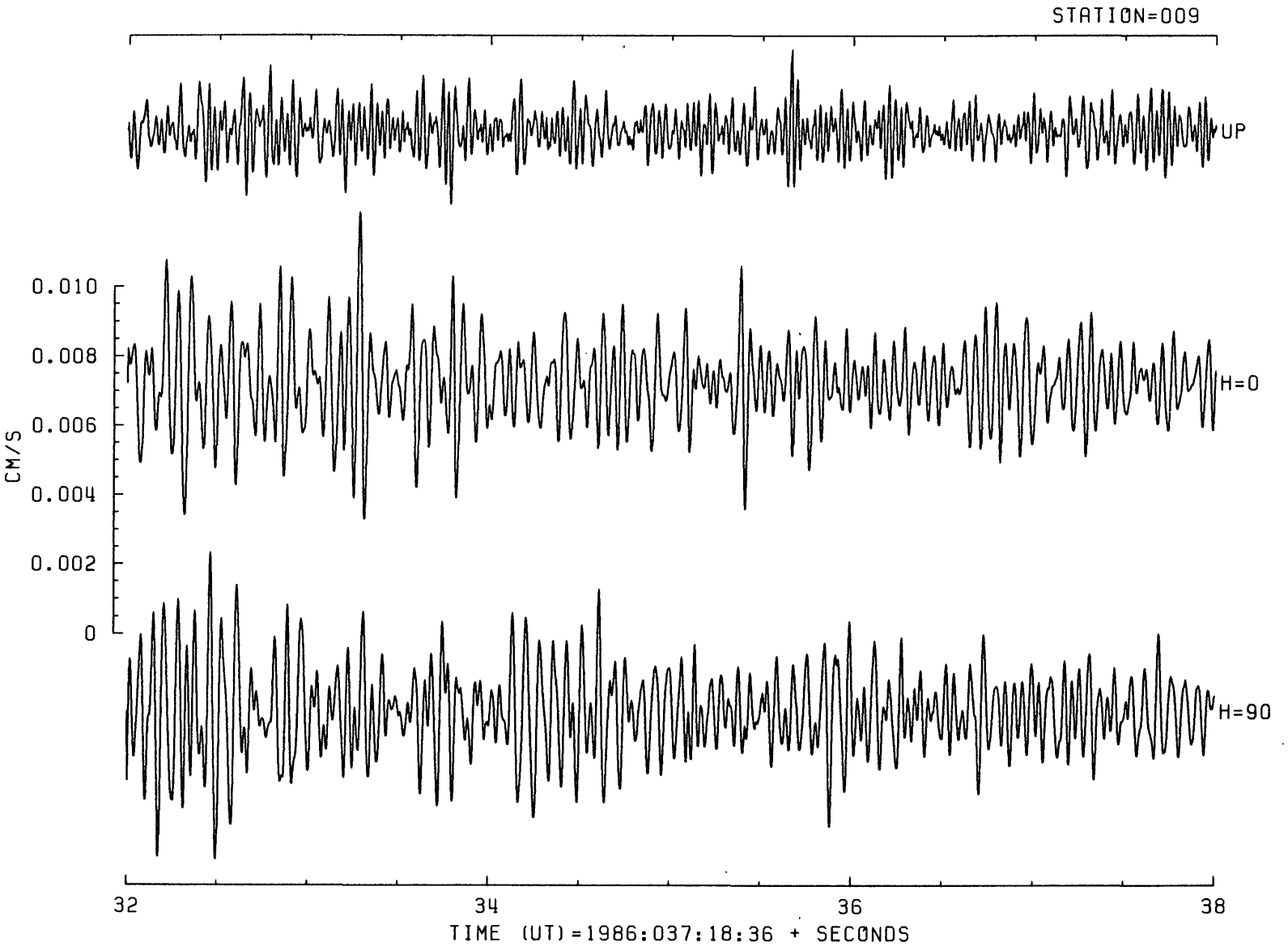

FIGURE A-23b: Three component velocity recording of event 036:18:36 at station 009.

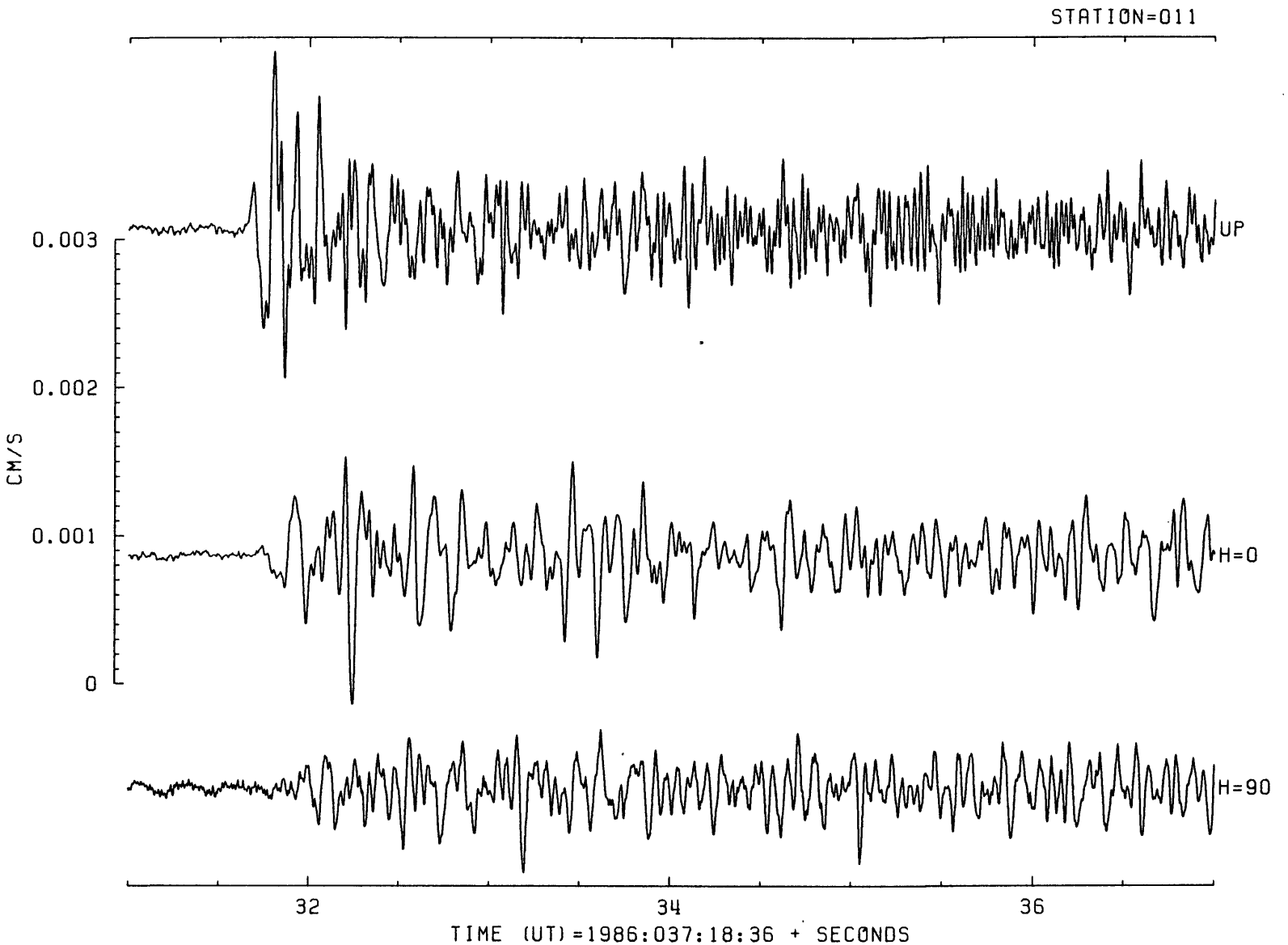

FIGURE A-24a: Three component velocity recording of event 036:18:36 at station 011.

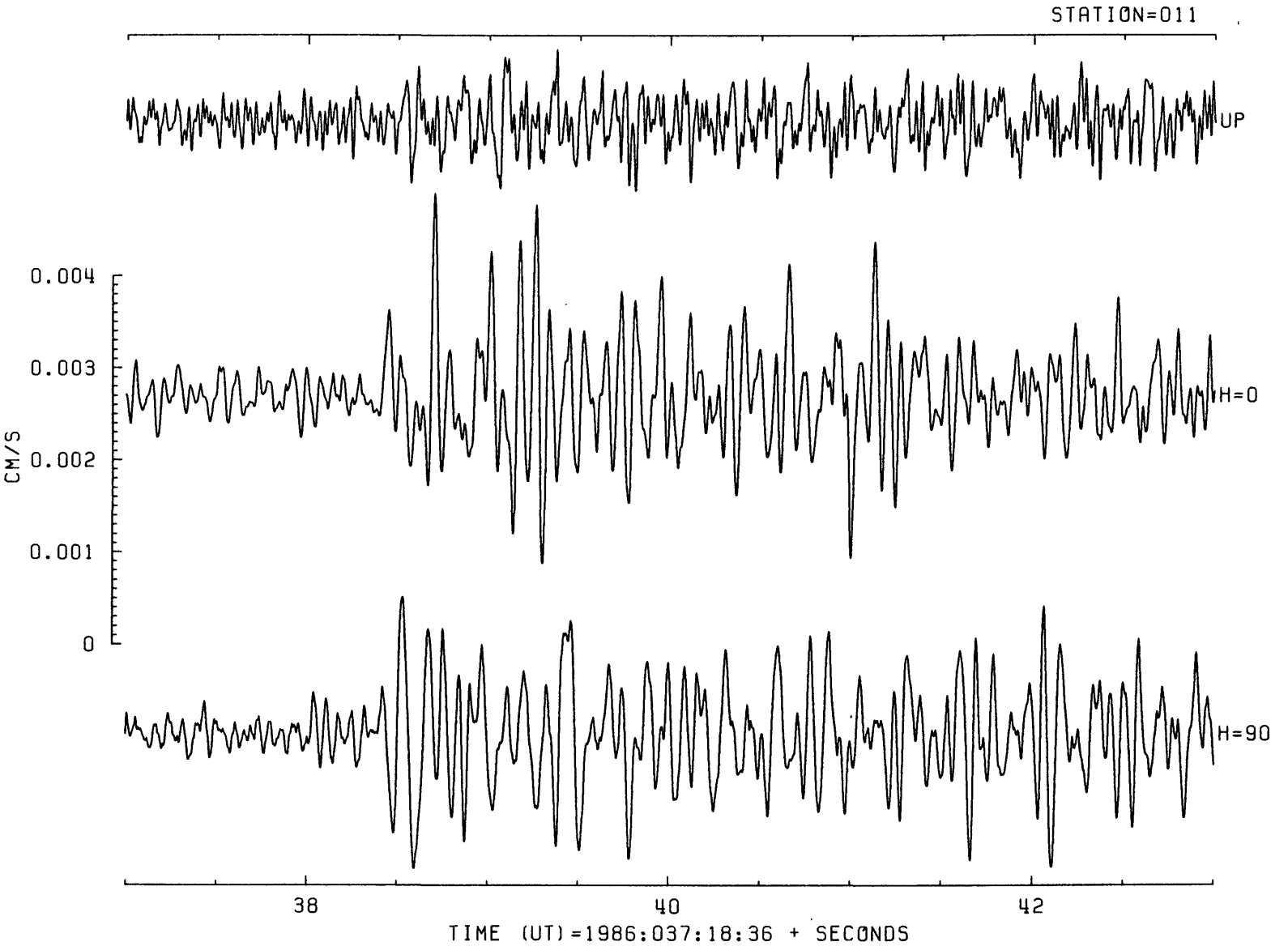

FIGURE A-24b: Three component velocity recording of event 036:18:36 at station 011.

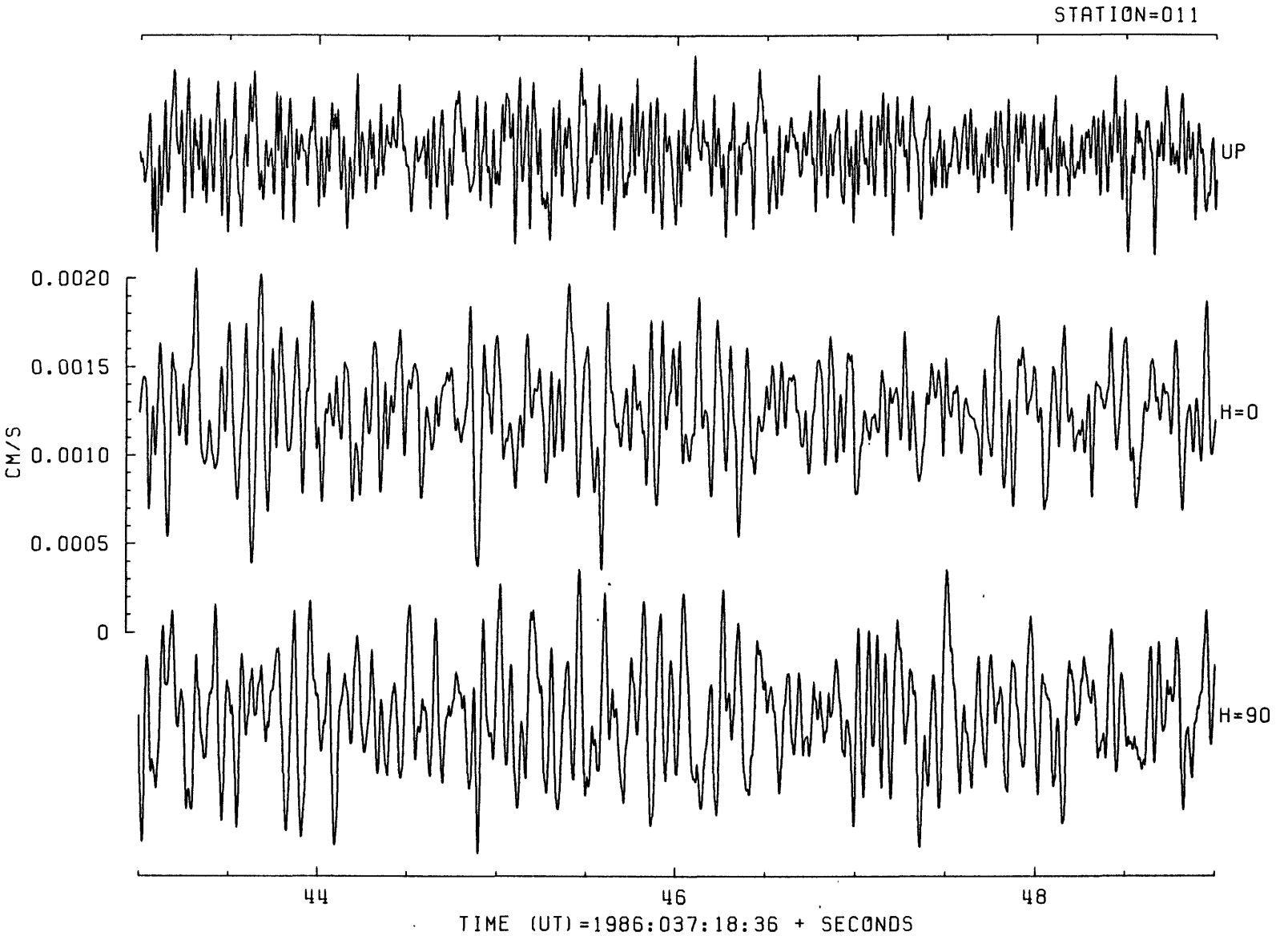

FIGURE A-24c: Three component velocity recording of event 036:18:36 at station 011.

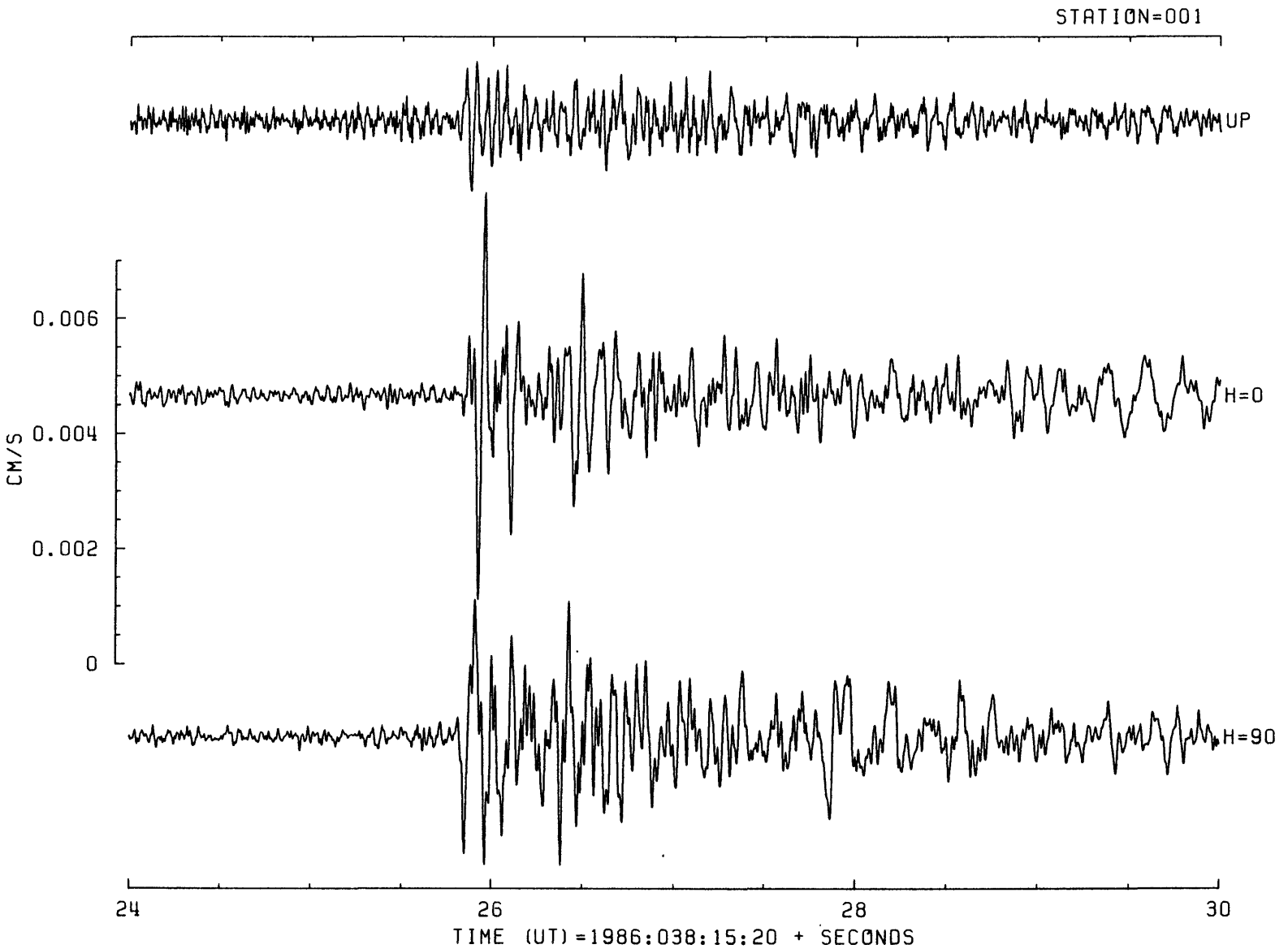

FIGURE A-25: Three component velocity recording of event 038:15:20 at station 001.

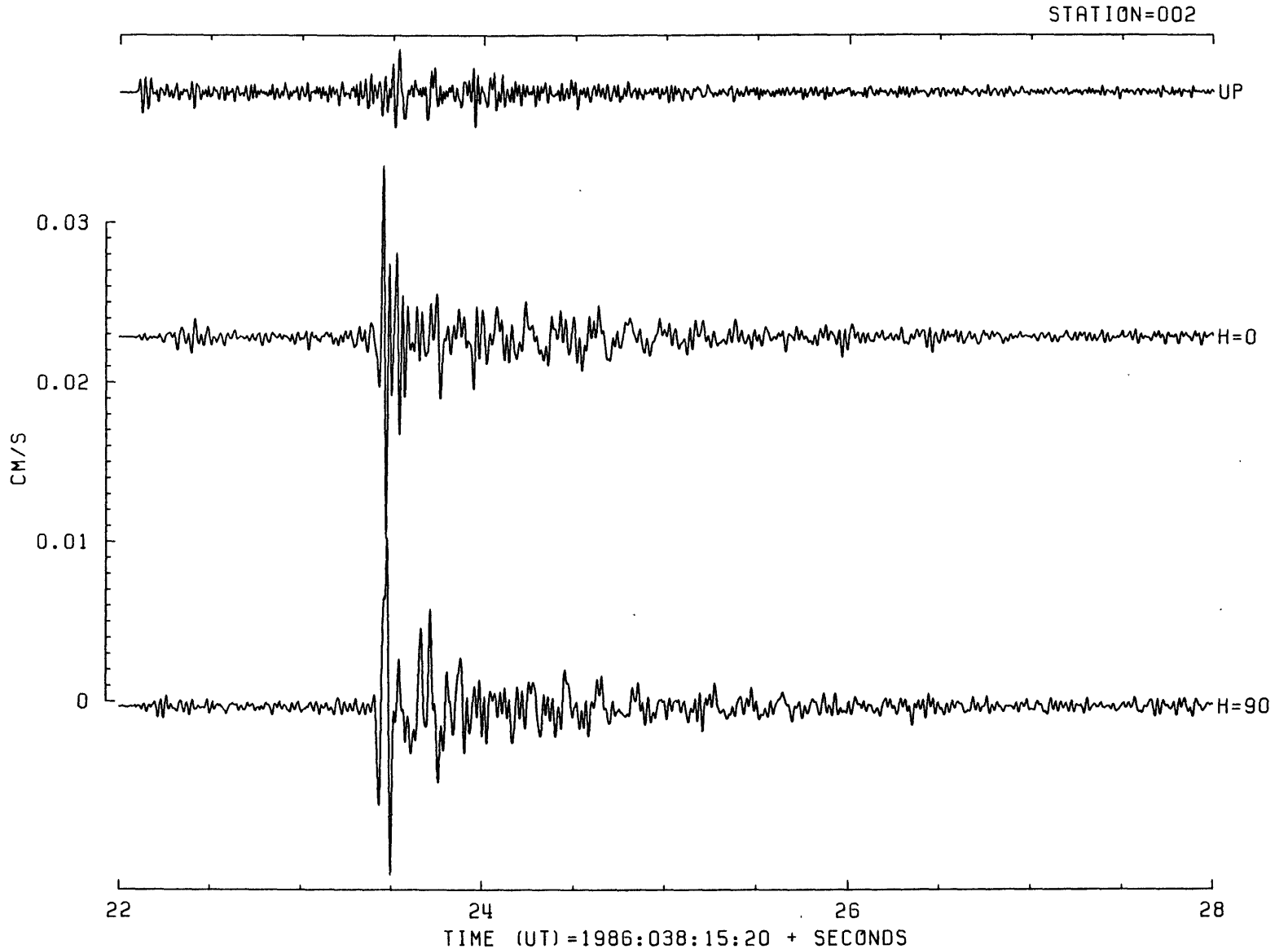

FIGURE A-26: Three component velocity recording of event 038:15:20 at station 002.

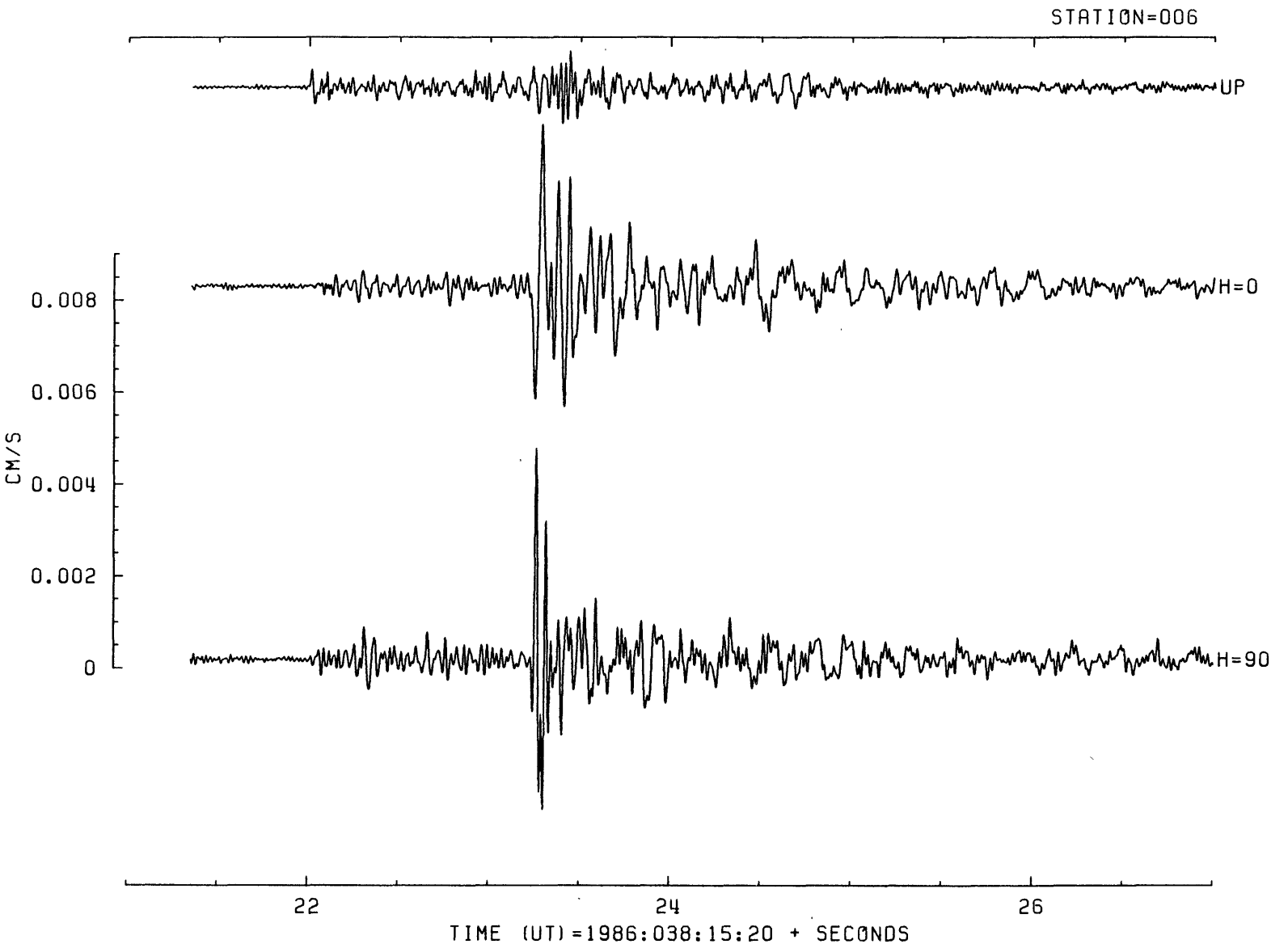

FIGURE A-27: Three component velocity recording of event 038:15:20 at station 006.

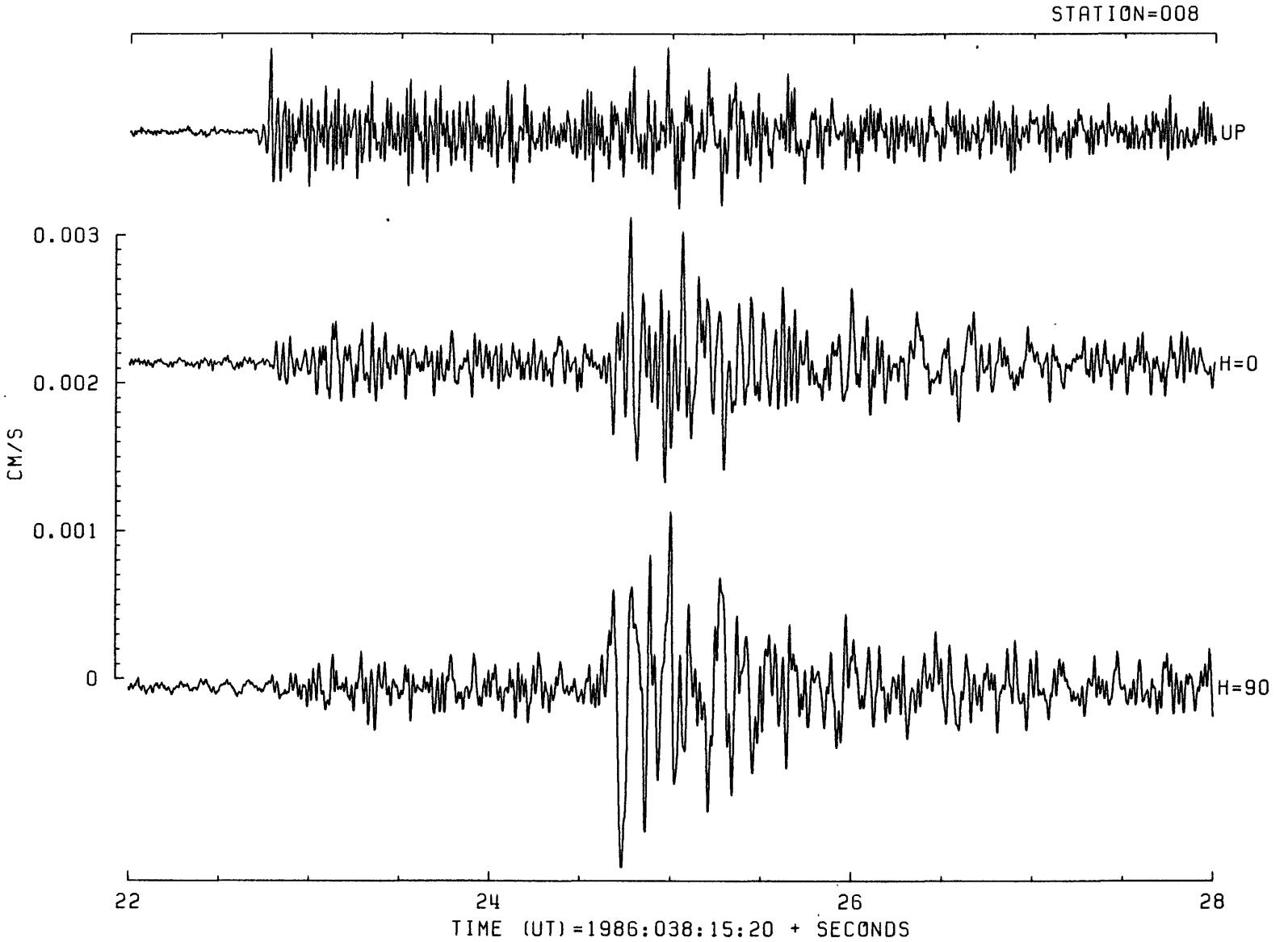

FIGURE A-28: Three component velocity recording of event 038:15:20 at station 008.

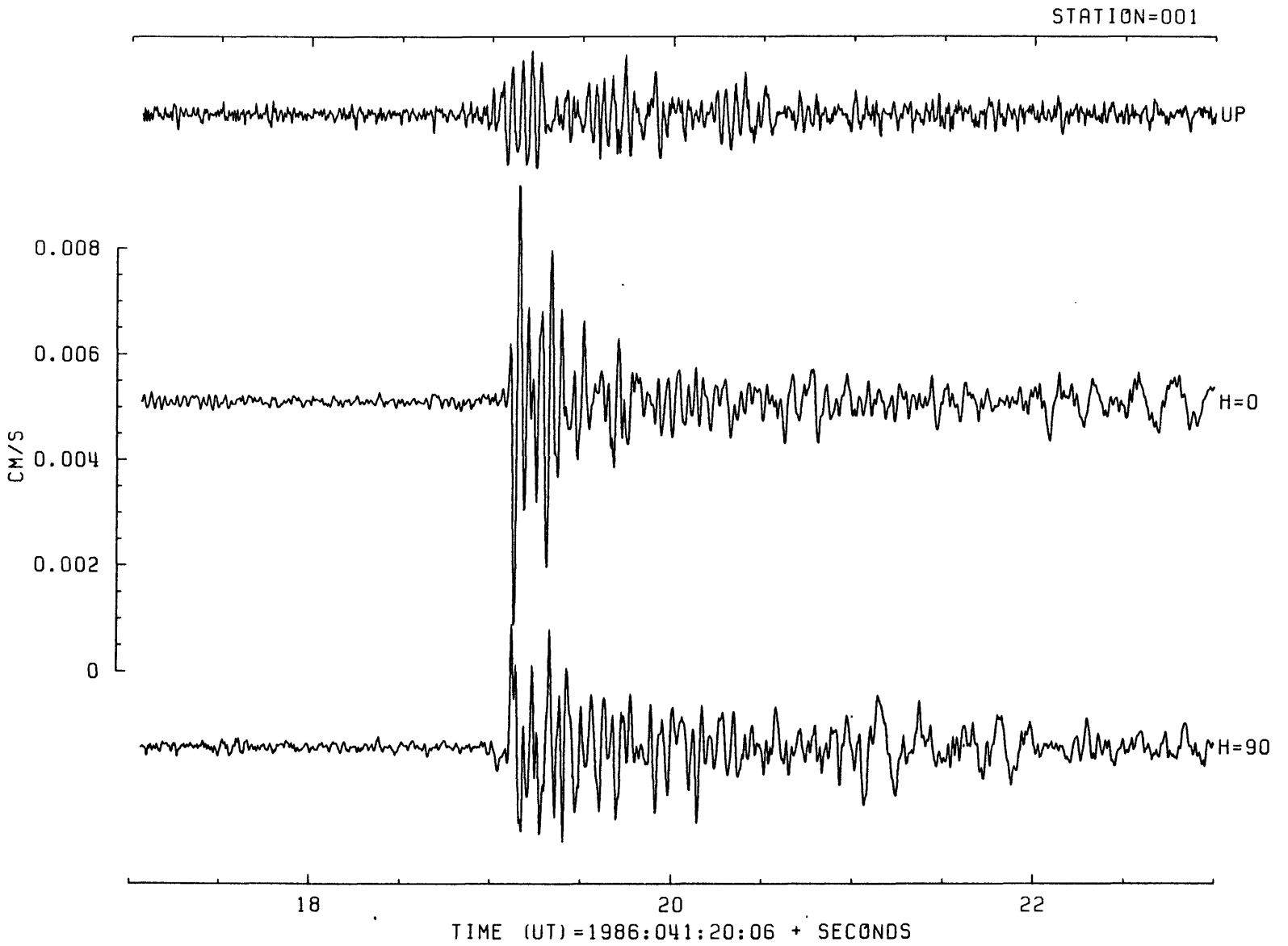

FIGURE A-29: Three component velocity recording of event 041:20:06 at station 001.

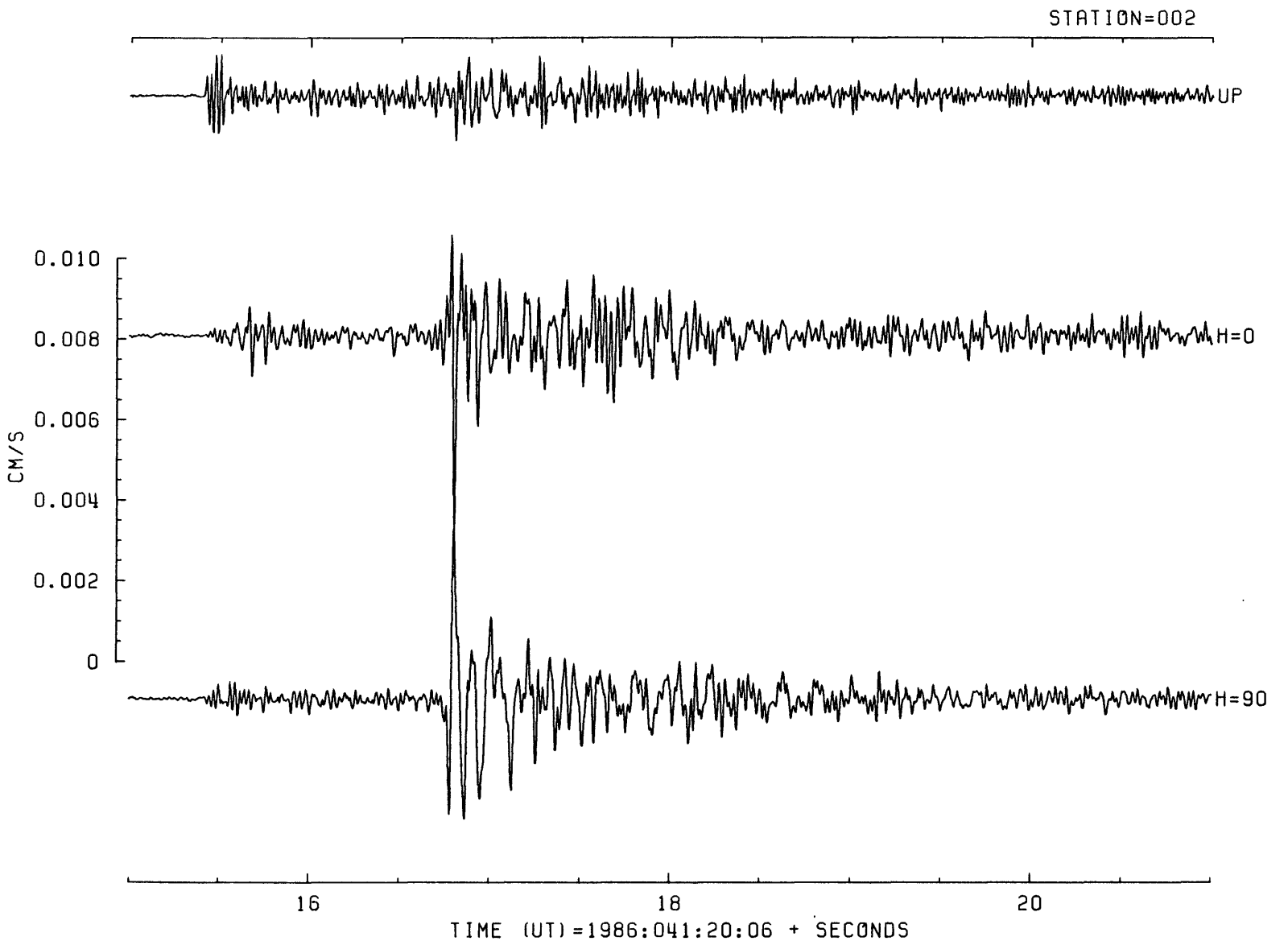

FIGURE A-30: Three component velocity recording of event 041:20:06 at station 002.

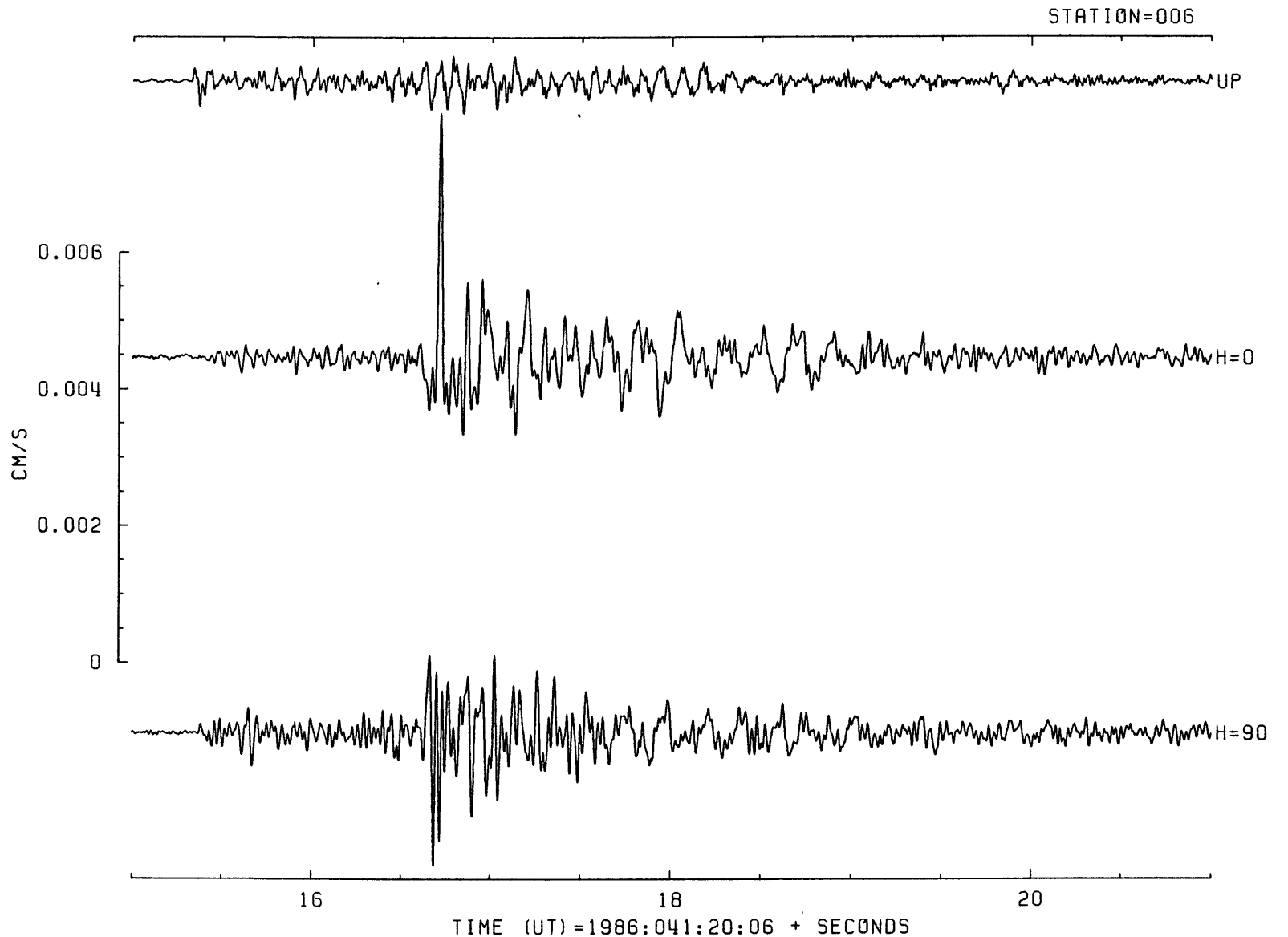

FIGURE A-31: Three component velocity recording of event 041:20:06 at station 006.

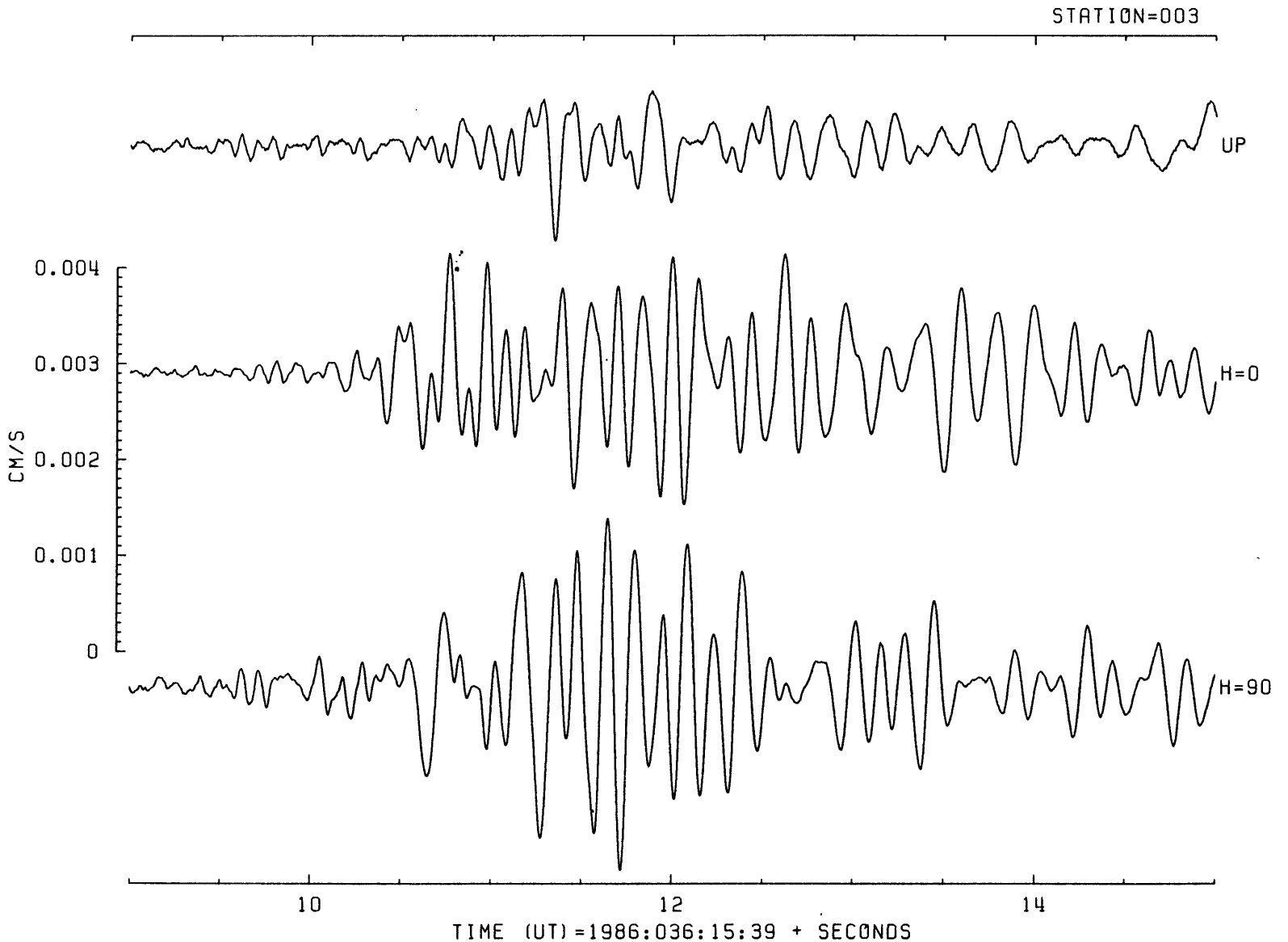

FIGURE A-32: Three component velocity recording of quarry blast 036:15:39 at station 003.

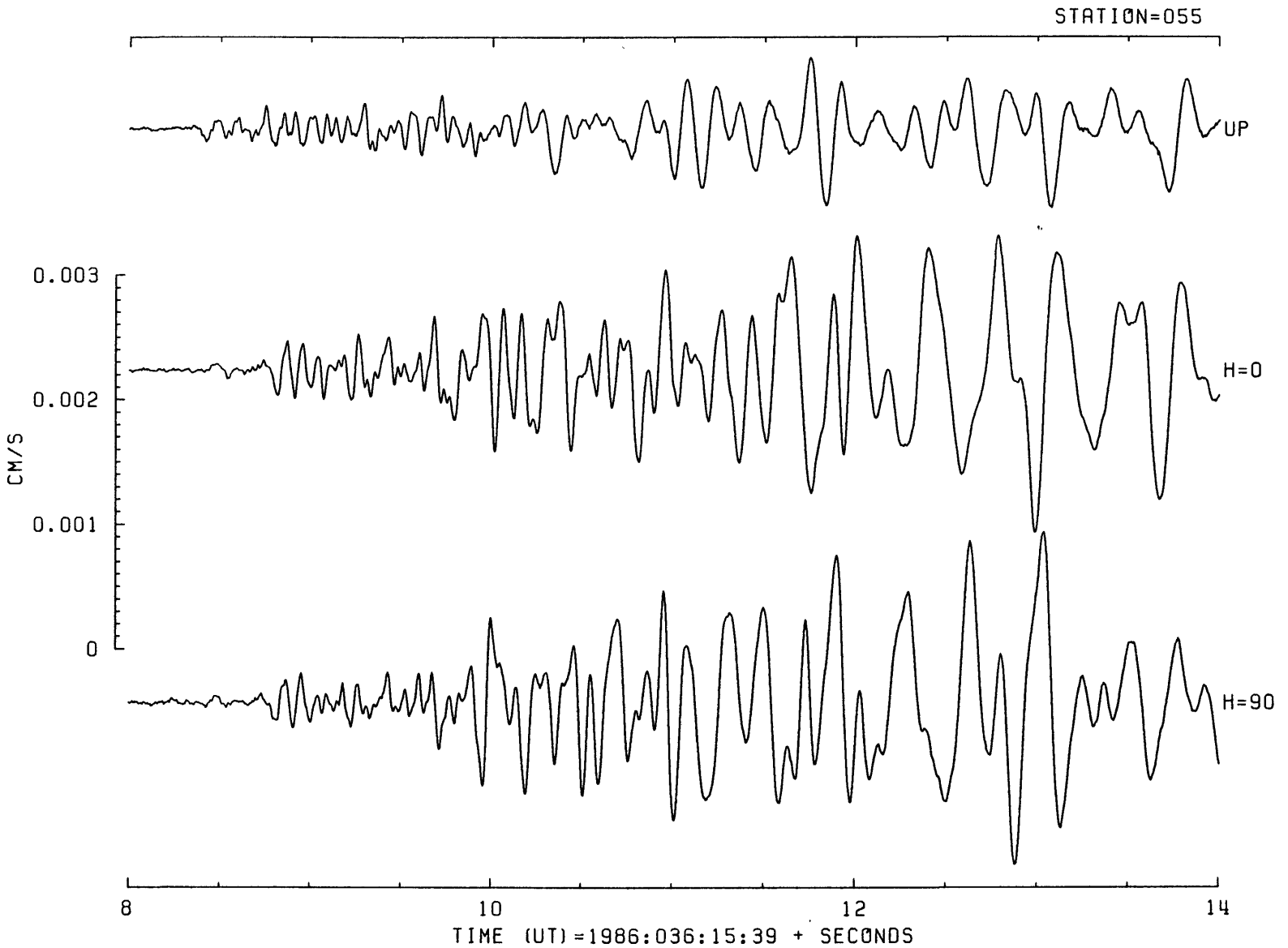

FIGURE A-33: Three component velocity recording of quarry blast 036:15:39 at station 055.

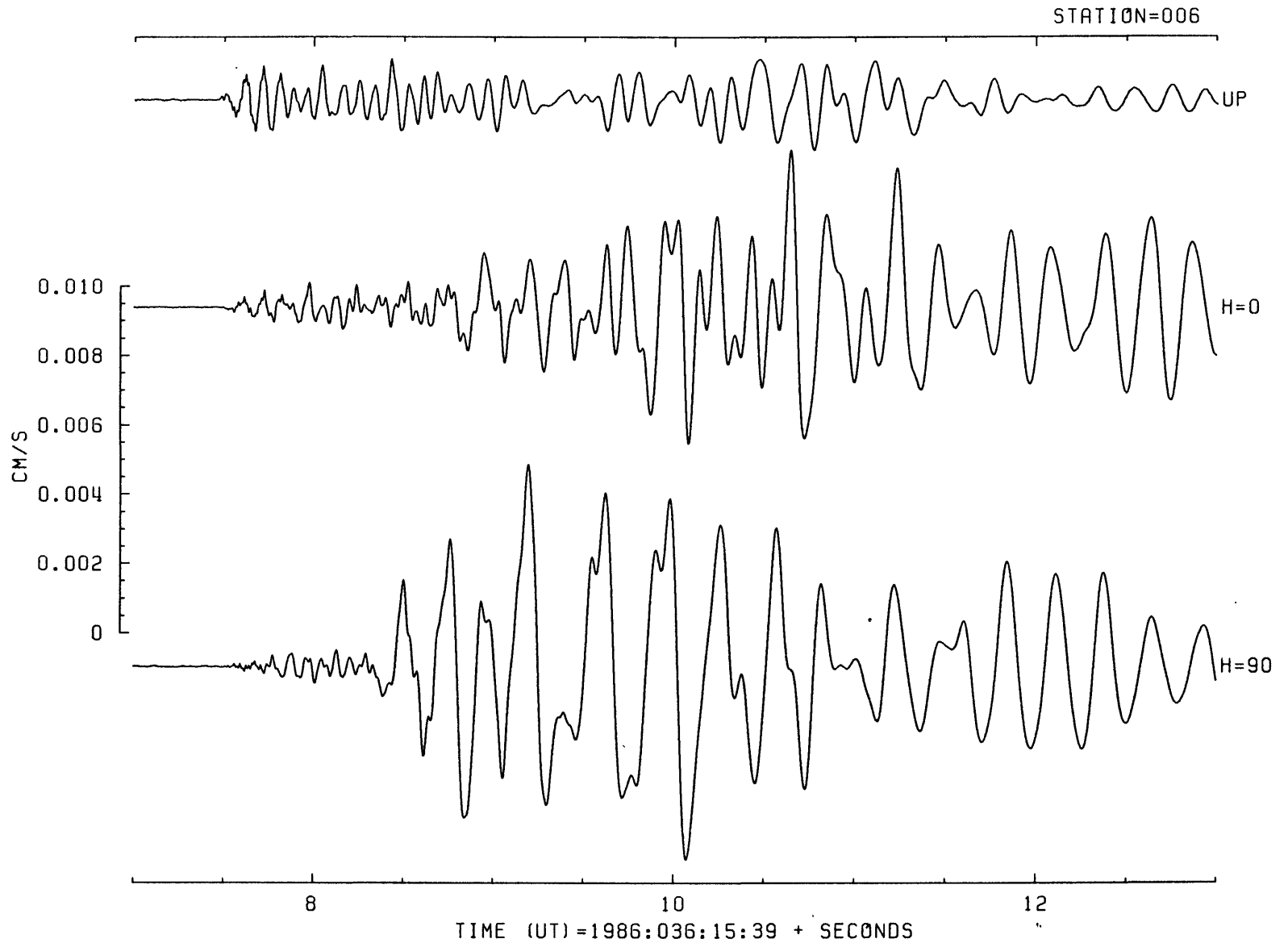

FIGURE A-34: Three component velocity recording of quarry blast 036:15:39 at station 006.

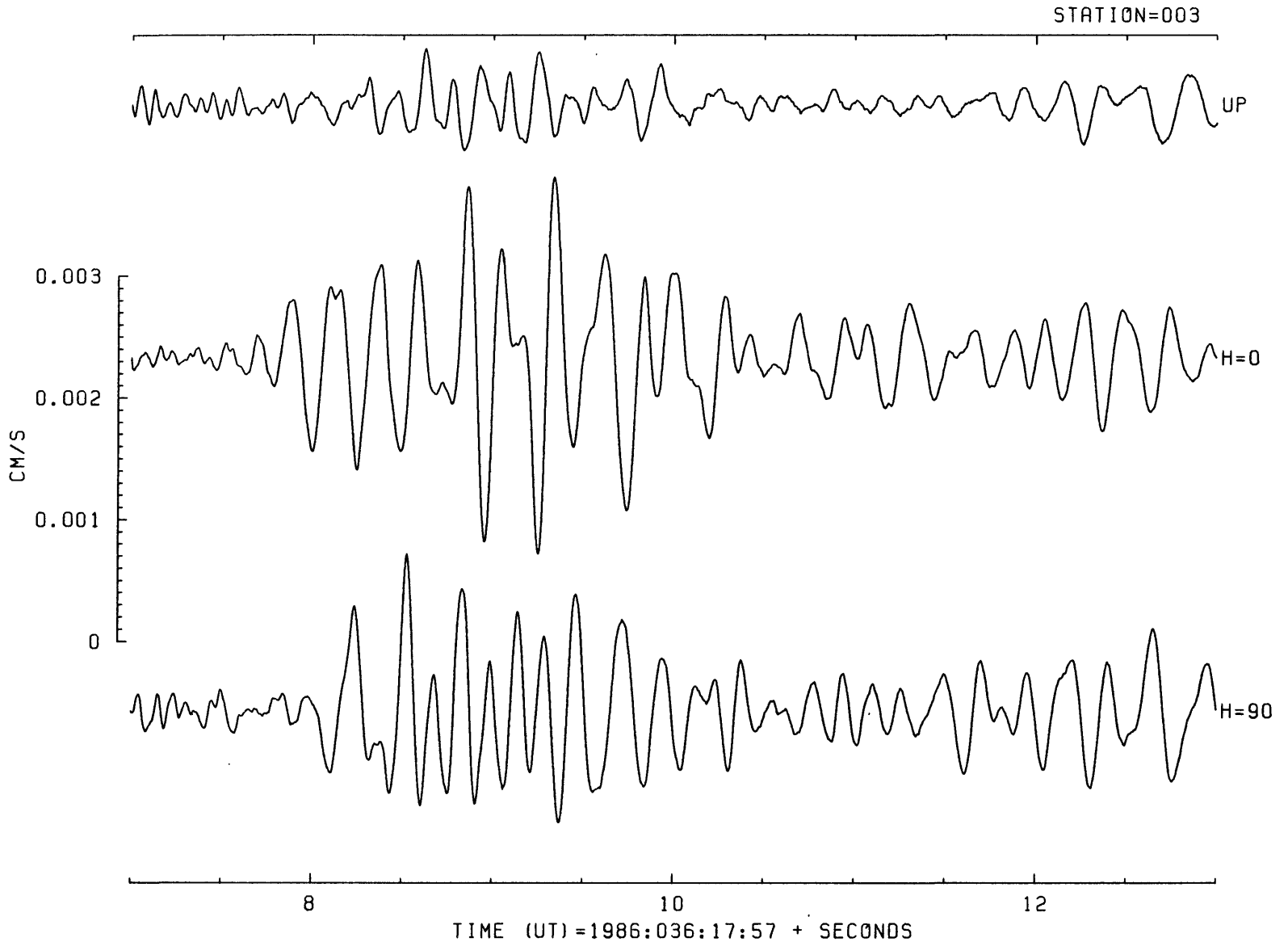

FIGURE A-35: Three component velocity recording of quarry blast 036:17:57 at station 003.

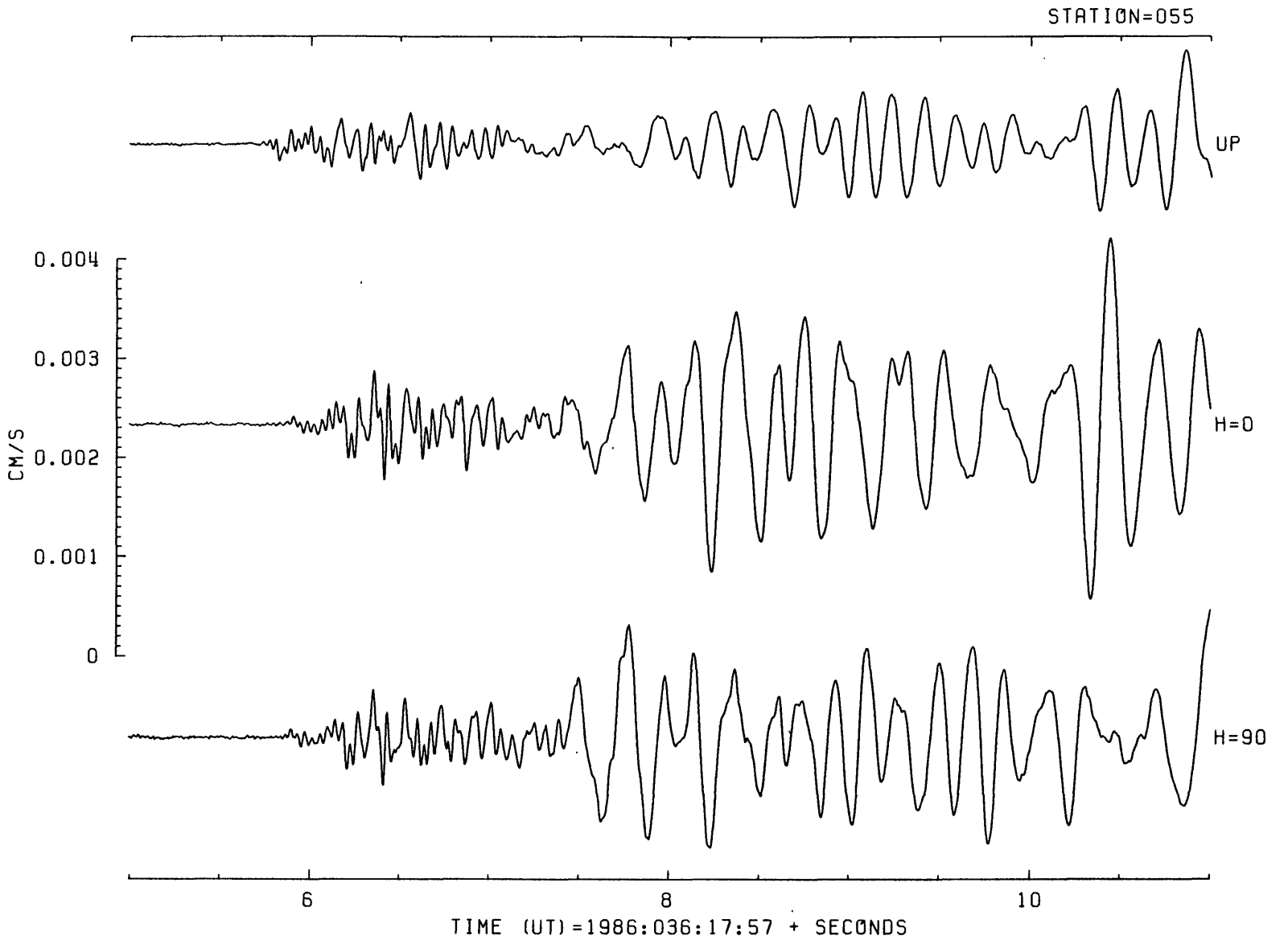

FIGURE A-36: Three component velocity recording of quarry blast 036:17:57 at station 055.

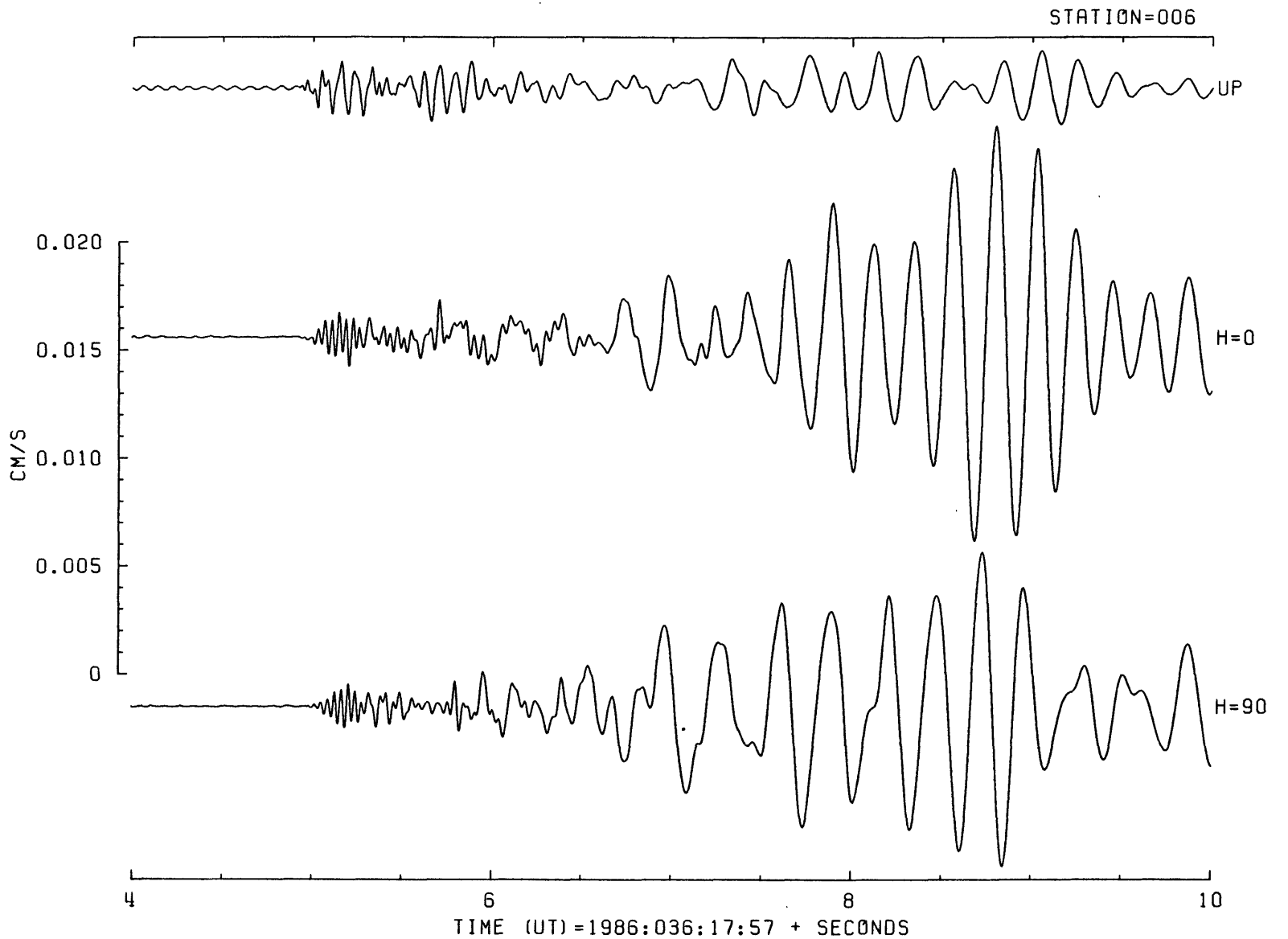

FIGURE A-37: Three component velocity recording of quarry blast 036:17:57 at station 006.

APPENDIX B

FOURIER AMPLITUDE SPECTRA FOR TIME HISTORIES SHOWN IN APPENDIX A.

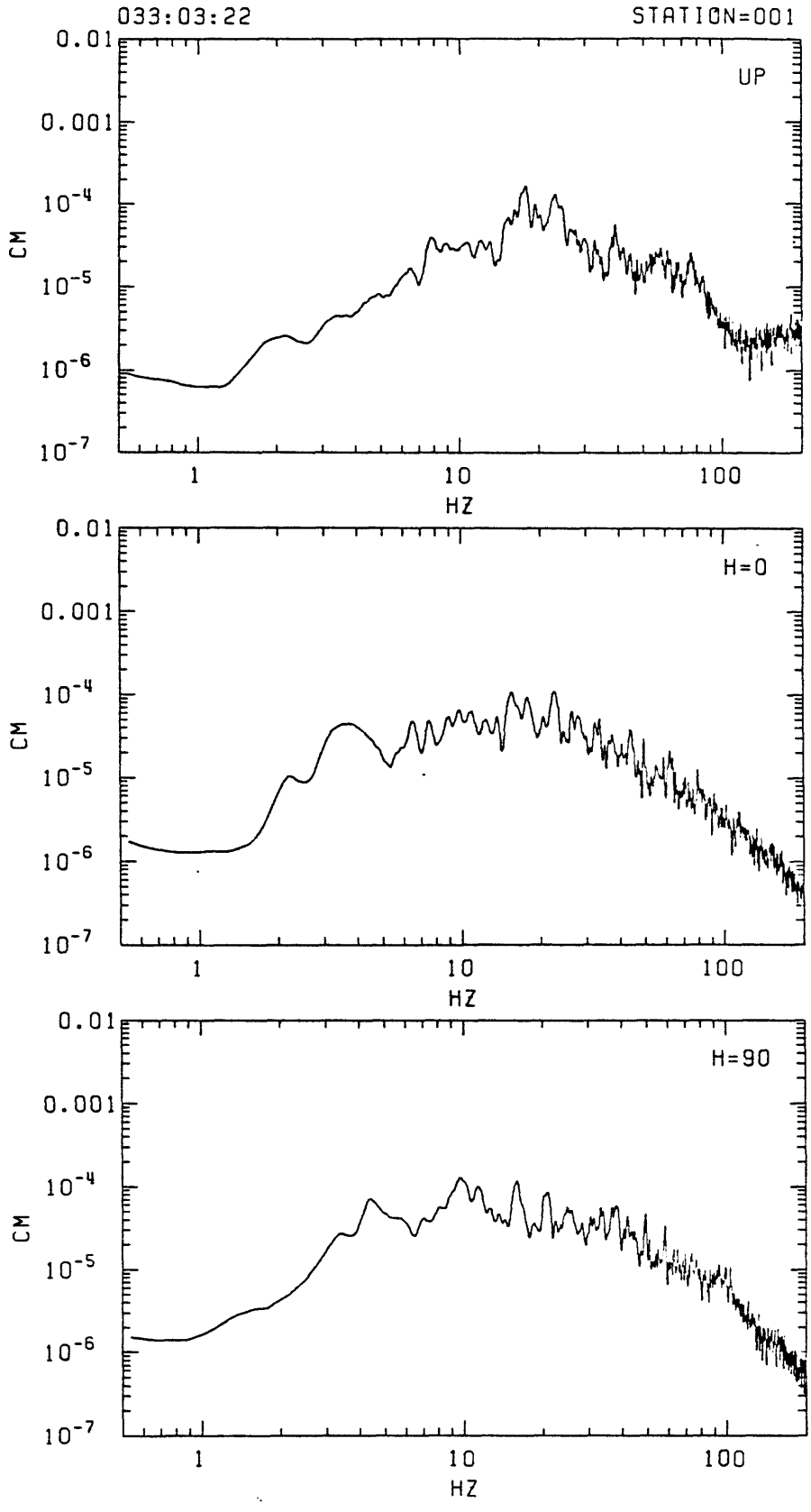

FIGURE B-1: Fourier amplitude spectrum for 10.24 seconds of 3 component recordings of event 033:03:22 at station 001.

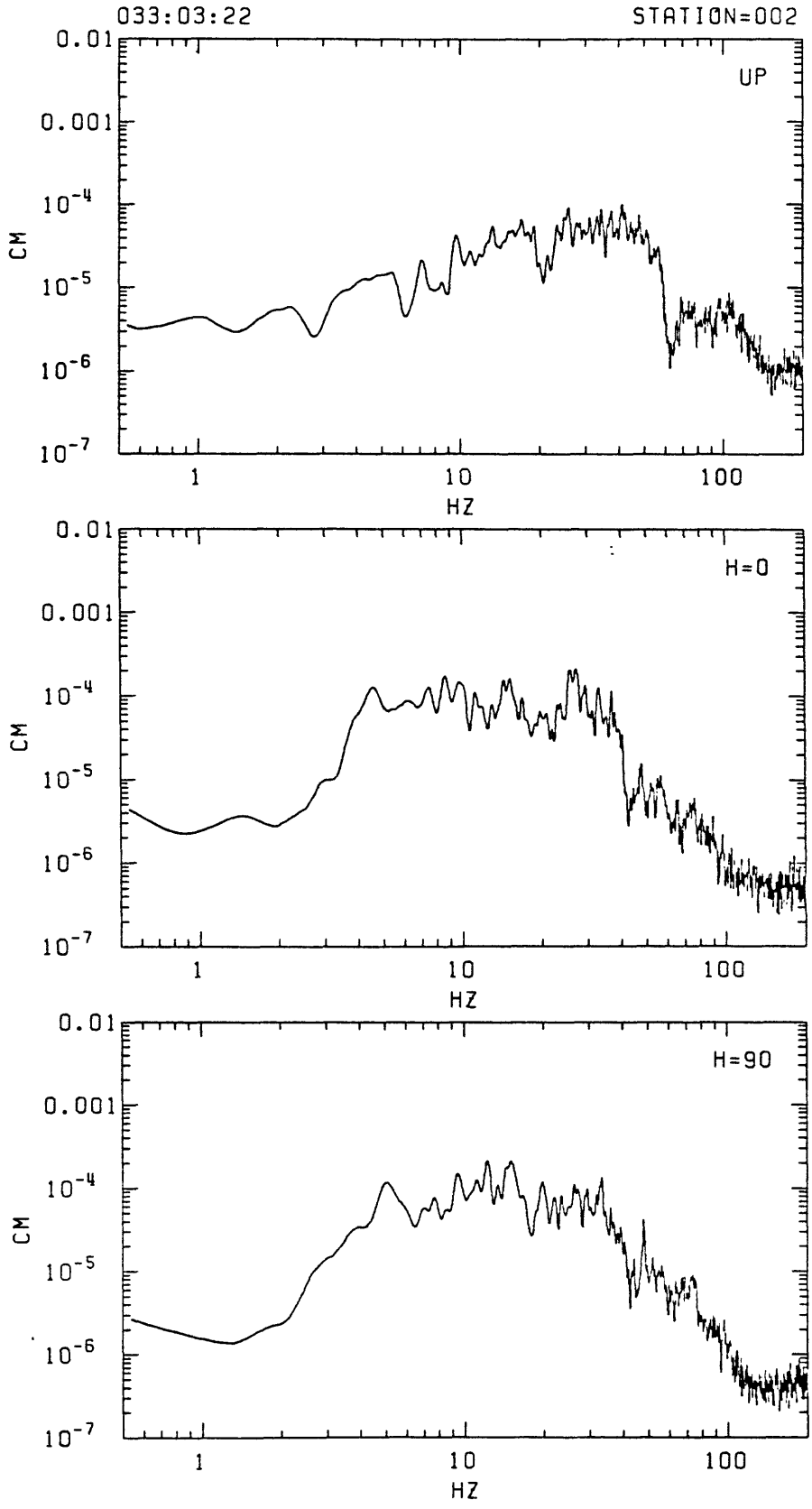

FIGURE B-2: Fourier amplitude spectrum for 10.24 seconds of 3 component recordings of event 033:03:22 at station 002.

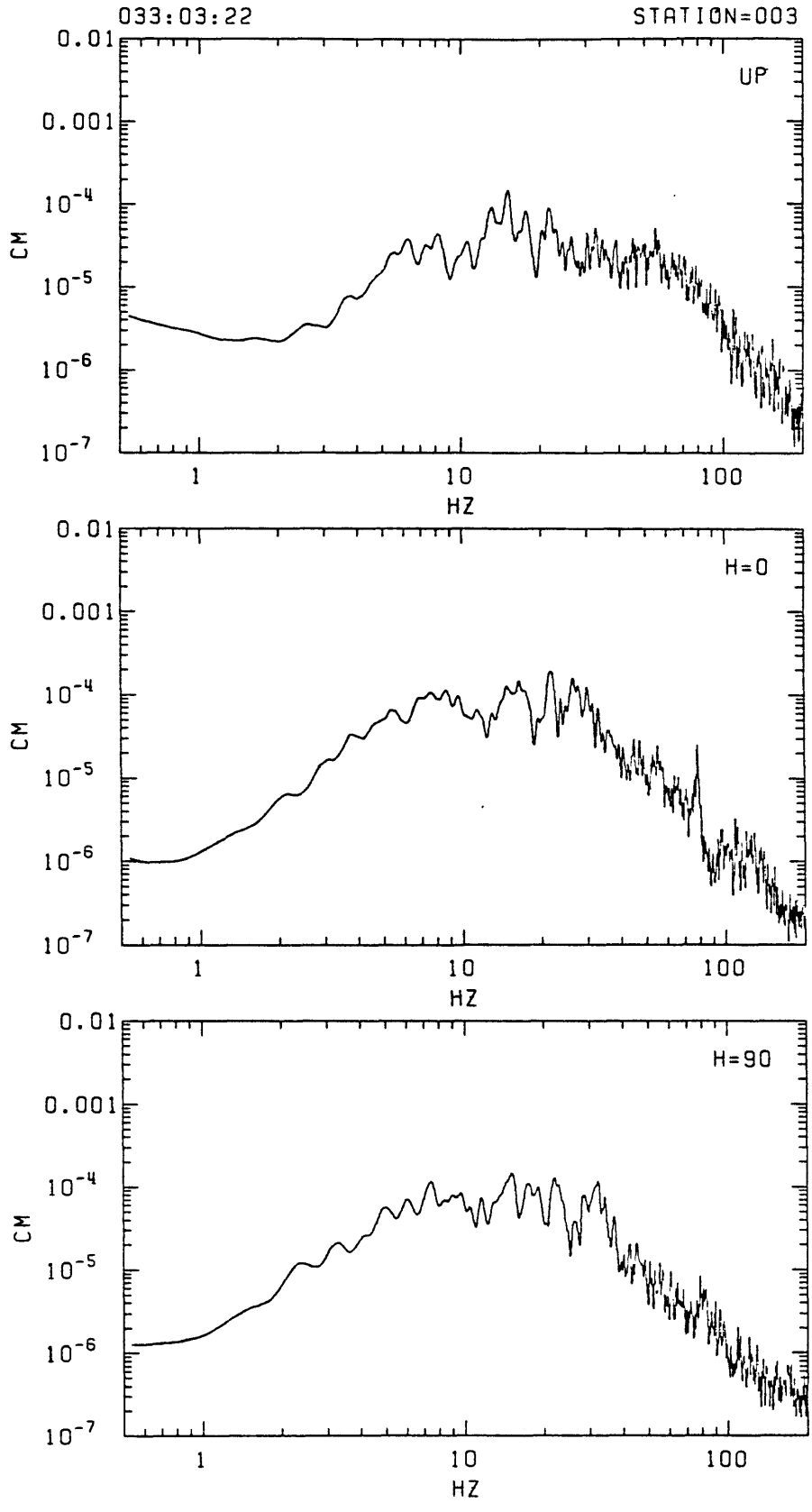

FIGURE B-3: Fourier amplitude spectrum for 10.24 seconds of 3 component recordings of event 033:03:22 at station 003.

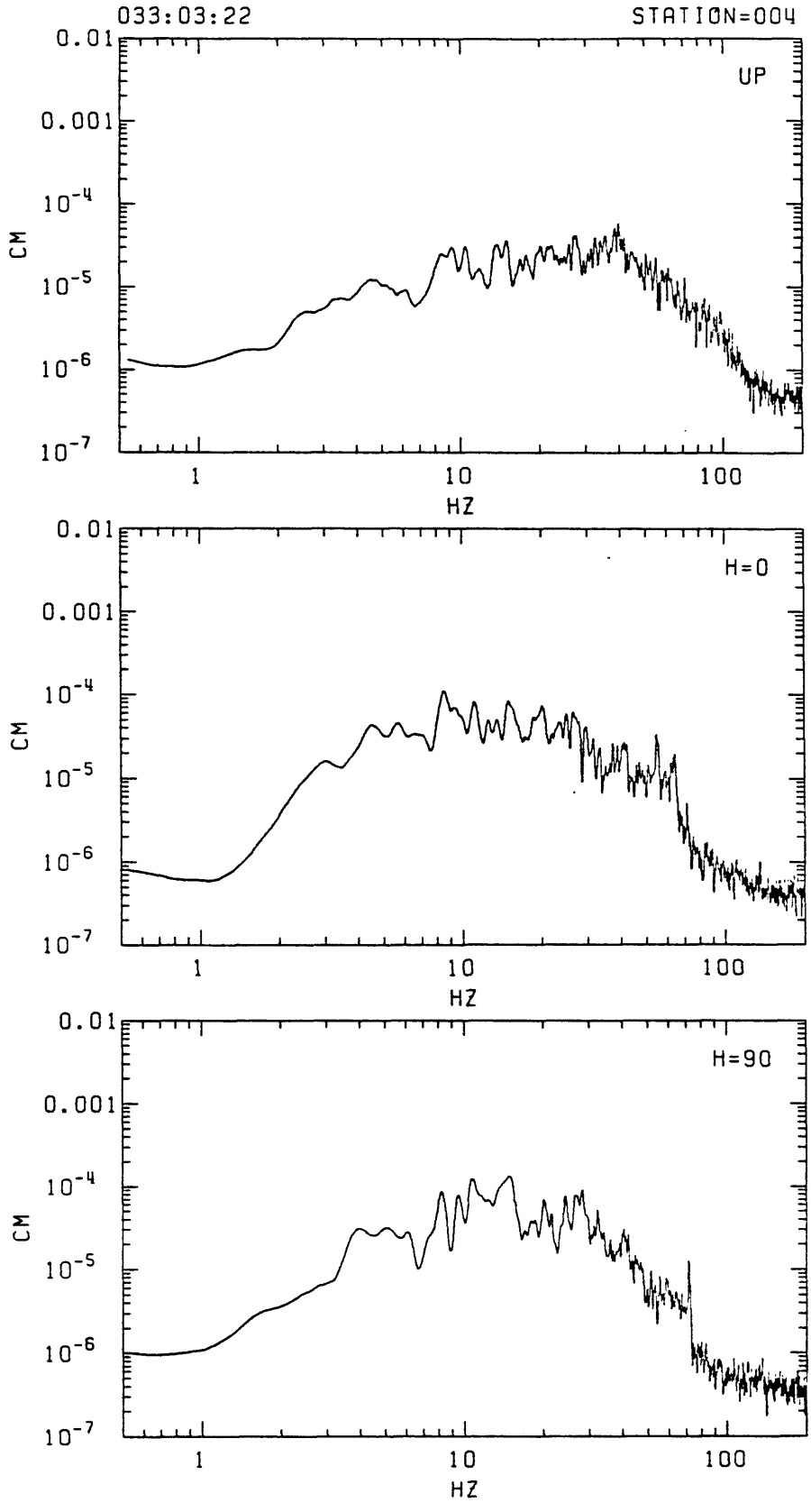

FIGURE B-4: Fourier amplitude spectrum for 10.24 seconds of 3 component recordings of event 033:03:22 at station 004.

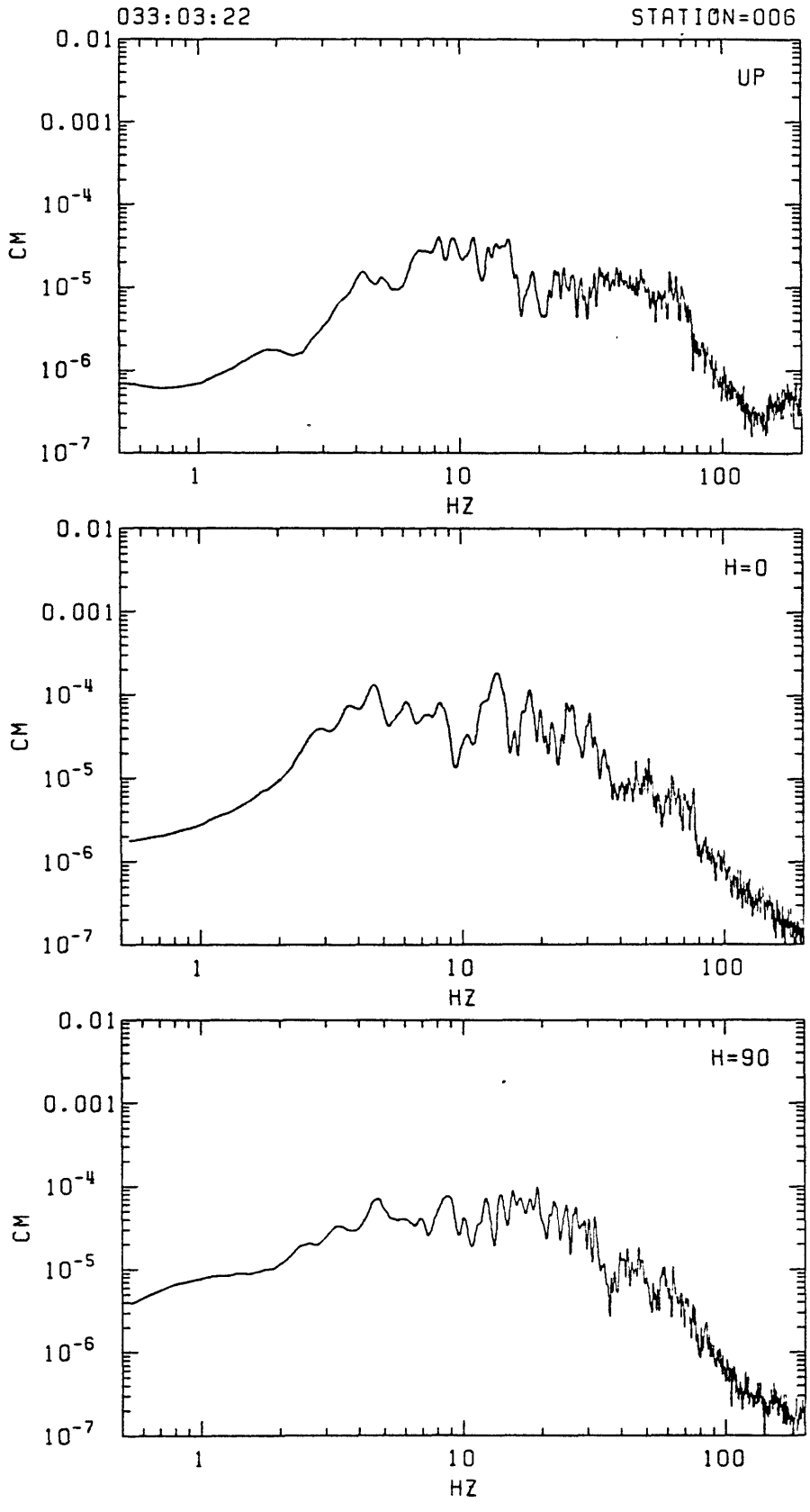

FIGURE B-5: Fourier amplitude spectrum for 10.24 seconds of 3 component recordings of event 033:03:22 at station 006.

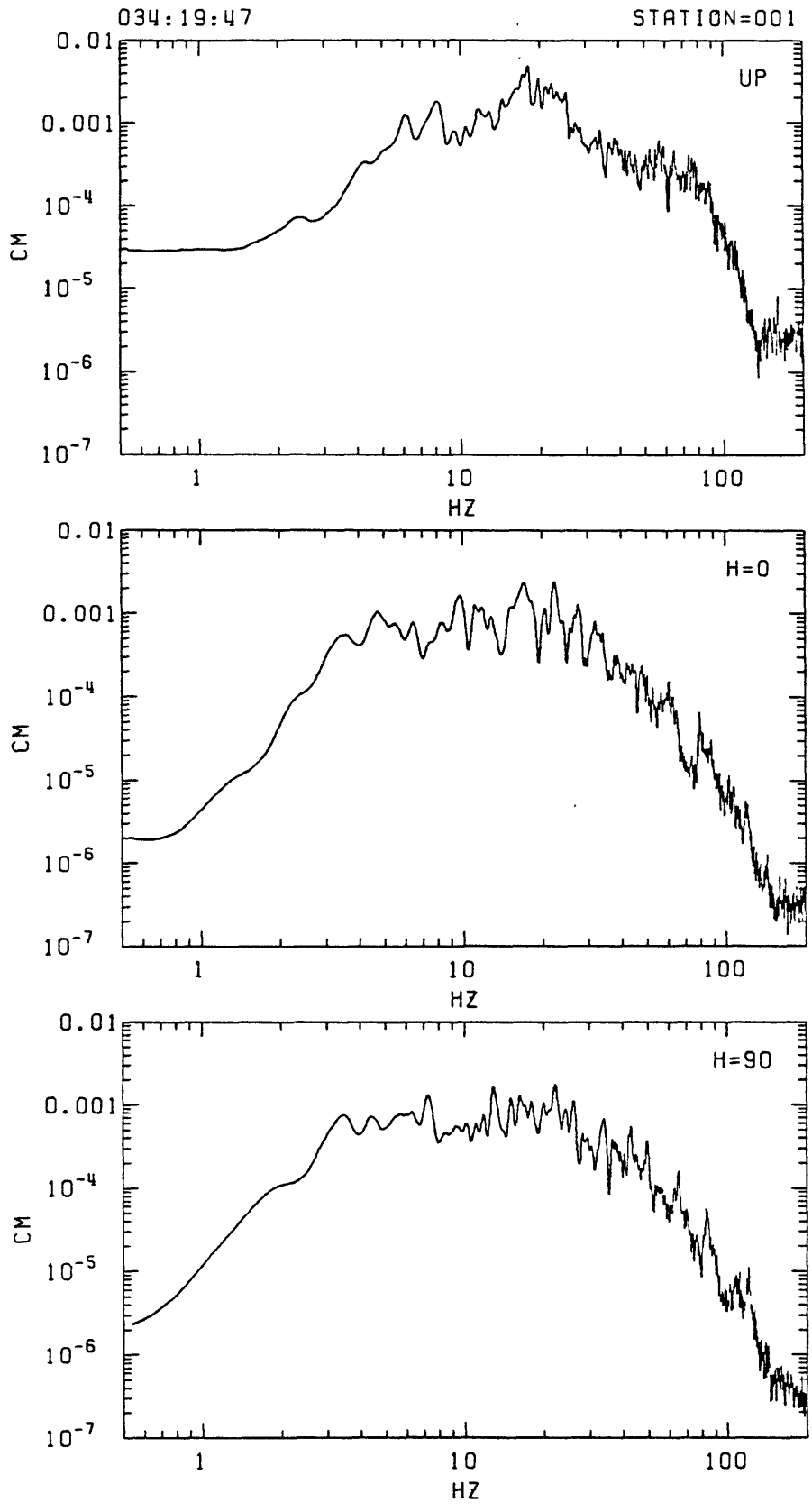

FIGURE B-6: Fourier amplitude spectrum for 10.24 seconds of 3 component recordings of event 034:19:47 at station 001.

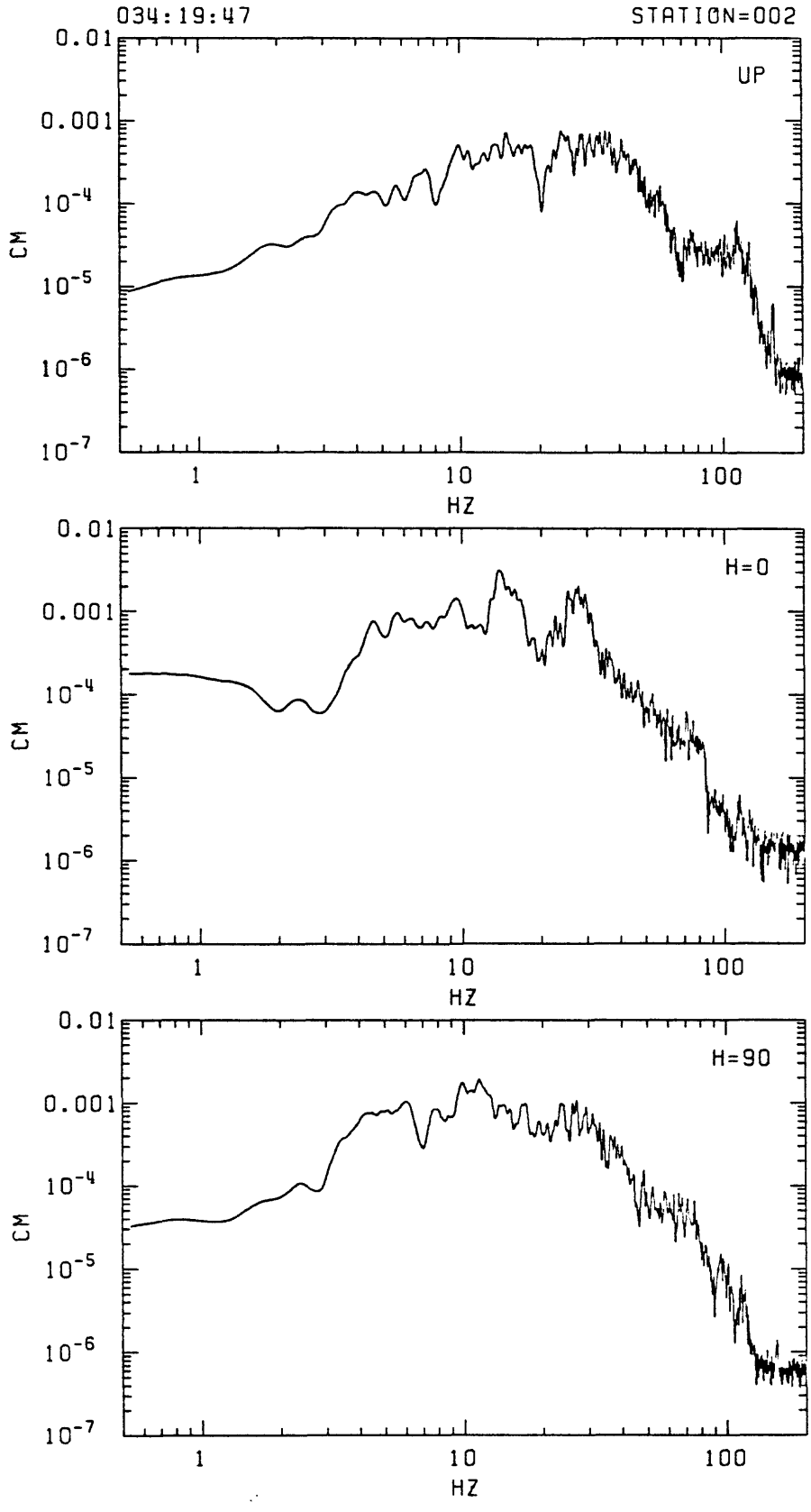

FIGURE B-7: Fourier amplitude spectrum for 10.24 seconds of 3 component recordings of event 034:19:47 at station 002.

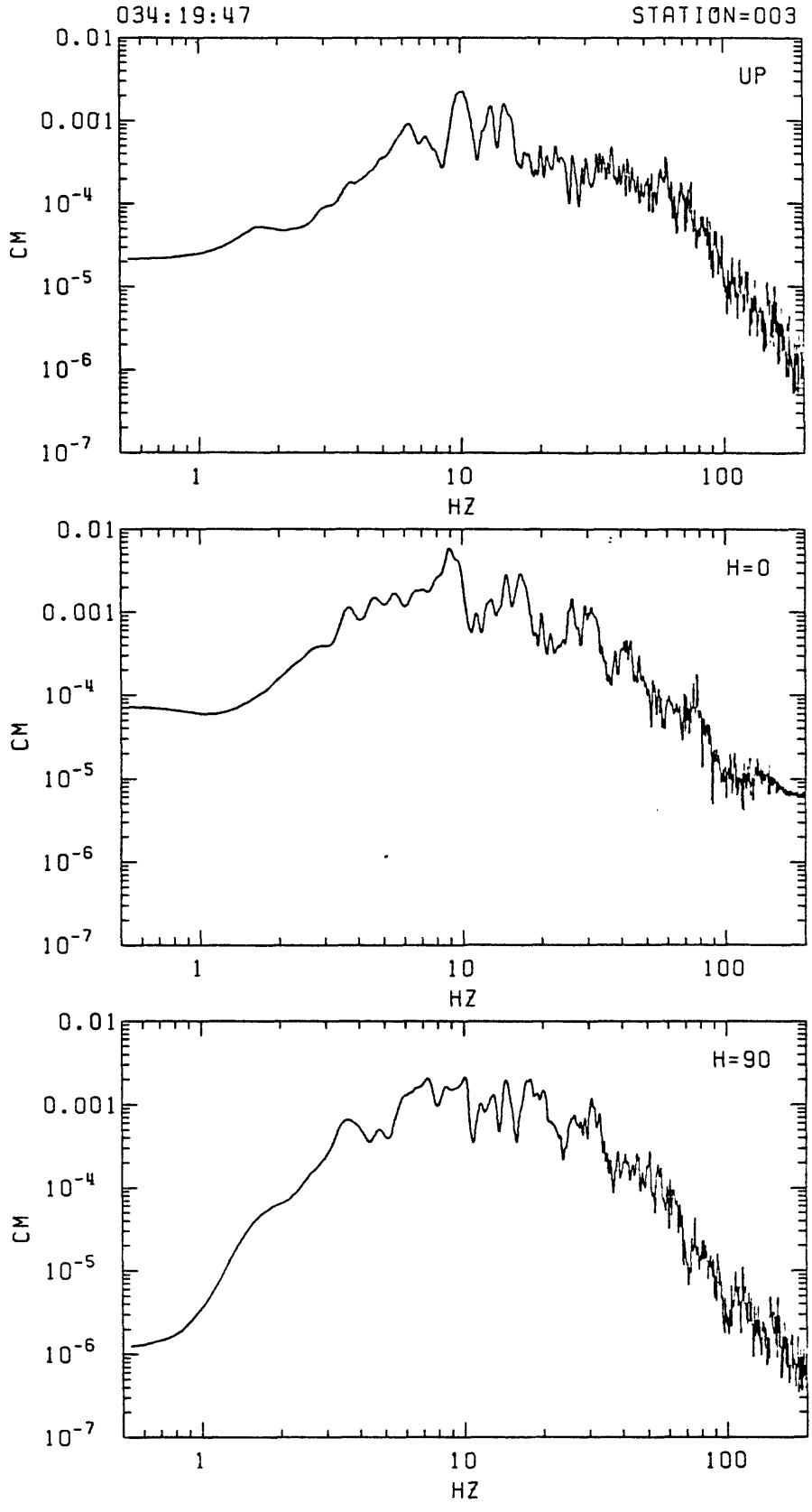

FIGURE B-8: Fourier amplitude spectrum for 10.24 seconds of 3 component recordings of event 034:19:47 at station 003.

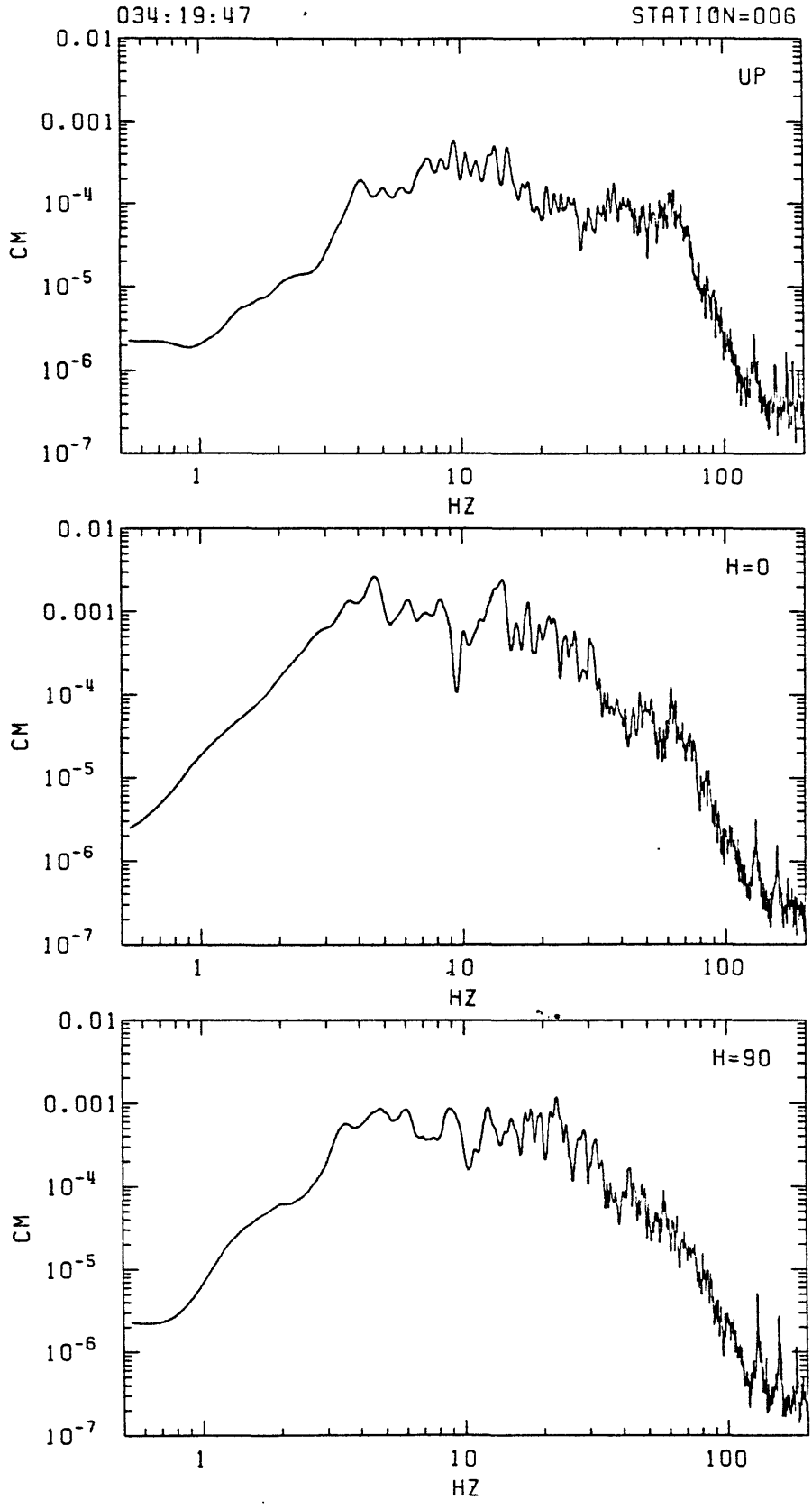

FIGURE B-9: Fourier amplitude spectrum for 10.24 seconds of 3 component recordings of event 034:19:47 at station 006.

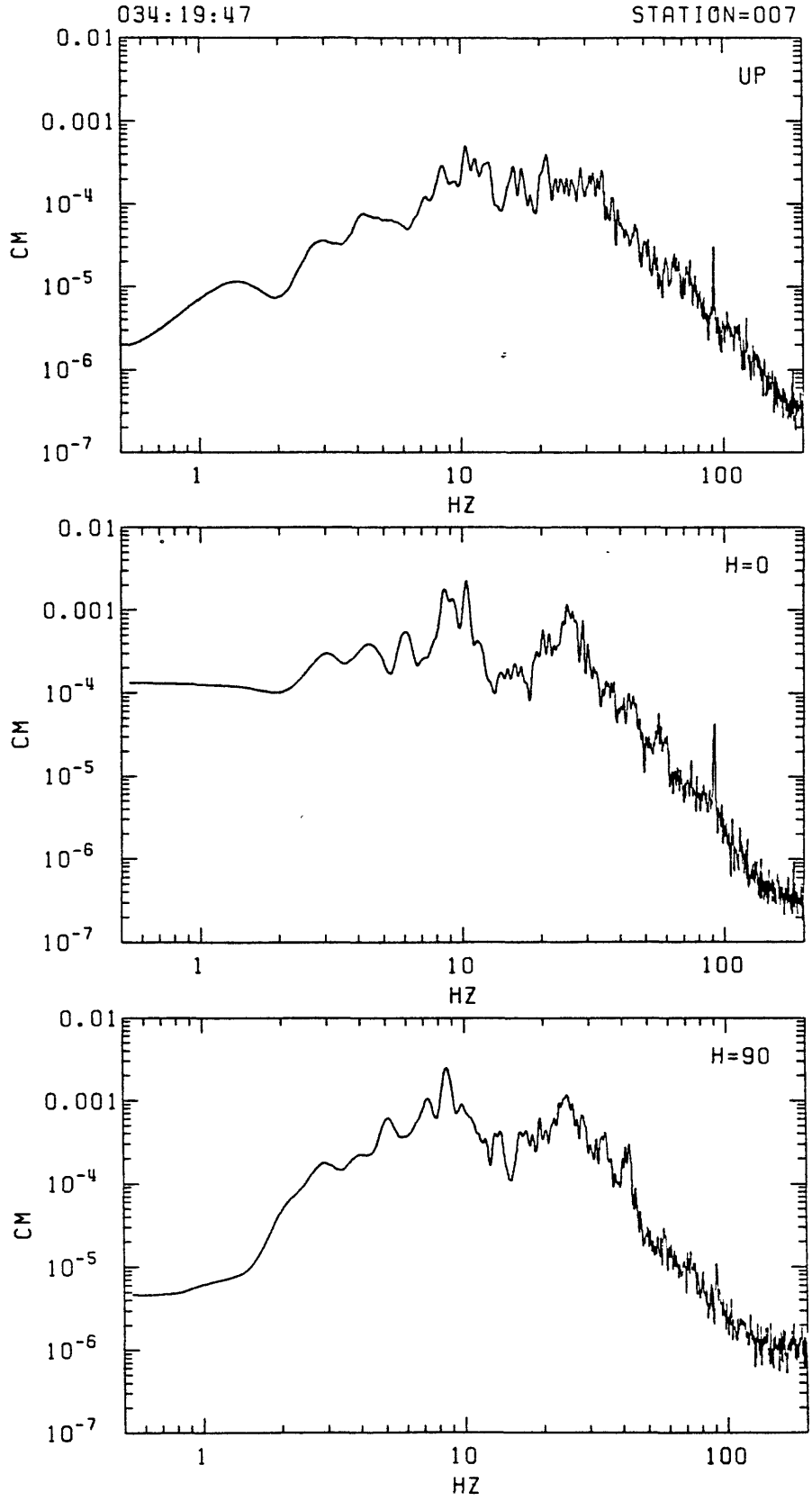

FIGURE B-10: Fourier amplitude spectrum for 10.24 seconds of 3 component recordings of event 034:19:47 at station 007.

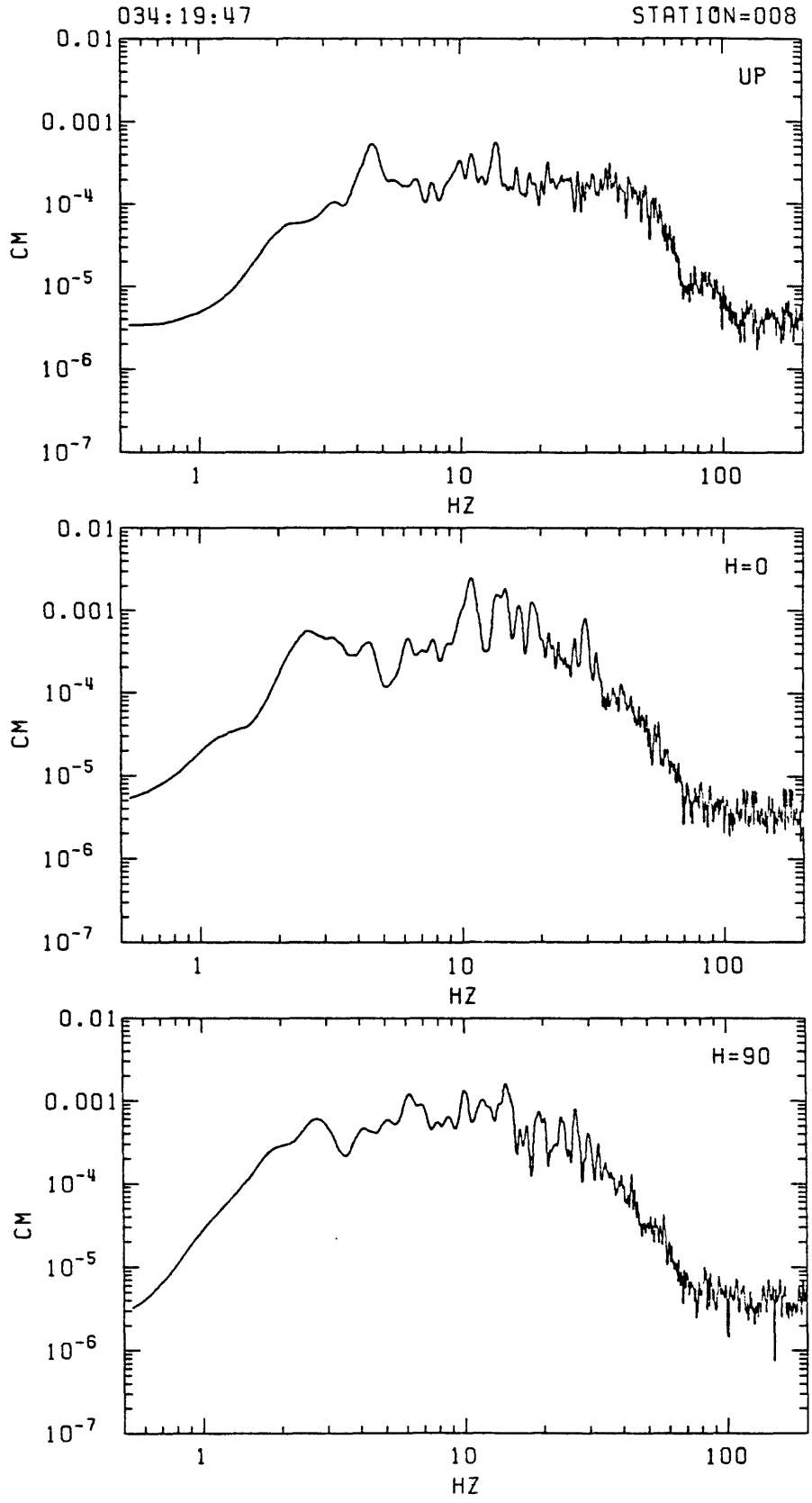

FIGURE B-11: Fourier amplitude spectrum for 10.24 seconds of 3 component recordings of event 034:19:47 at station 008.

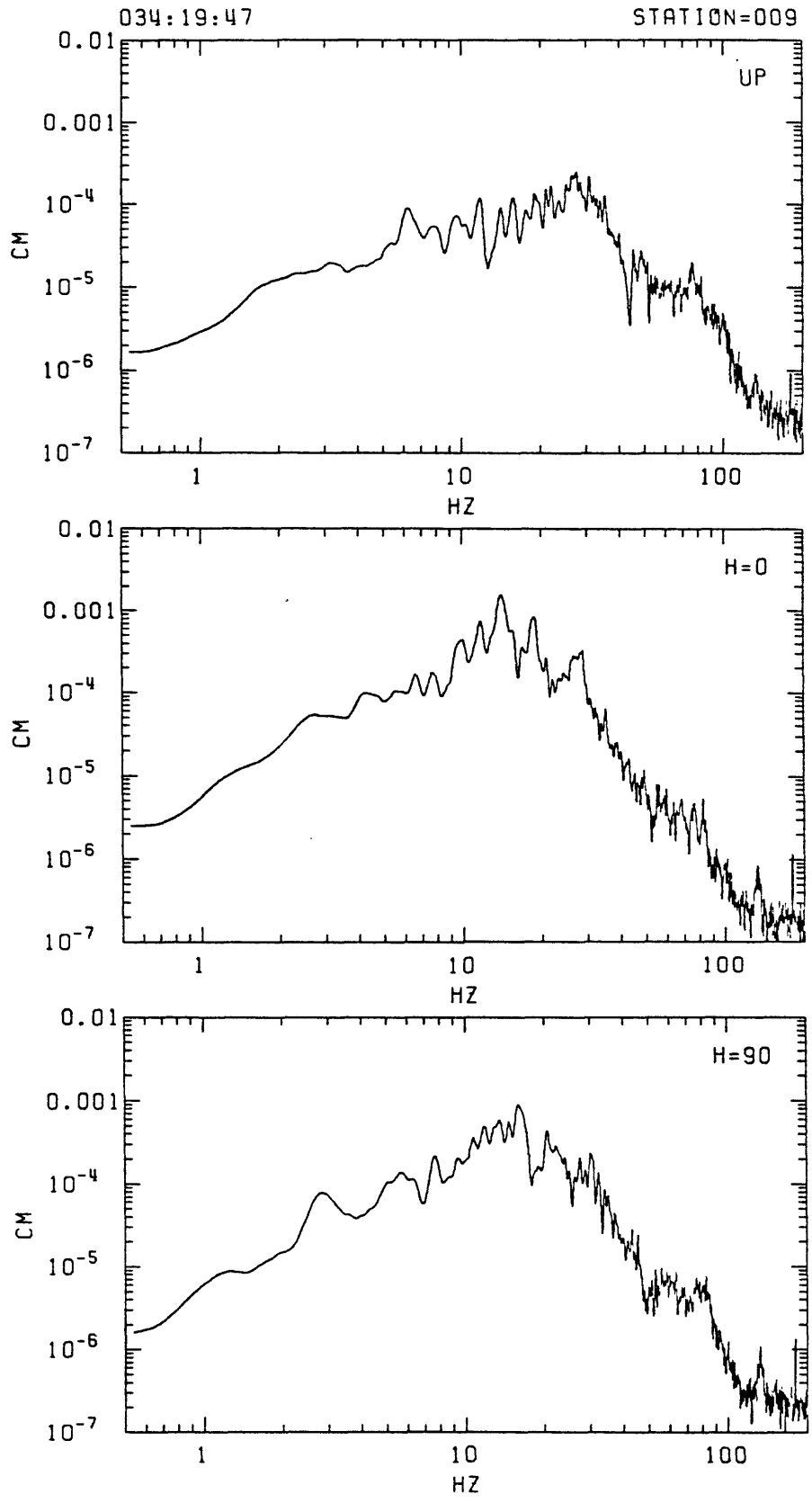

FIGURE B-12: Fourier amplitude spectrum for 10.24 seconds of 3 component recordings of event 034:19:47 at station 009.

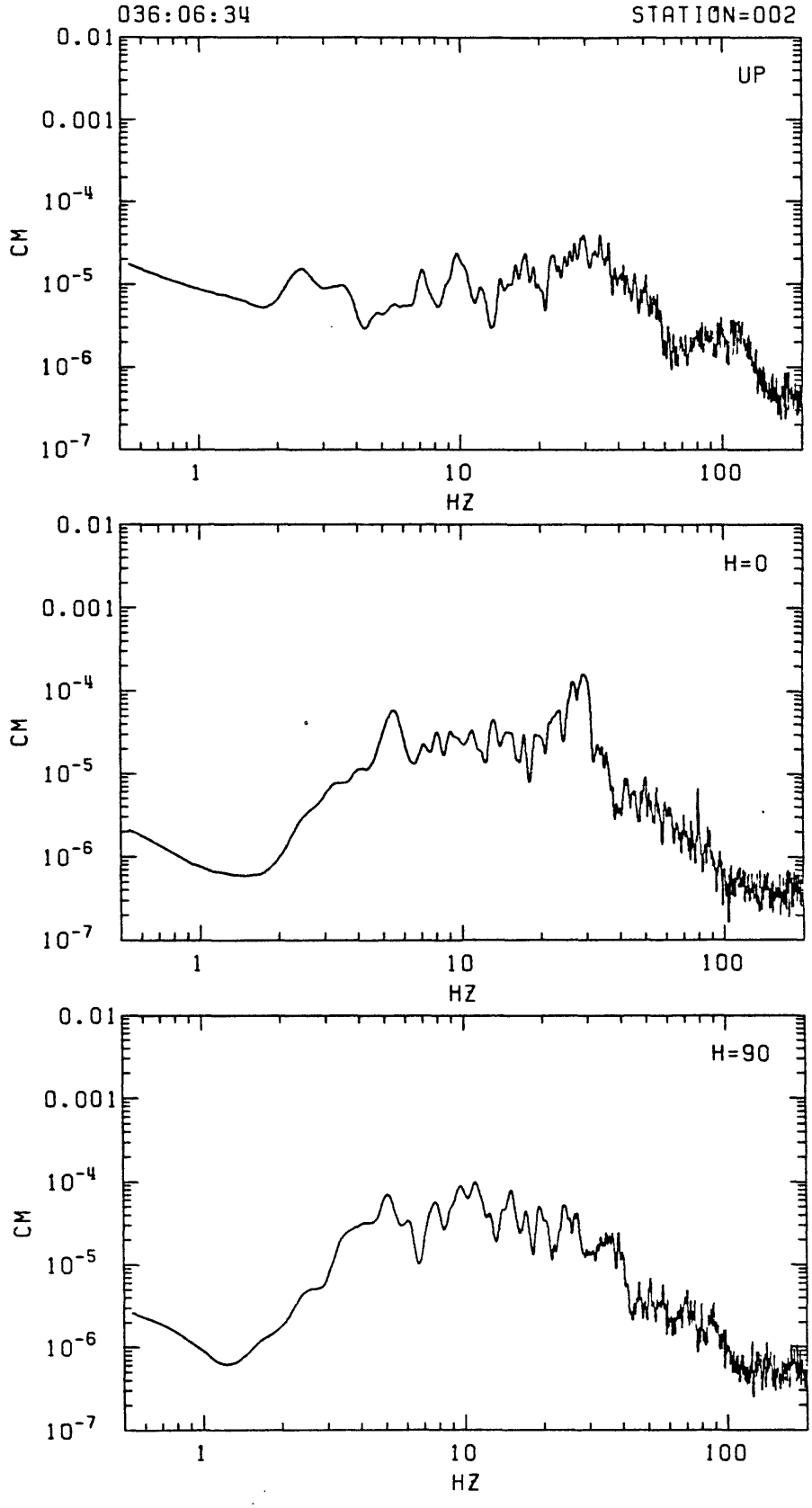

FIGURE B-13: Fourier amplitude spectrum for 10.24 seconds of 3 component recordings of event 036:06:34 at station 002.

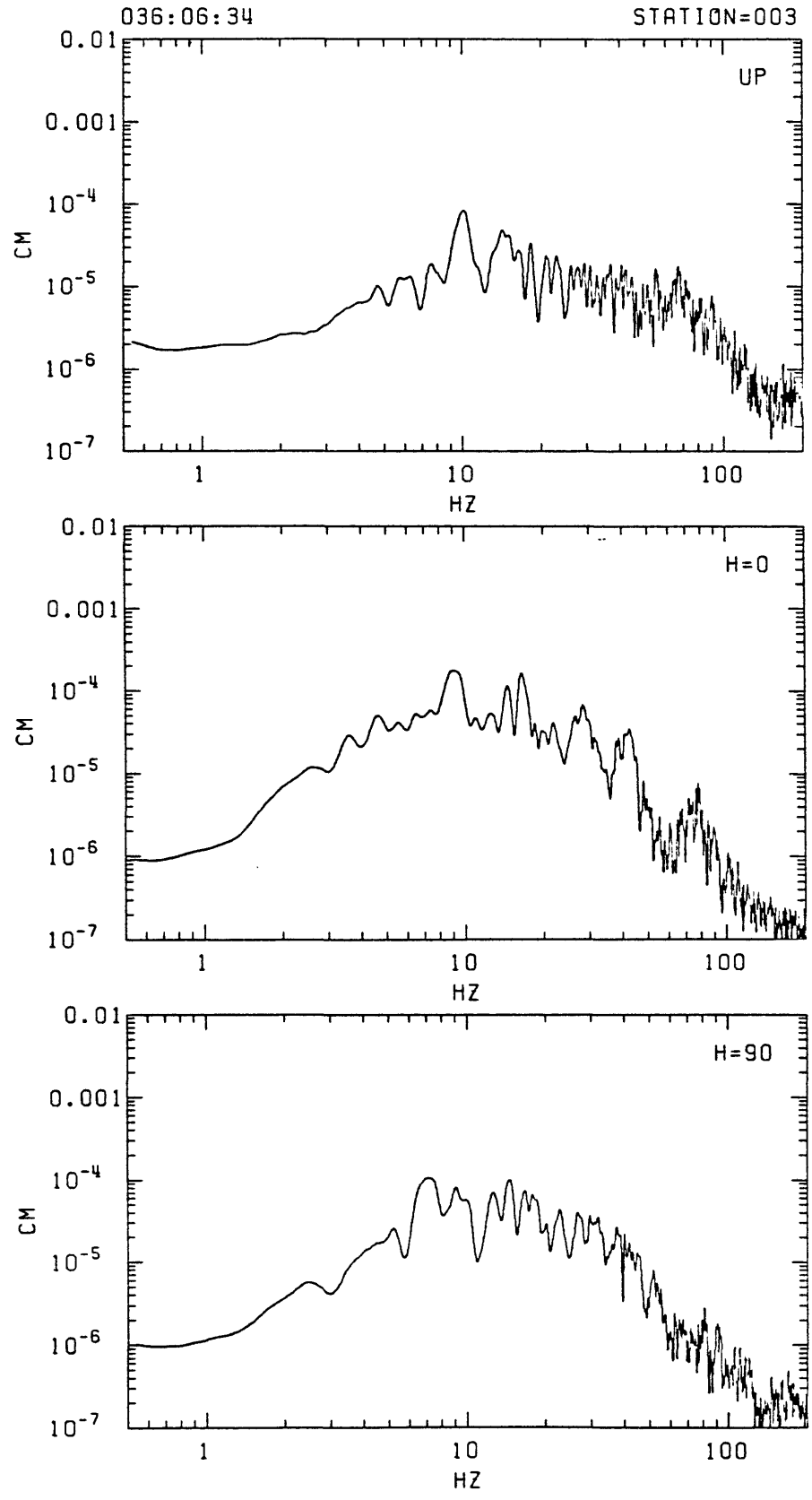

FIGURE B-14: Fourier amplitude spectrum for 10.24 seconds of 3 component recordings of event 036:06:34 at station 003.

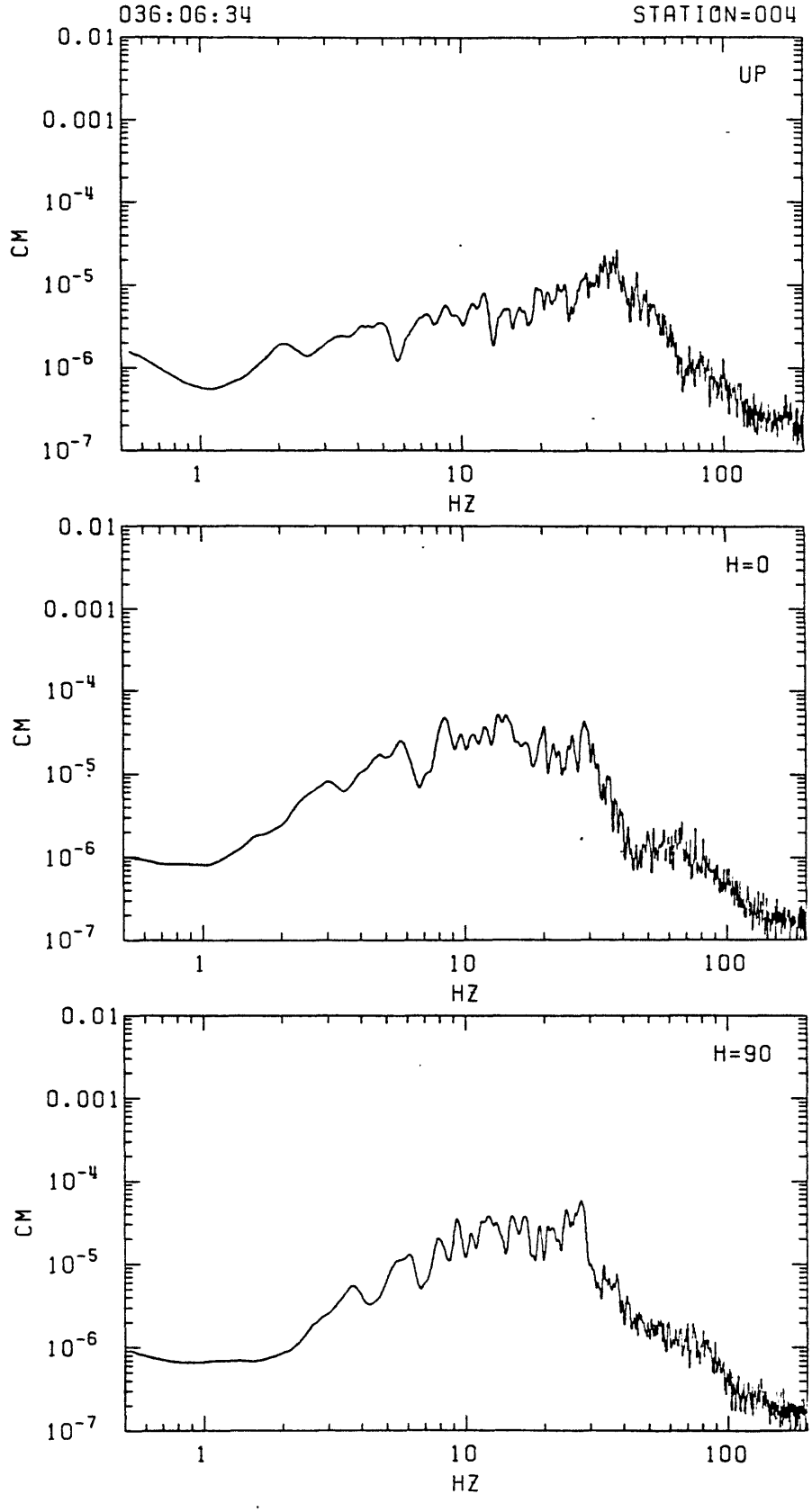

FIGURE B-15: Fourier amplitude spectrum for 10.24 seconds of 3 component recordings of event 036:06:34 at station 004.

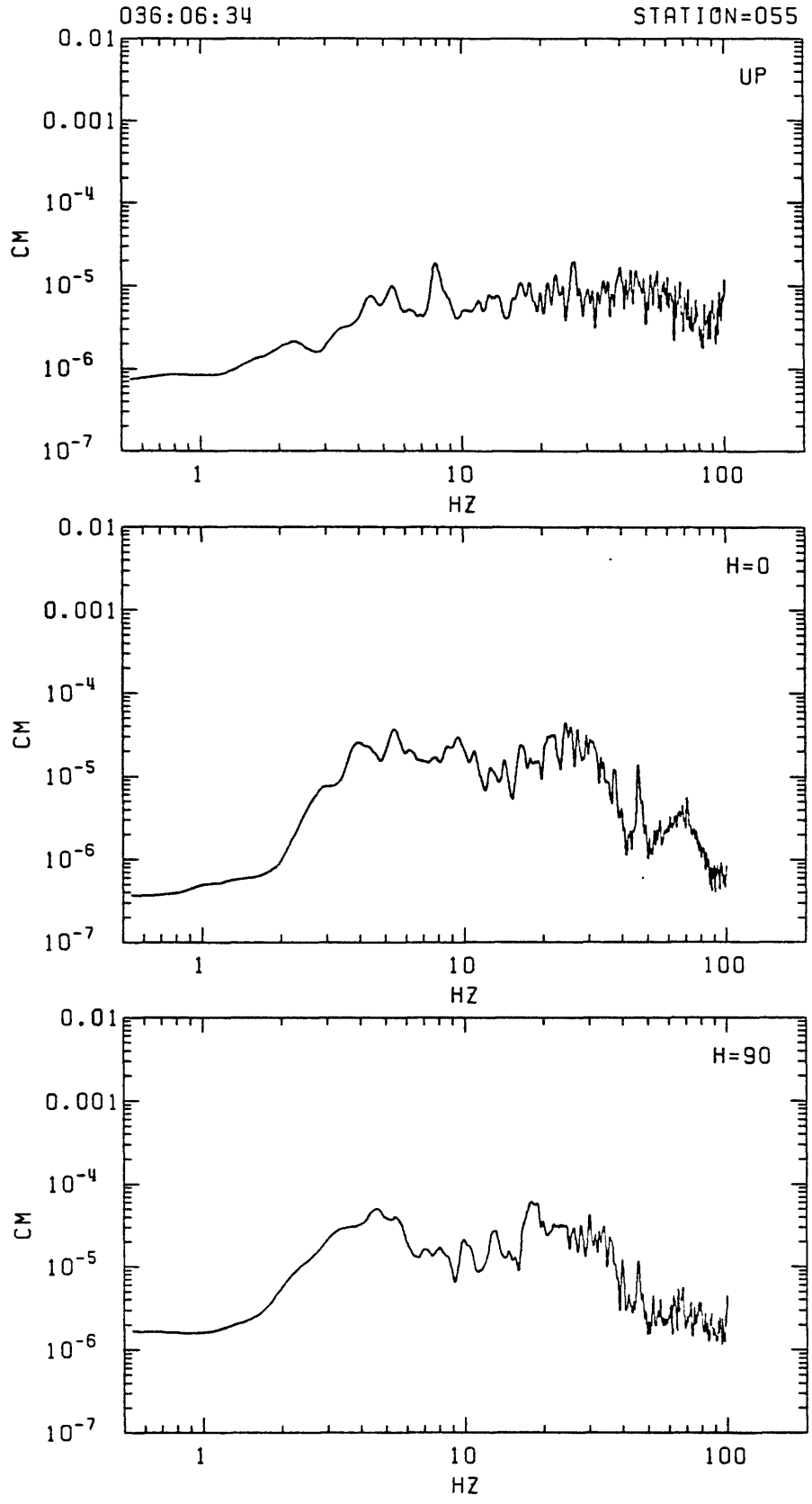

FIGURE B-16: Fourier amplitude spectrum for 10.24 seconds of 3 component recordings of event 036:06:34 at station 055.

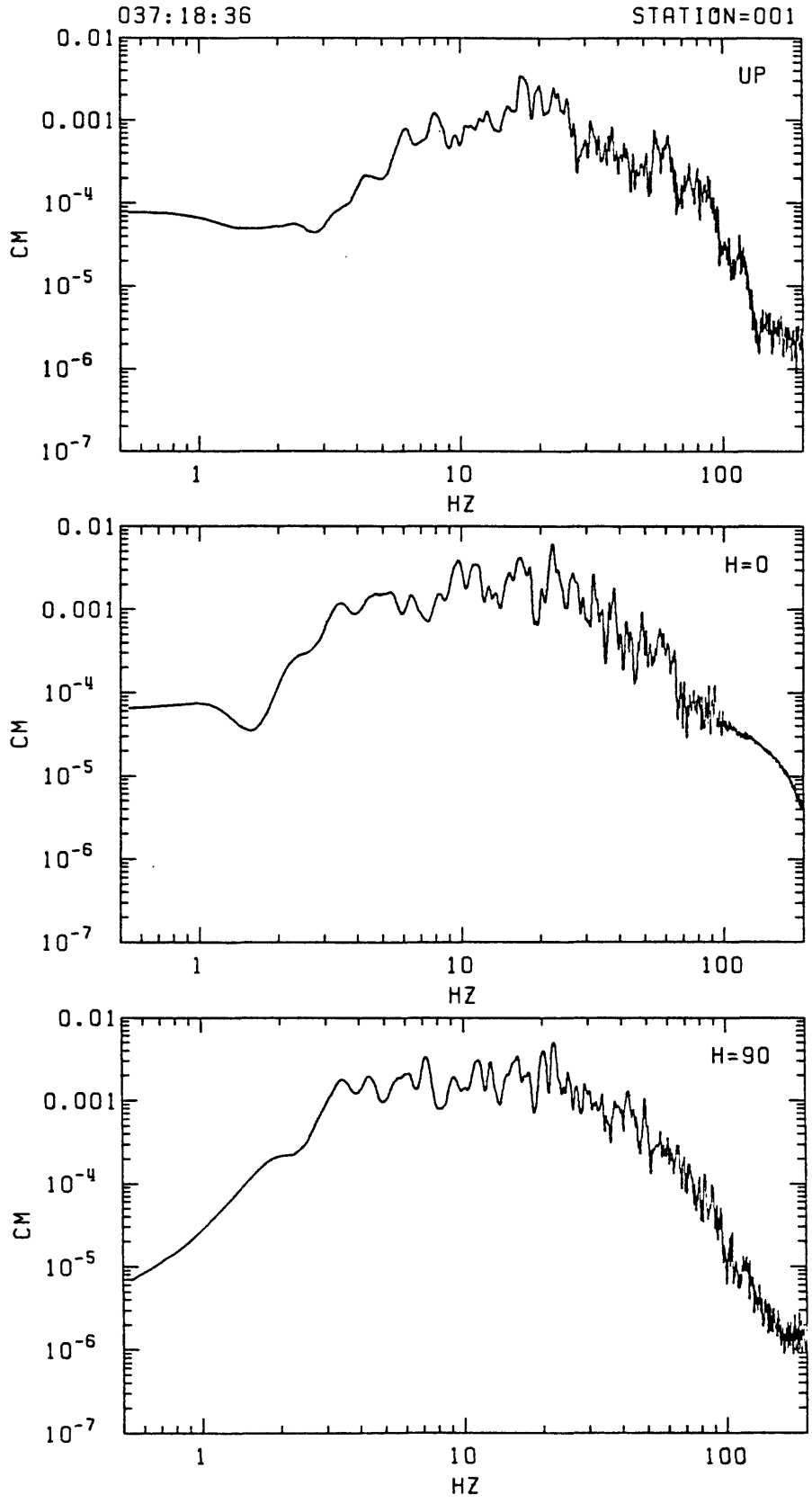

FIGURE B-17: Fourier amplitude spectrum for 10.24 seconds of 3 component recordings of event 037:18:36 at station 001.

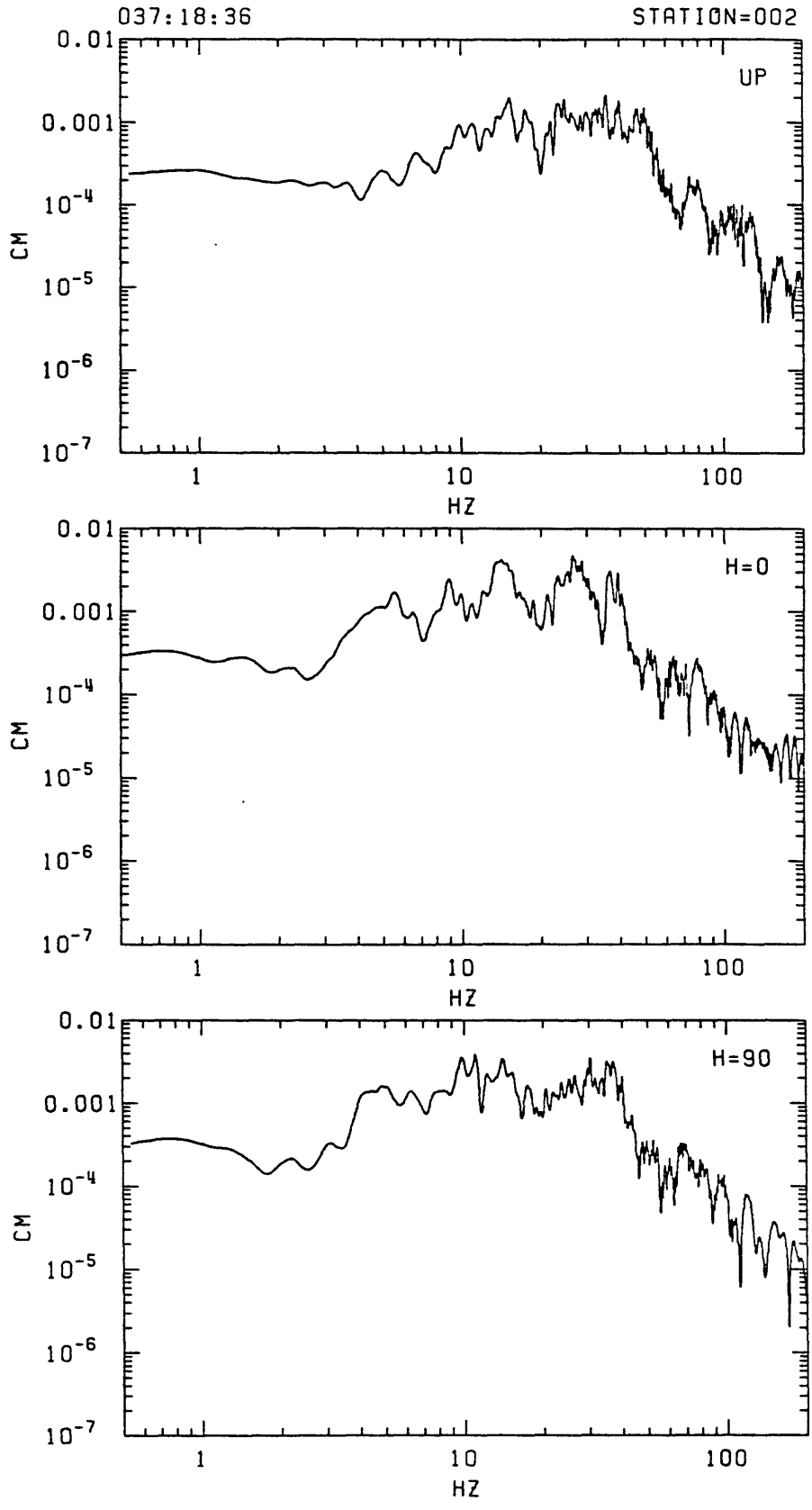

FIGURE B-18: Fourier amplitude spectrum for 10.24 seconds of 3 component recordings of event 037:18:36 at station 002.

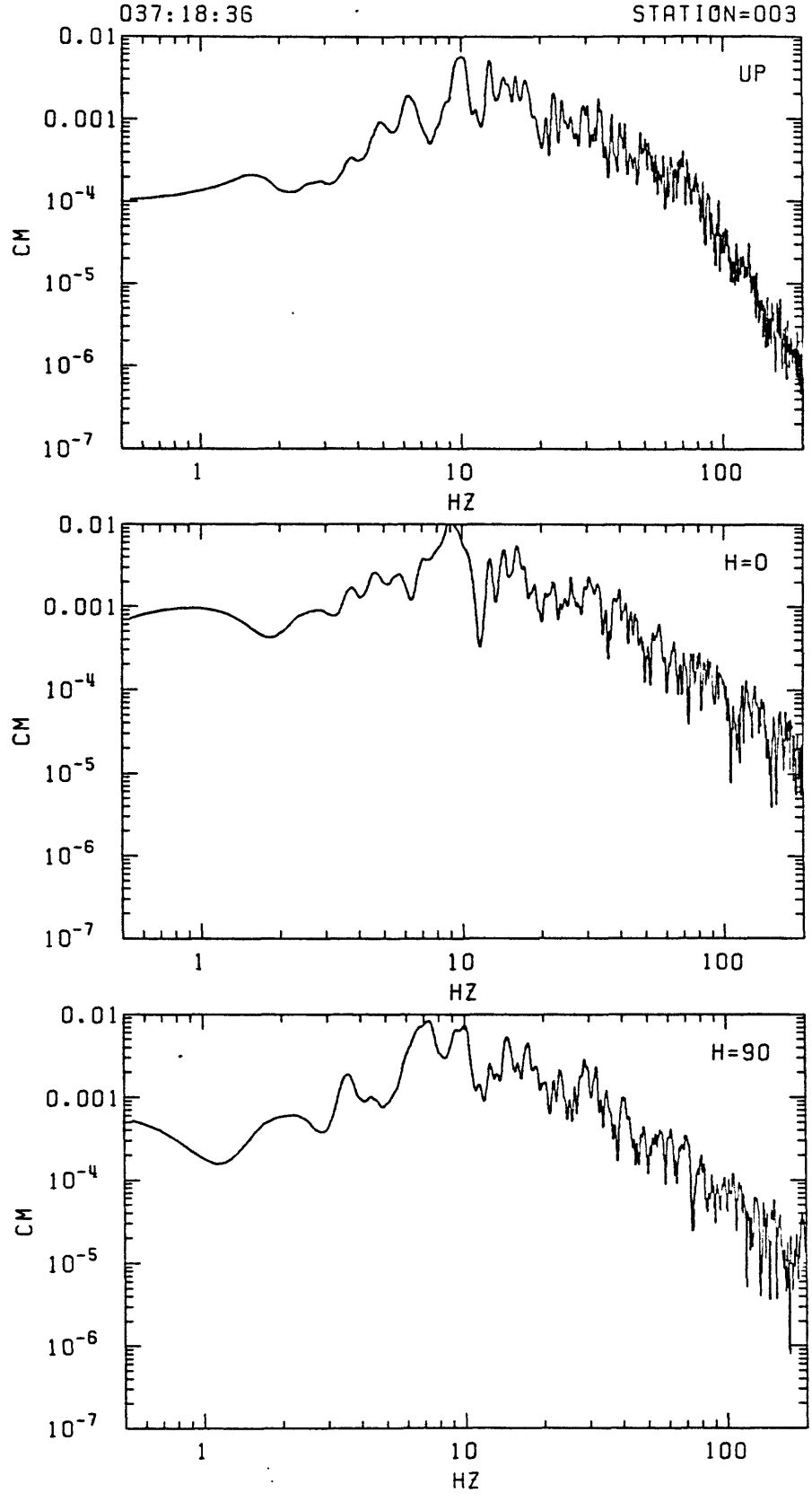

FIGURE B-19: Fourier amplitude spectrum for 10.24 seconds of 3 component recordings of event 037:18:36 at station 003.

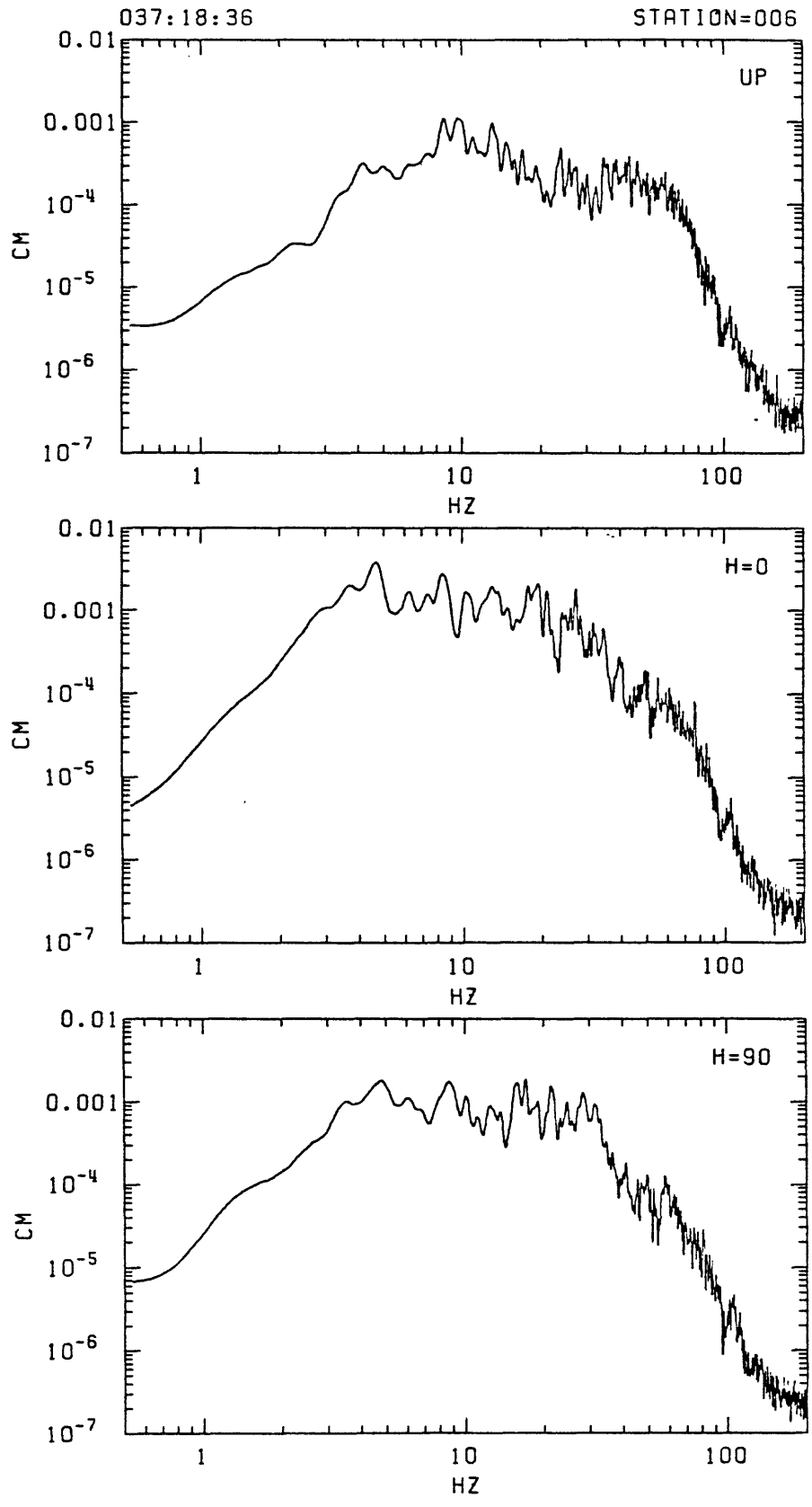

FIGURE B-20: Fourier amplitude spectrum for 10.24 seconds of 3 component recordings of event 037:18:36 at station 006.

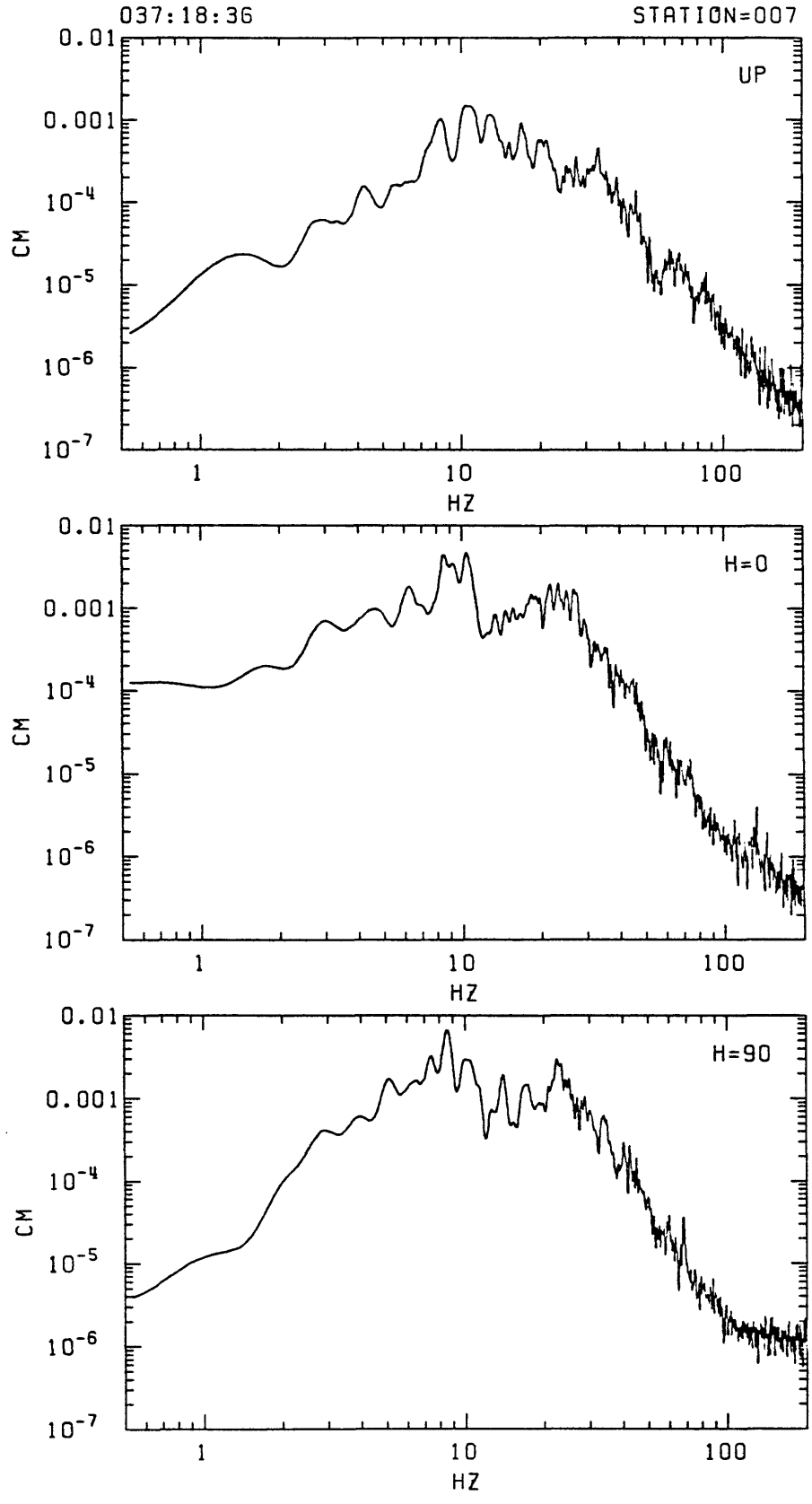

FIGURE B-21: Fourier amplitude spectrum for 10.24 seconds of 3 component recordings of event 037:18:36 at station 007.

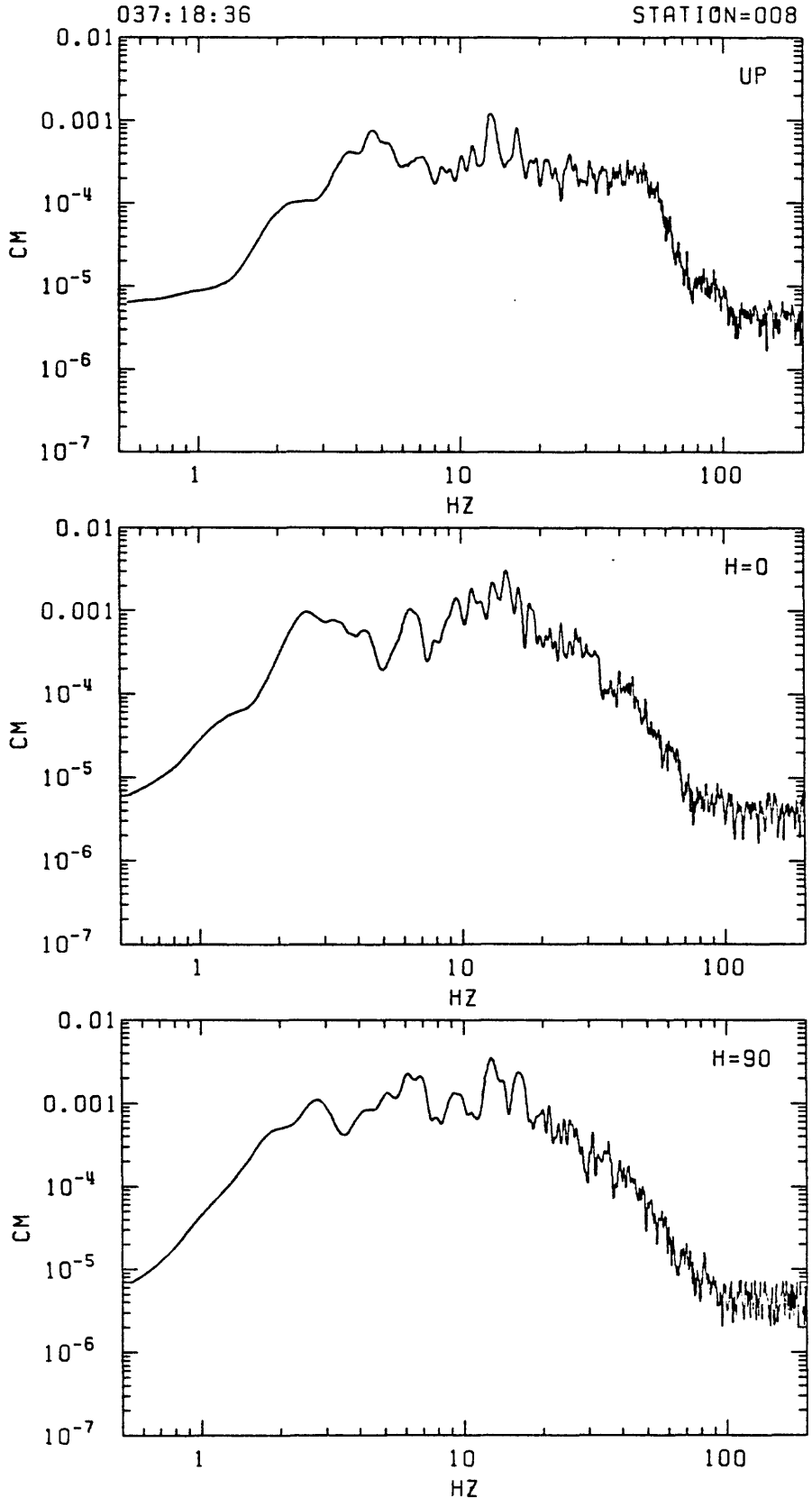

FIGURE B-22: Fourier amplitude spectrum for 10.24 seconds of 3 component recordings of event 037:18:36 at station 008.

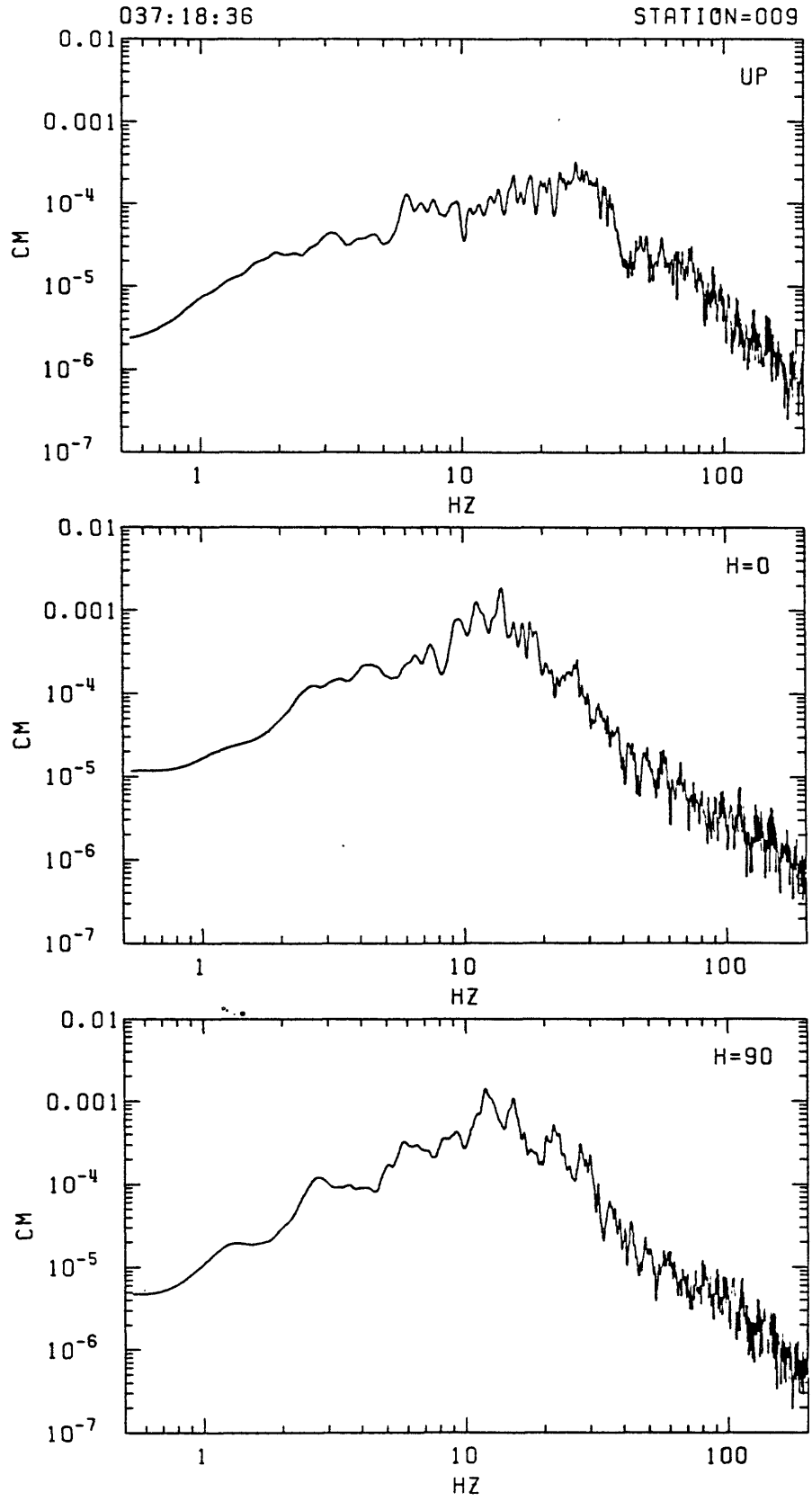

FIGURE B-23: Fourier amplitude spectrum for 10.24 seconds of 3 component recordings of event 037:18:36 at station 009.

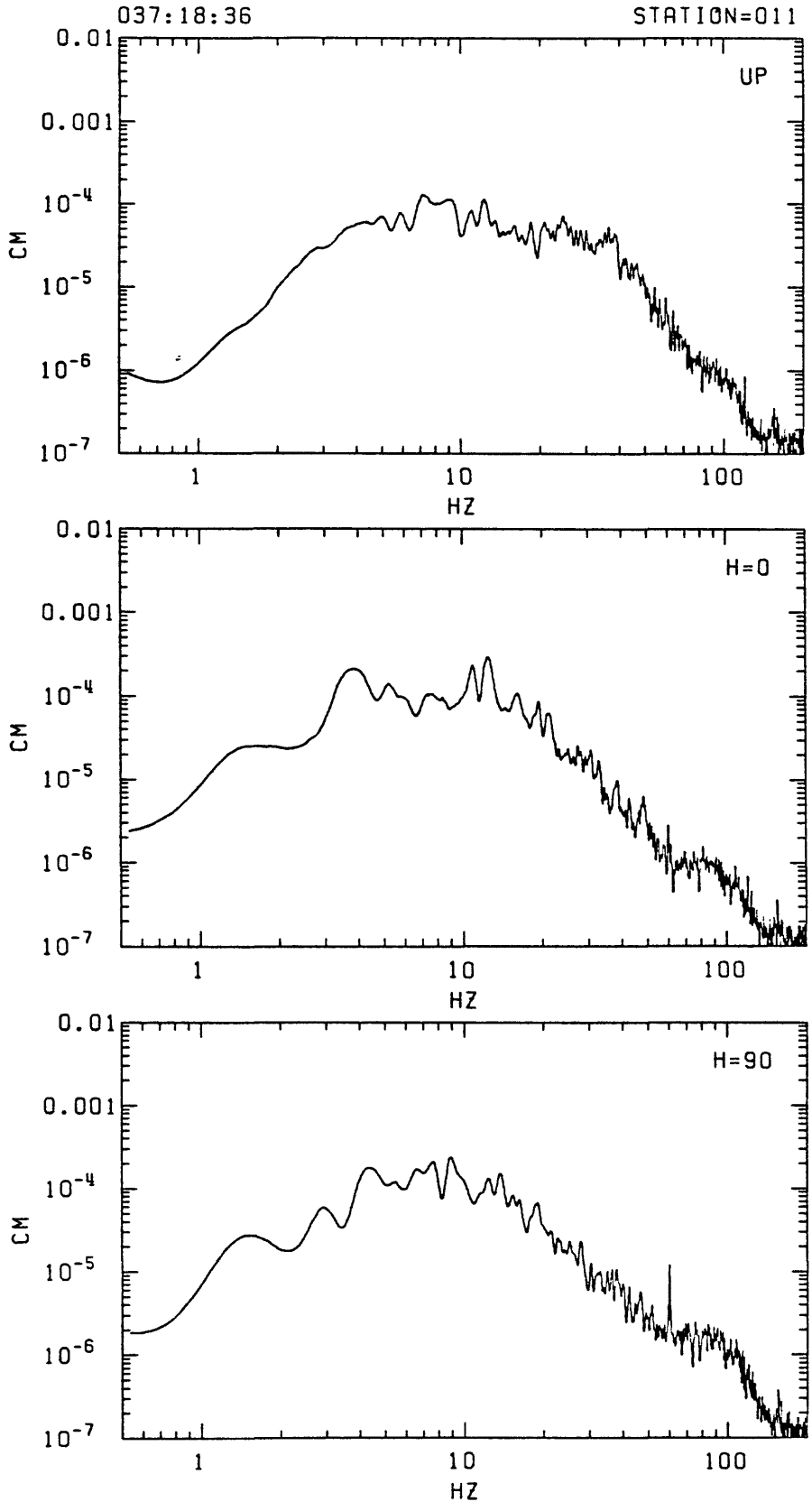

FIGURE B-24: Fourier amplitude spectrum for 10.24 seconds of 3 component recordings of event 037:18:36 at station 011.

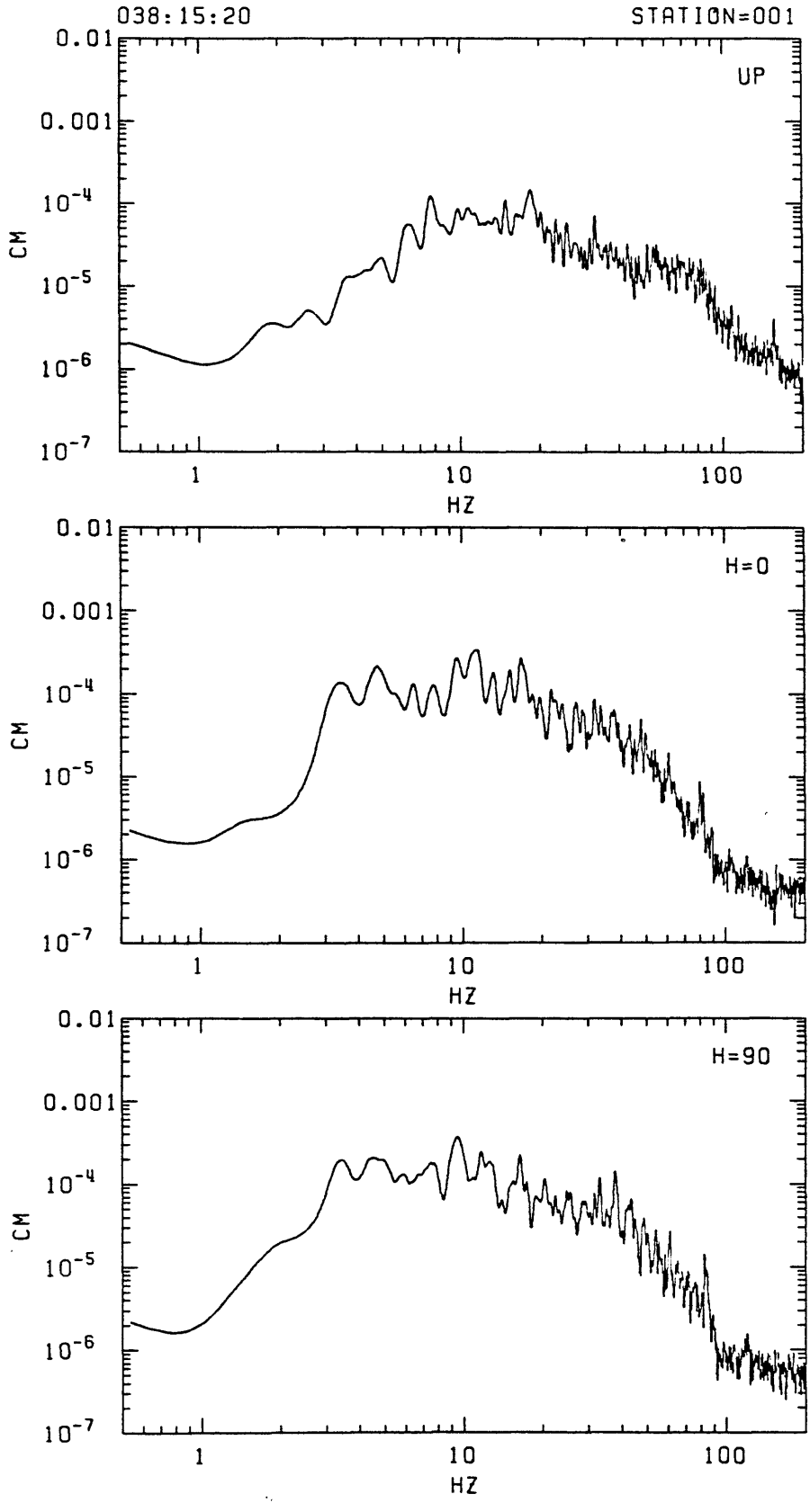

FIGURE B-25: Fourier amplitude spectrum for 10.24 seconds of 3 component recordings of event 038:15:20 at station 001.

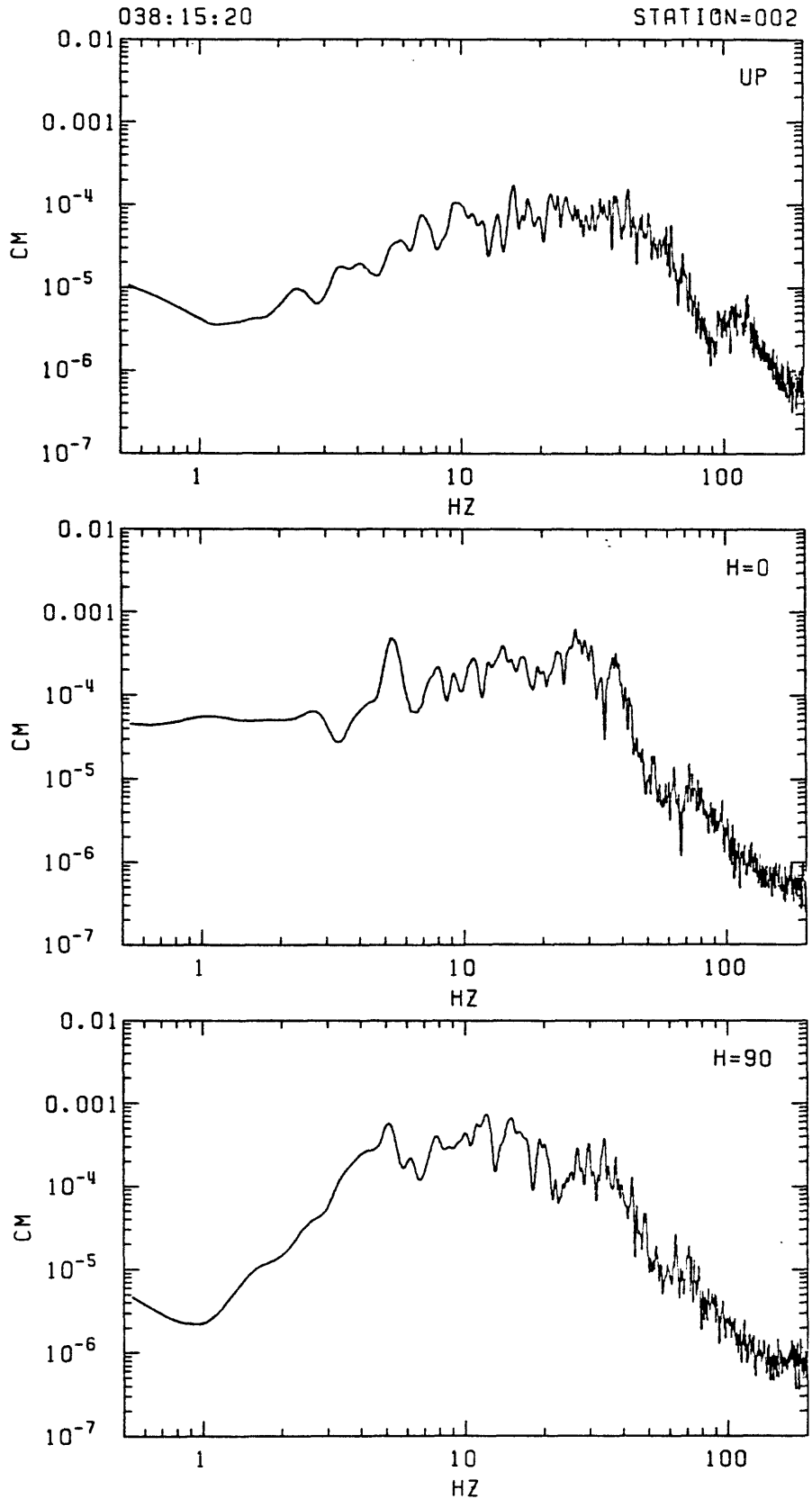

FIGURE B-26: Fourier amplitude spectrum for 10.24 seconds of 3 component recordings of event 038:15:20 at station 002.

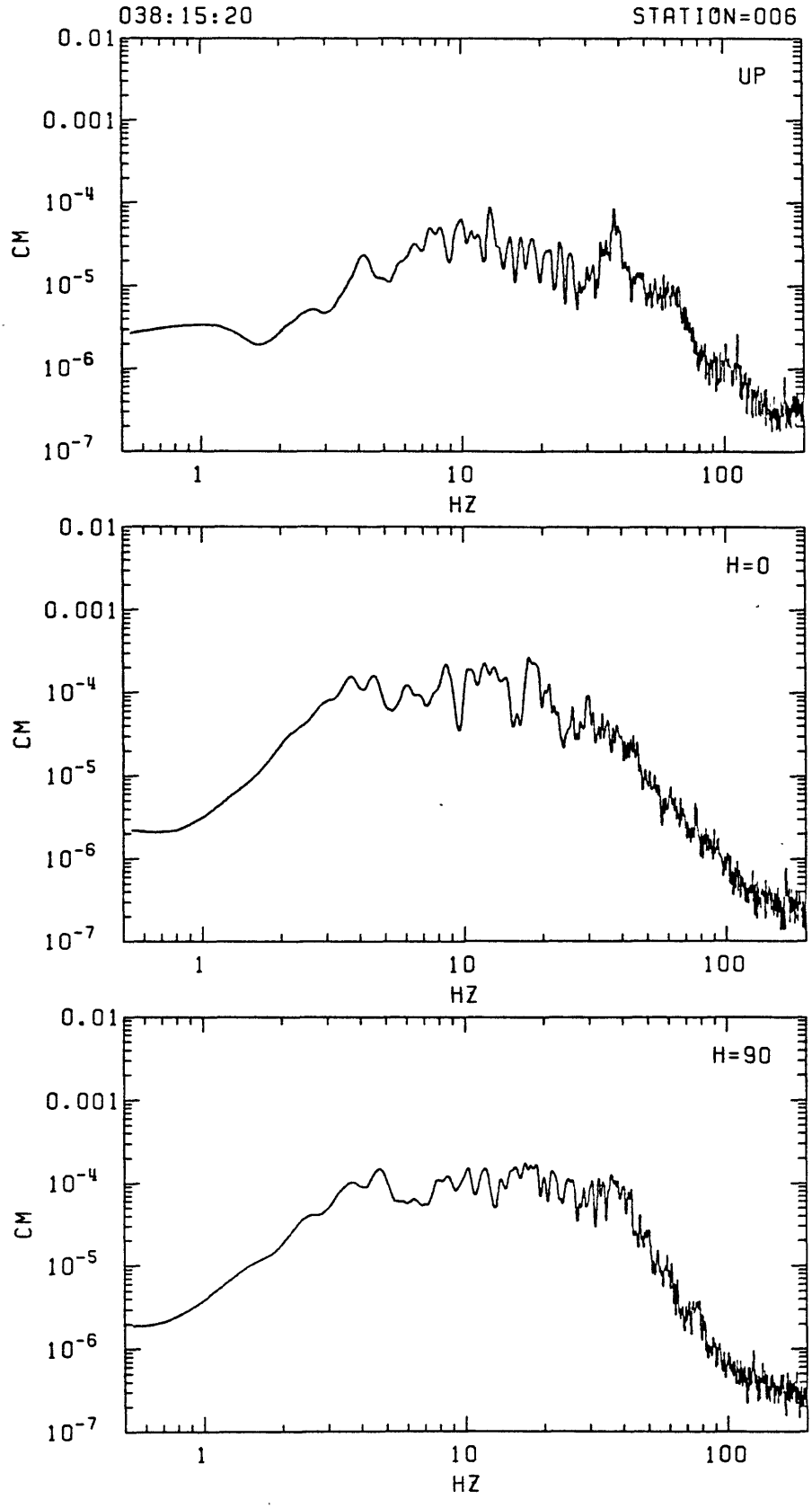

FIGURE B-27: Fourier amplitude spectrum for 10.24 seconds of 3 component recordings of event 038:15:20 at station 006.

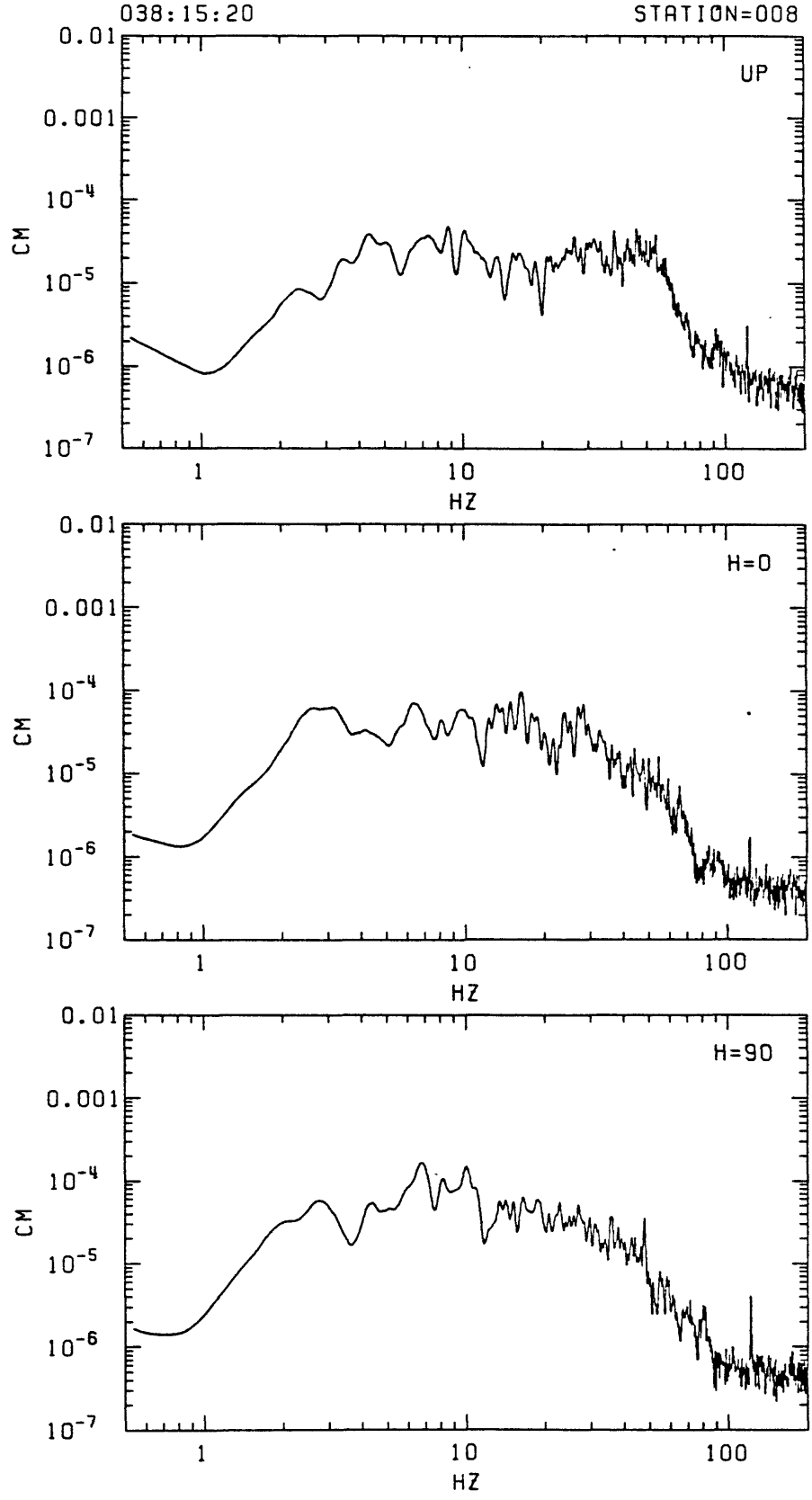

FIGURE B-28: Fourier amplitude spectrum for 10.24 seconds of 3 component recordings of event 038:15:20 at station 008.

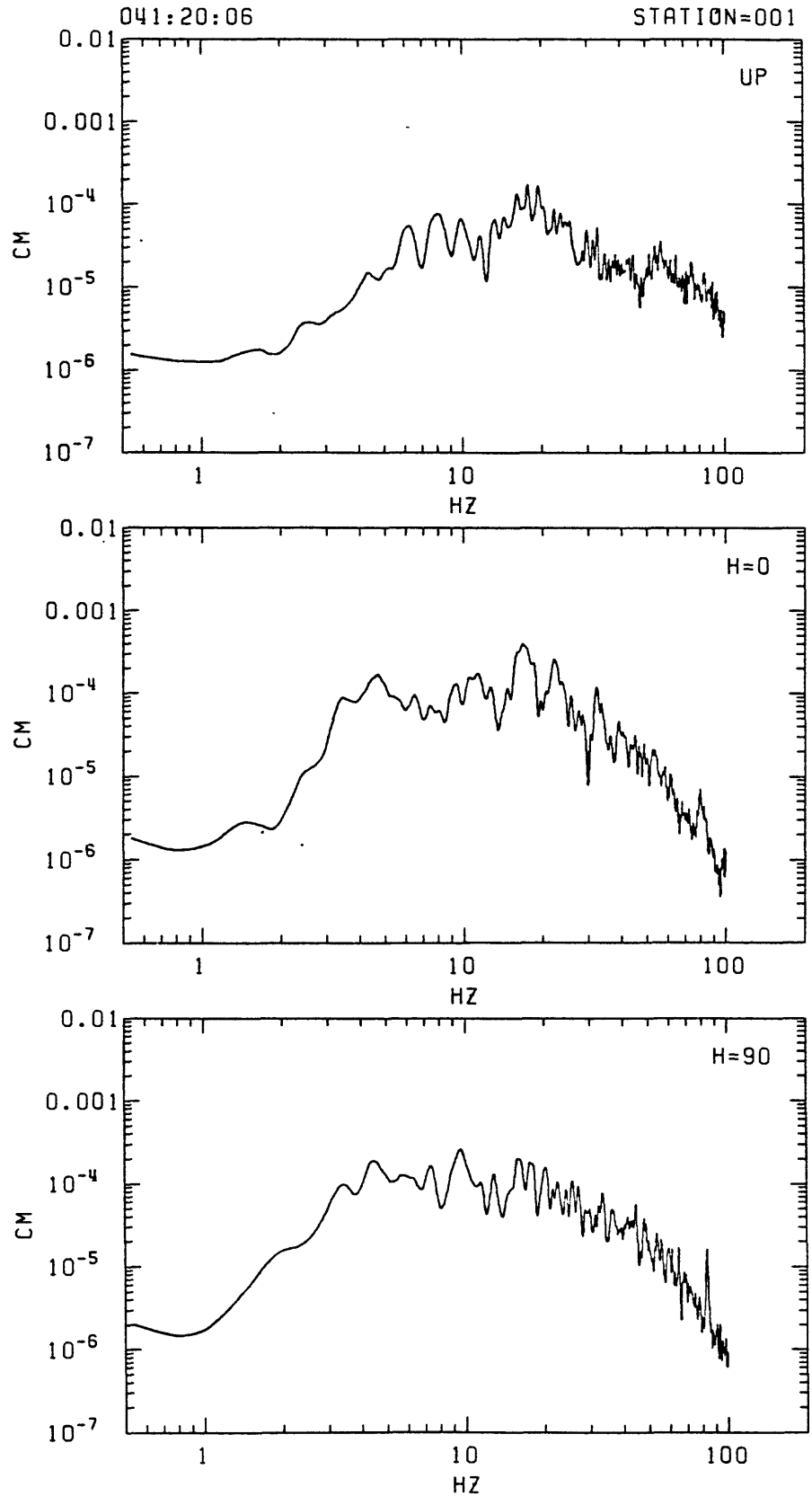

FIGURE B-29: Fourier amplitude spectrum for 10.24 seconds of 3 component recordings of event 041:20:06 at station 001.

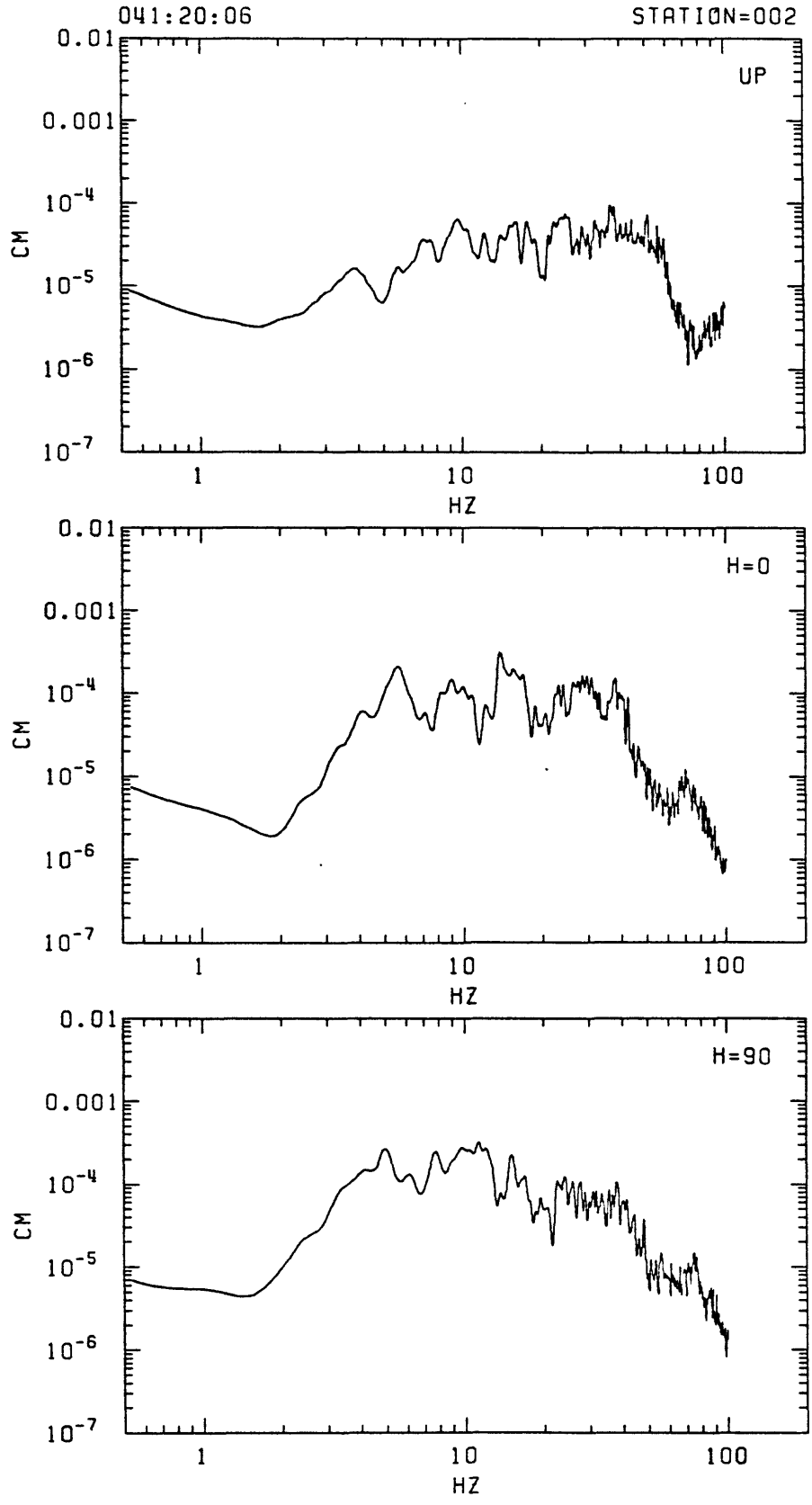

FIGURE B-30: Fourier amplitude spectrum for 10.24 seconds of 3 component recordings of event 041:20:06 at station 002.

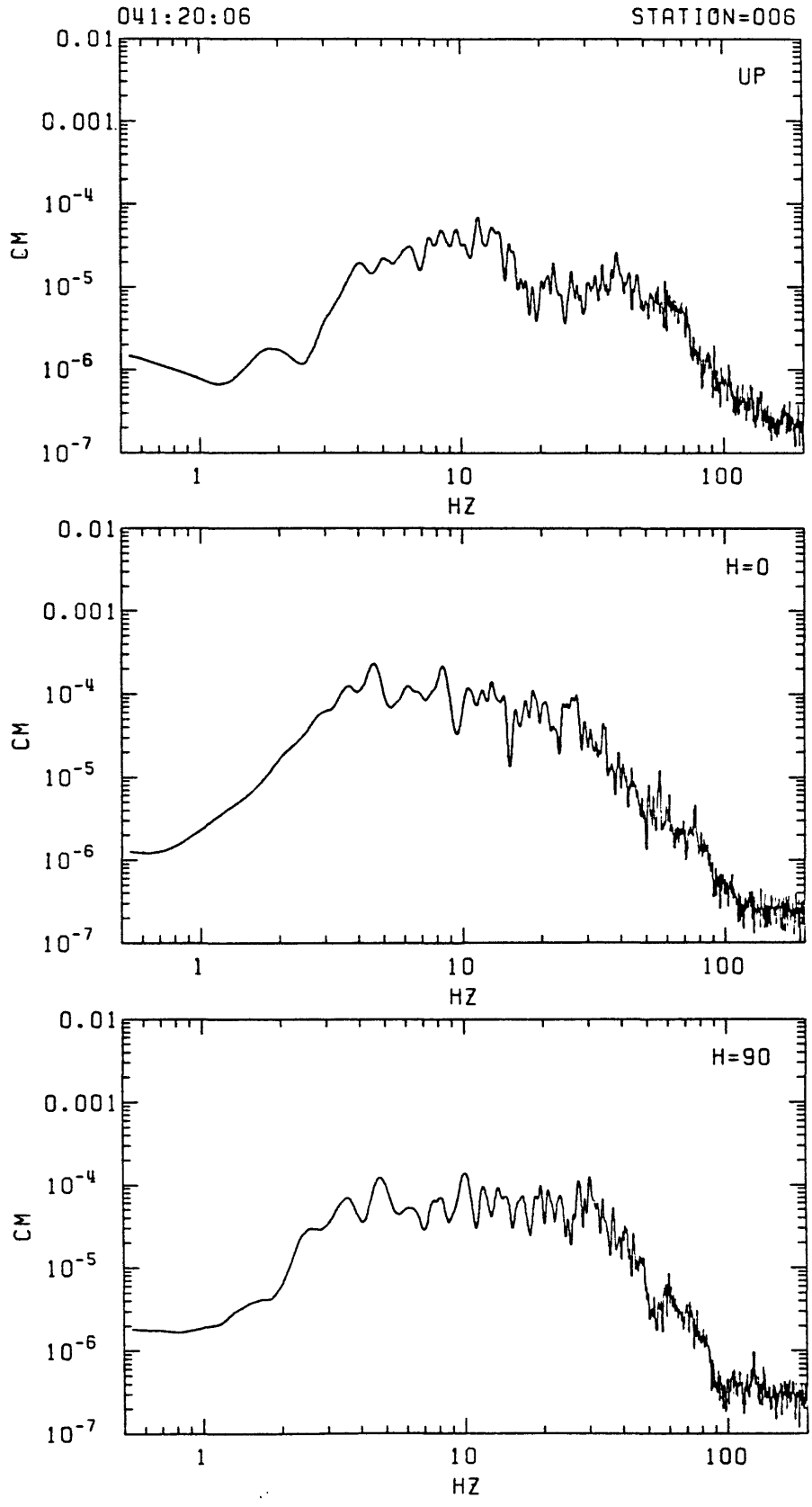

FIGURE B-31: Fourier amplitude spectrum for 10.24 seconds of 3 component recordings of event 041:20:06 at station 006.

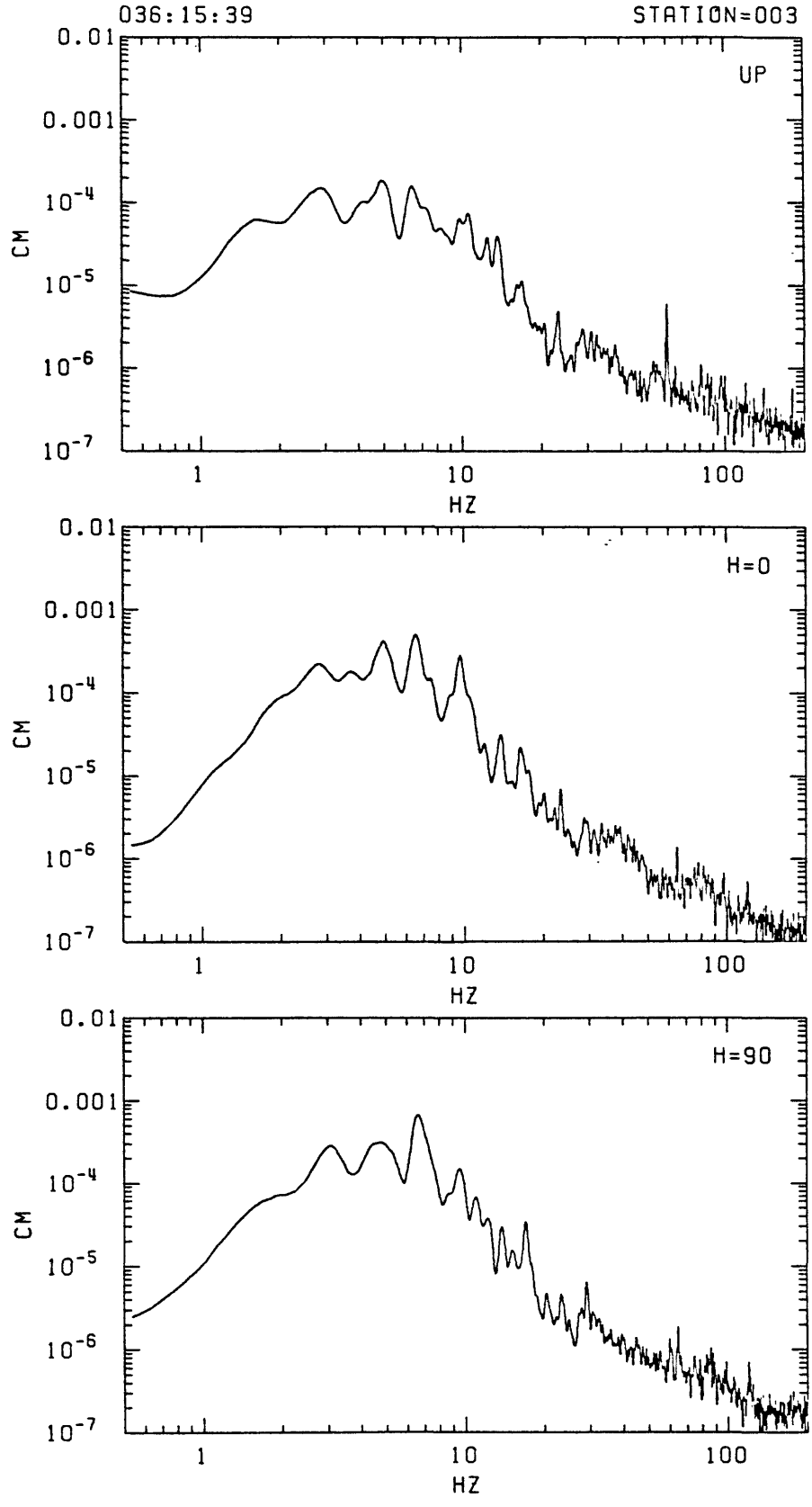

FIGURE B-32: Fourier amplitude spectrum for 10.24 seconds of 3 component recordings of quarry blast 036:15:39 at station 003.

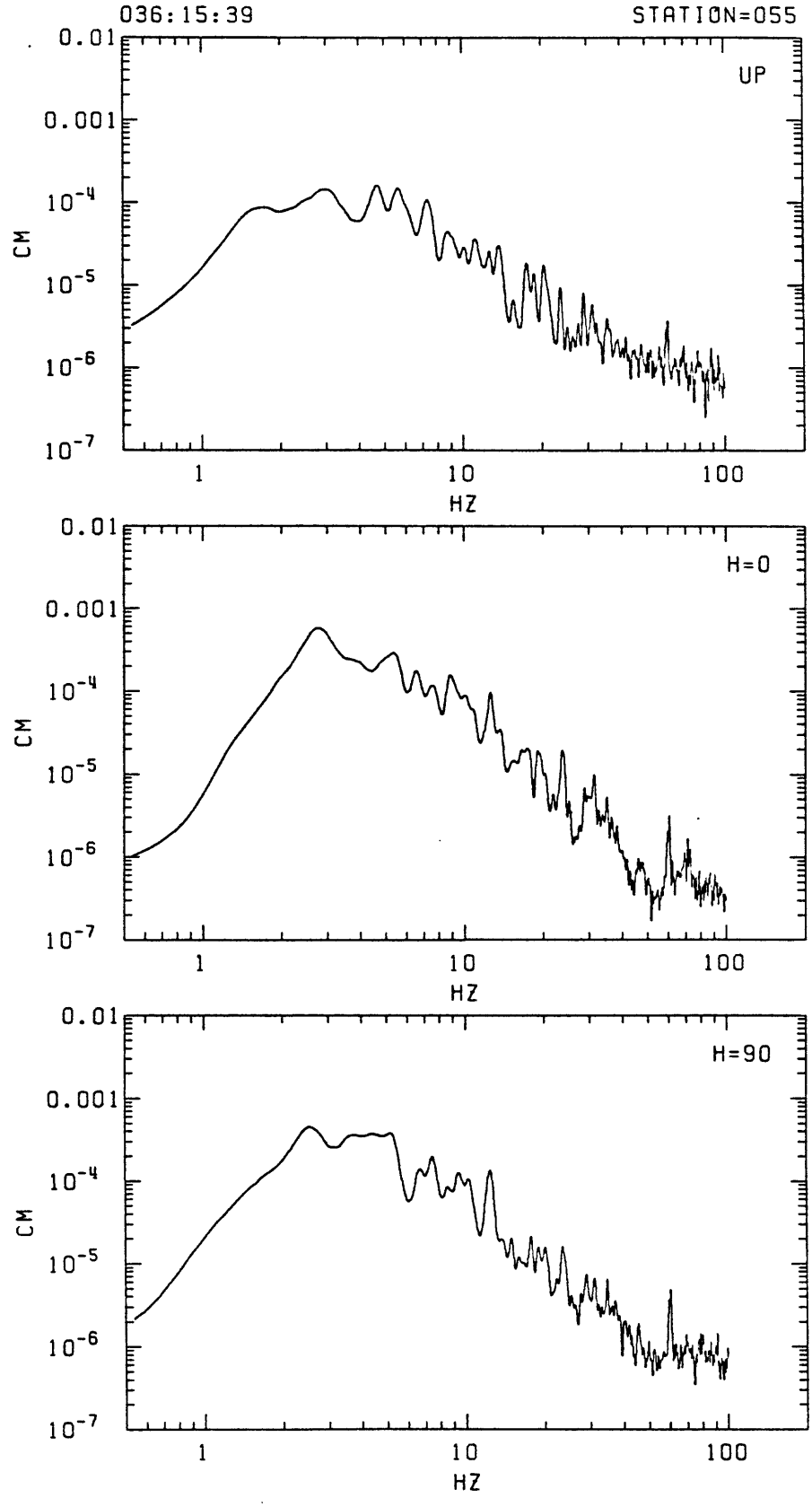

FIGURE B-33: Fourier amplitude spectrum for 10.24 seconds of 3 component recordings of quarry blast 036:15:39 at station 055.

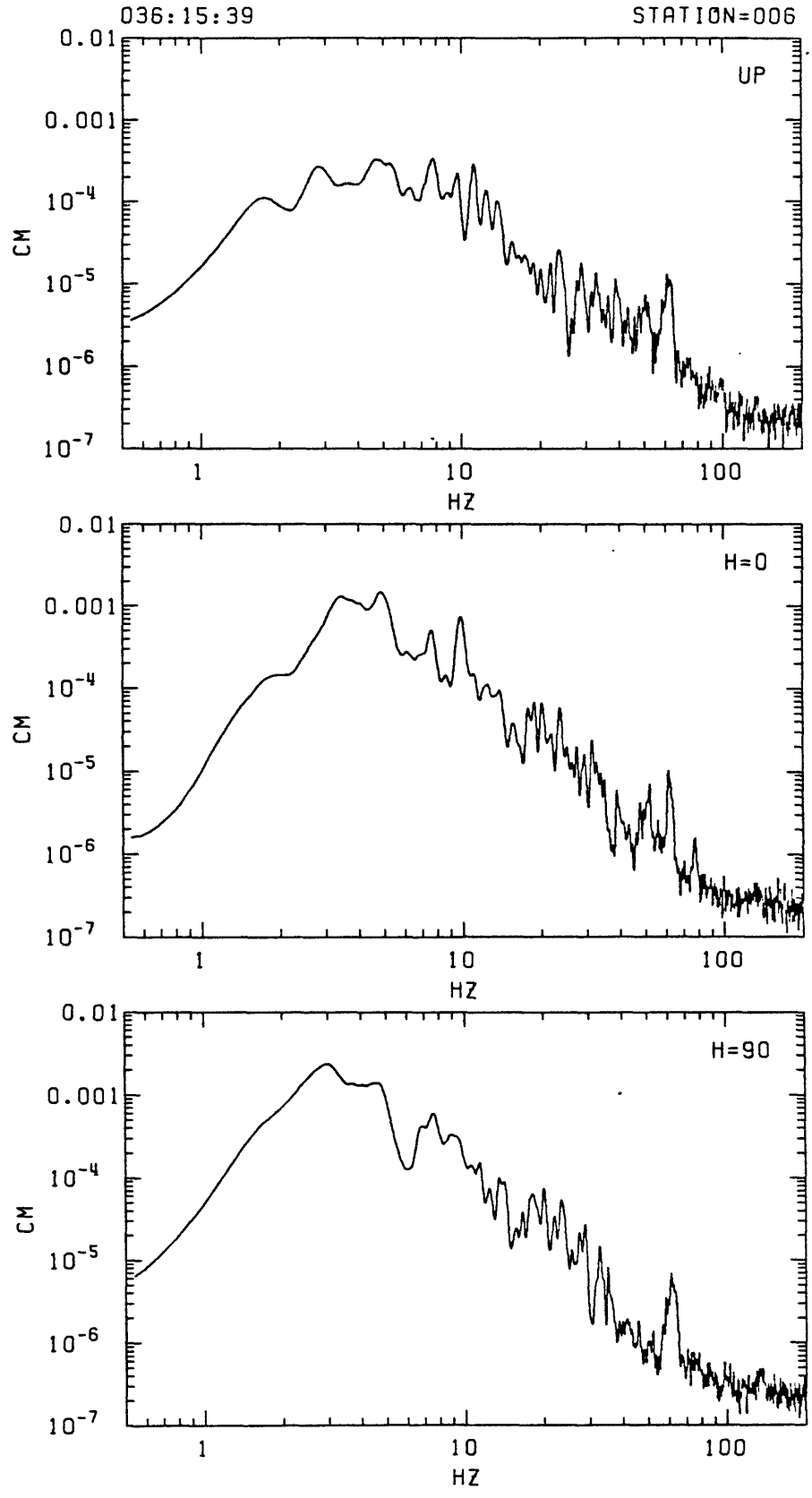

FIGURE B-34: Fourier amplitude spectrum for 10.24 seconds of 3 component recordings of quarry blast 036:15:39 at station 006.

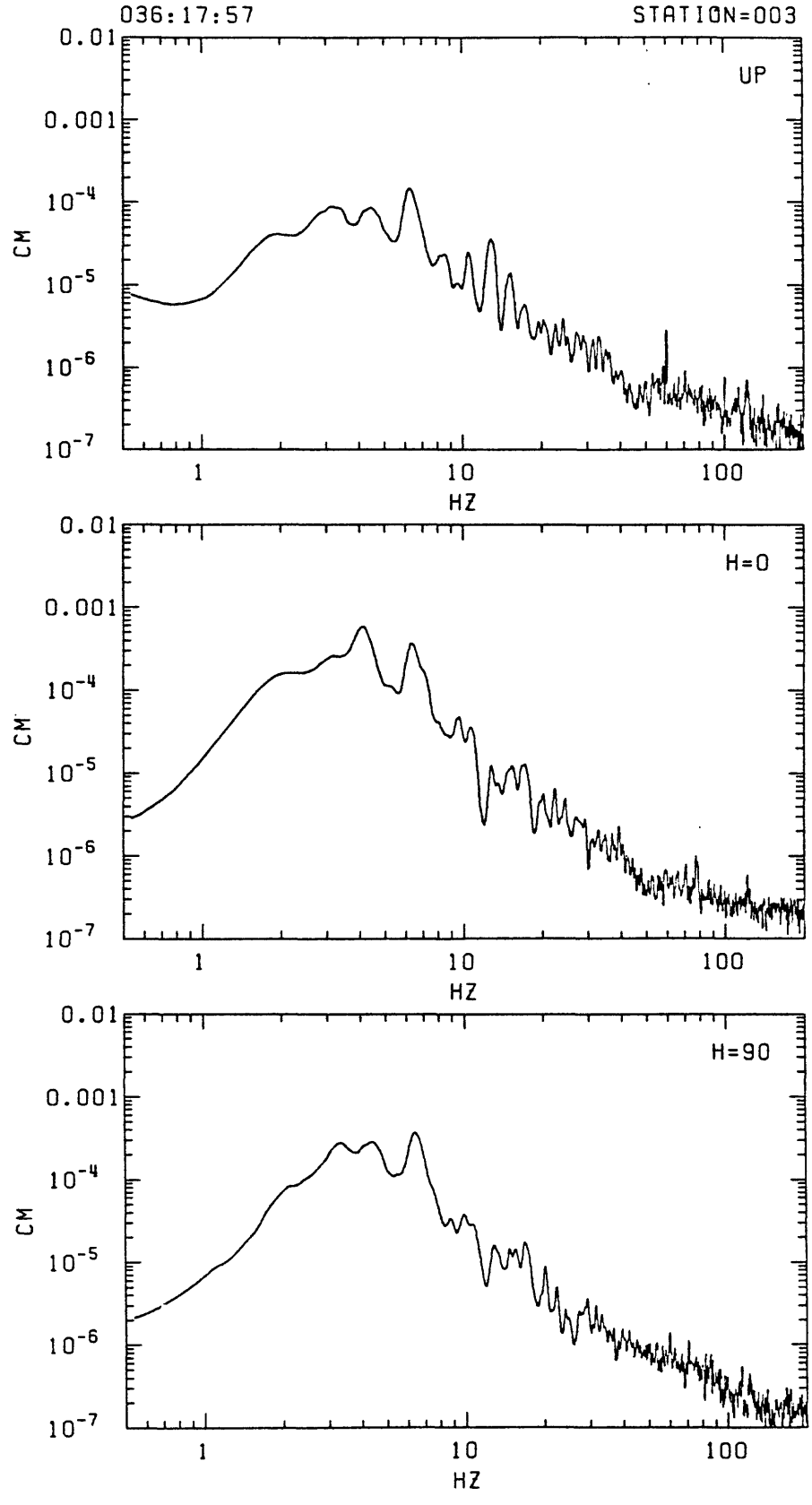

FIGURE B-35: Fourier amplitude spectrum for 10.24 seconds of 3 component recordings of quarry blast 036:17:57 at station 003.

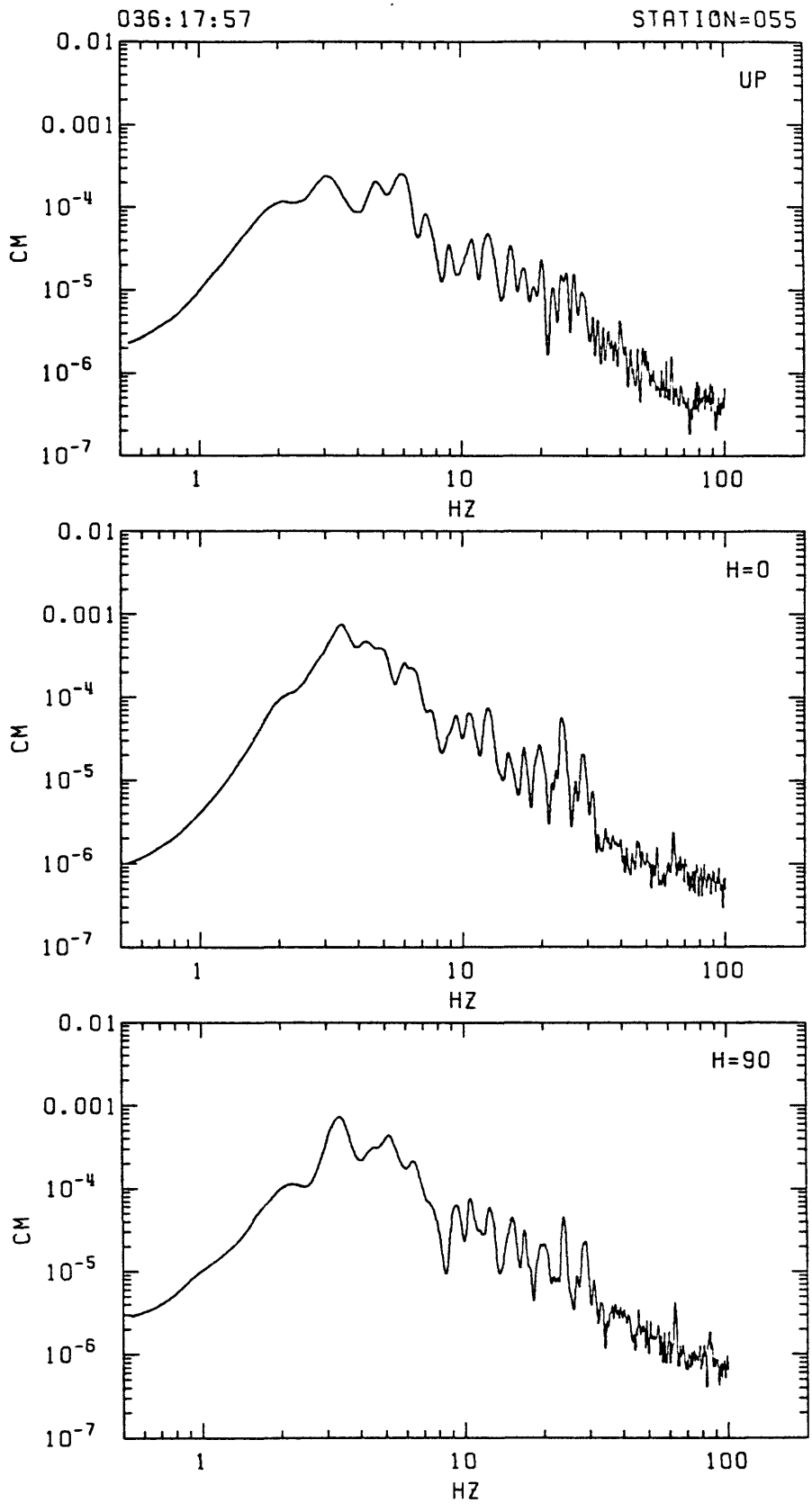

FIGURE B-36: Fourier amplitude spectrum for 10.24 seconds of 3 component recordings of quarry blast 036:17:57 at station 055.

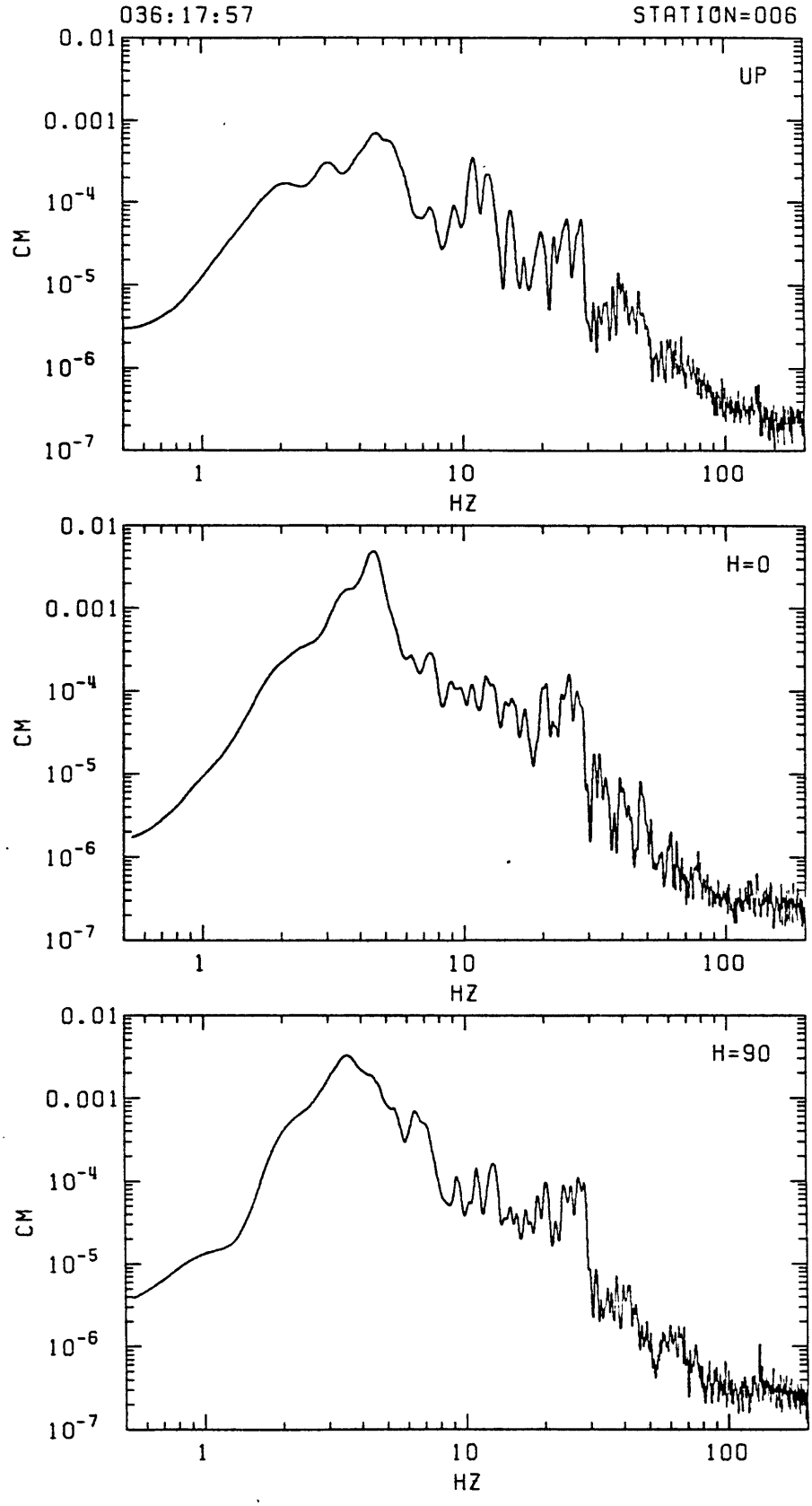

FIGURE B-37: Fourier amplitude spectrum for 10.24 seconds of 3 component recordings of quarry blast 036:17:57 at station 006.

APPENDIX C

LOCATION PARAMETERS (HYPOINVERSE) FOR SEISMIC EVENTS LOCATED NEAR PAINESVILLE, OHIO DURING TIME PERIOD FEB. 1, 1986 THROUGH FEB. 10, 1986 AS INDICATED IN FIGURES 4 AND 5

TABLE C-1 -- EVENT: 2 FEB 86, 3:22

I	ORIGIN	LAT N	LON W	Z	NWR	RMS	DT	ADJUSTMENTS (KM) DLAT	DLON	DZ	RR
1	47.62	41 39.74	81 10.36	7.00	9	0.73	0.65	-2.133	-0.830	0.000	2.28
FOCAL DEPTH FREED											
2	48.27	41 38.59	81 9.76	7.00	9	0.14	0.29	0.265	-0.292	-1.732	1.77
3	48.56	41 38.73	81 9.55	5.27	9	0.02	0.01	0.047	-0.063	-0.145	0.16
4	48.57	41 38.76	81 9.50	5.12	9	0.01	0.00	-0.001	-0.037	-0.008	0.03

YR	MO	DA	ORIGIN	LAT N	LON W	DEPTH	RMS	ERH	ERZ	GAP	XMAG	FMAG
86-	2-	2	322 48.57	41 38.76	81 9.50	5.12	0.01	1.16	0.78	150		

RMSWT	DMIN	ITR	NFM	NWR	NWS	REMK
0.01	1.5	4	0	9	4	

STA	DIST	AZM	AN	P/S	W	SEC	+CCOR	(TOBS	-TCAL	-DLY	=RES)	WT	XMG	FMG	R	INFO
003	1.5	329	160	P		49.62	0.00	1.05	1.07	0.00	-0.02	1.57				0.309
				S		50.47	0.00	1.90	1.89	0.00	0.00	1.57				0.824
006	8.2	103	114	P		50.41	0.00	1.84	1.84	0.00	0.00	1.57				0.675
				S	2	51.75	0.00	3.18	3.20	0.00	-0.02	0.78				0.383
002	9.3	0	111	P	1	50.54	0.00	1.97	2.01	-0.03	-0.01	1.17				0.465
				S	3	51.96	0.00	3.39	3.47	-0.08	-0.01	0.39				0.127
004	11.7	253	106	P	2	50.96	0.00	2.39	2.37	0.00	0.01	0.78				0.780
				S	4	52.67	0.00	4.10	4.10	0.00	0.00	0.00				0.000
001	17.6	4	100	P	2	51.90	0.00	3.33	3.32	0.00	0.00	0.78				0.275
				S	3	54.31	0.00	5.74	5.68	0.05	0.01	0.39				0.158

TABLE C-2 -- EVENT: 3 FEB 86, 19:47

I	ORIGIN	LAT N	LON W	Z	NWR	RMS	DT	ADJUSTMENTS (KM) DLAT	DLON	DZ	RR
1	18.83	41 39.74	81 10.36	7.00	11	0.64	0.61	-1.568	-0.986	0.000	1.85
FOCAL DEPTH FREED											
2	19.44	41 38.89	81 9.65	7.00	11	0.09	0.19	-0.019	-0.263	-1.120	1.15
3	19.64	41 38.88	81 9.46	5.88	11	0.03	0.01	0.068	-0.040	-0.073	0.10
4	19.65	41 38.92	81 9.43	5.81	11	0.03	0.00	0.006	0.032	0.005	0.03

YR	MO	DA	ORIGIN	LAT N	LON W	DEPTH	RMS	ERH	ERZ	GAP	XMAG	FMAG
86-	2-	3	1947 19.65	41 38.92	81 9.43	5.81	0.03	0.88	0.76	116		

RMSWT	DMIN	ITR	NEM	NWR	NWS	REMK
0.03	1.3	4	0	11	4	

STA	DIST	AZM	AN	P/S	W	SEC+CCOR	(TOBS	-TCAL	-DLY	=RES)	WT	XMG	FMG	R	INFO
003	1.3	318	165	P		20.83 0.00	1.18	1.17	0.00	0.01	1.76				0.310
				S		21.69 0.00	2.04	2.06	0.00	-0.02	1.76				0.817
CAL	4.3	9	137	P	5	21.24 0.00	1.59	1.40	0.00	0.19	0.00				0.000
				S	5	22.54 0.00	2.89	2.45	0.00	0.44	0.00				0.000
HAM	5.3	165	131	P	5	21.16 0.00	1.51	1.51	0.00	0.00	0.00				0.000
				S	5	21.66 0.00	2.01	2.64	0.00	-0.63	0.00				0.000
WSH	5.8	246	128	P	5	21.32 0.00	1.67	1.58	0.00	0.09	0.00				0.000
				S	5	22.30 0.00	2.65	2.76	0.00	-0.11	0.00				0.000
BUR	6.2	84	126	P	5	21.40 0.00	1.75	1.63	0.00	0.13	0.00				0.000
				S	5	22.75 0.00	3.10	2.83	0.00	0.27	0.00				0.000
006	8.1	105	118	P		21.54 0.00	1.89	1.88	0.00	0.01	1.76				0.615
				S	2	22.89 0.00	3.24	3.27	0.00	-0.03	0.88				0.444
002	8.9	0	116	P	1	21.60 0.00	1.95	2.01	0.00	-0.06	1.32				0.455
				S	3	23.01 0.00	3.36	3.47	0.00	-0.11	0.44				0.100
COT	9.2	148	115	P	5	21.72 0.00	2.07	2.04	0.00	0.04	0.00				0.000
				S	5	23.16 0.00	3.51	3.52	0.00	-0.01	0.00				0.000
CUY	10.0	186	113	P	5	21.76 0.00	2.11	2.16	0.00	-0.05	0.00				0.000
				S	5	23.28 0.00	3.63	3.73	0.00	-0.10	0.00				0.000
MON	11.6	122	110	P	5	22.06 0.00	2.41	2.40	0.00	0.01	0.00				0.000
				S	5	23.62 0.00	3.97	4.14	0.00	-0.17	0.00				0.000
004	11.9	252	110	P	4	22.12 0.00	2.47	2.44	0.00	0.03	0.00				0.000
008	13.1	202	107	P	2	22.25 0.00	2.60	2.63	0.00	-0.03	0.88				0.608
				S	4	24.19 0.00	4.54	4.51	0.00	0.03	0.00				0.000
007	14.1	149	106	P	3	22.47 0.00	2.82	2.78	0.00	0.04	0.44				0.072
				S	5	24.47 0.00	4.82	4.77	0.00	0.05	0.00				0.000
LOX	14.1	42	106	P	5	22.50 0.00	2.85	2.78	0.00	0.07	0.00				0.000
				S	5	24.55 0.00	4.90	4.77	0.00	0.13	0.00				0.000
HAR	14.2	107	106	P	5	22.45 0.00	2.80	2.81	0.00	0.00	0.00				0.000
				S	5	24.39 0.00	4.74	4.81	0.00	-0.07	0.00				0.000
001	17.4	4	103	P	2	22.97 0.00	3.32	3.30	0.00	0.02	0.88				0.286
				S	3	25.44 0.00	5.79	5.64	0.00	0.15	0.44				0.134
009	26.4	188	98	P	3	24.32 0.00	4.67	4.74	0.00	-0.06	0.44				0.154
				S	5	27.69 0.00	8.04	8.04	0.00	0.00	0.00				0.000

TABLE C-3 -- EVENT: 5 FEB 86, 6:34

I	ORIGIN	LAT N	LON W	Z	NWR	RMS	DT	ADJUSTMENTS (KM) DLAT	DLON	DZ	RR
1	1.26	41 39.74	81 10.36	7.00	8	0.79	0.73	-1.337	-1.569	0.000	2.06
FOCAL DEPTH FREED											
2	1.99	41 39.02	81 9.23	7.00	8	0.12	0.47	0.008	0.775	-3.101	3.19
3	2.45	41 39.02	81 9.79	3.90	8	0.05	-0.05	-0.113	-0.144	0.149	0.23
4	2.40	41 38.96	81 9.68	4.05	8	0.02	0.00	-0.016	0.011	-0.034	0.03

YR	MO	DA	ORIGIN	LAT N	LON W	DEPTH	RMS	ERH	ERZ	GAP	XMAG	FMAG
86-	2-	5	634 2.40	41 38.96	81 9.68	4.05	0.02	0.88	1.31	134		

RMSWT	DMIN	ITR	NFM	NWR	NWS	REMK
0.02	1.1	4	0	8	4	

STA	DIST	AZM	AN	P/S	W	SEC+CCOR	(TOBS	-TCAL	-DLY	=RES)	WT	XMG	FMG	R	INFO
003	1.1	330	161	P		3.26 0.00	0.86	0.88	0.00	-0.03	1.68				0.506
				S	2	4.00 0.00	1.60	1.58	0.00	0.02	0.84				0.544
055	4.8	135	119	P		3.69 0.00	1.29	1.28	0.00	0.00	1.68				0.873
				S	3	4.62 0.00	2.22	2.27	0.00	-0.05	0.42				0.117
002	8.9	1	105	P	2	4.24 0.00	1.84	1.89	-0.03	-0.02	0.84				0.362
				S	2	5.62 0.00	3.22	3.28	-0.08	0.02	0.84				0.610
004	11.6	251	101	P	1	4.71 0.00	2.31	2.31	0.00	-0.01	1.26				0.799
				S	3	6.43 0.00	4.03	4.00	0.00	0.03	0.42				0.185

TABLE C-4 -- EVENT: 6 FEB 86, 18:36

I	ORIGIN	LAT N	LON W	Z	NWR	RMS	DT	ADJUSTMENTS (KM) DLAT	DLON	DZ	RR
1	21.52	41 39.74	81 10.36	7.00	11	0.62	0.61	-1.905	-1.314	0.000	2.31
FOCAL DEPTH FREED											
2	22.13	41 38.71	81 9.41	7.00	11	0.07	0.12	-0.068	-0.090	-0.848	0.85
3	22.25	41 38.68	81 9.35	6.15	11	0.03	0.01	0.005	-0.018	-0.094	0.09
4	22.26	41 38.68	81 9.33	6.06	11	0.03	0.00	0.005	-0.001	0.035	0.03

YR	MO	DA	ORIGIN	LAT N	LON W	DEPTH	RMS	ERH	ERZ	GAP	XMAG	FMAG
86-	2-	6	1836 22.26	41 38.68	81 9.33	6.06	0.03	0.82	0.80	121		

RMSWT	DMIN	ITR	NFM	NWR	NWS	REMK
0.03	1.8	4	0	11	4	

STA	DIST	AZM	AN	P/S	W	SEC+CCOR	(TOBS	-TCAL	-DLY	=RES)	WT	XMG	FMG	R	INFO
003	1.8	325	161	P		23.52	0.00	1.26	1.23	0.00	0.03	1.76			0.307
				S		24.40	0.00	2.14	2.16	0.00	-0.02	1.76			0.821
CAL	4.7	7	136	P	5	23.81	0.00	1.55	1.47	0.00	0.08	0.00			0.000
				S	5	25.06	0.00	2.80	2.58	0.00	0.22	0.00			0.000
HAM	4.8	166	136	P	5	23.70	0.00	1.44	1.48	0.00	-0.04	0.00			0.000
				S	5	24.33	0.00	2.07	2.59	0.00	-0.52	0.00			0.000
WSH	5.8	251	130	P	5	23.91	0.00	1.65	1.60	0.00	0.05	0.00			0.000
				S	5	24.93	0.00	2.67	2.80	0.00	-0.13	0.00			0.000
ERJ	6.2	77	128	P	5	23.95	0.00	1.69	1.65	0.00	0.05	0.00			0.000
				S	5	25.07	0.00	2.81	2.87	0.00	-0.06	0.00			0.000
006	7.9	102	121	P		24.13	0.00	1.87	1.88	0.00	-0.01	1.76			0.615
				S	2	25.51	0.00	3.25	3.26	0.00	-0.01	0.88			0.443
COT	8.7	147	118	P	5	24.34	0.00	2.08	1.99	0.00	0.09	0.00			0.000
				S	5	25.49	0.00	3.23	3.45	0.00	-0.21	0.00			0.000
002	9.4	359	116	P	1	24.31	0.00	2.05	2.09	0.00	-0.04	1.32			0.449
				S	3	25.74	0.00	3.48	3.62	0.00	-0.14	0.44			0.096
CUY	9.6	187	115	P	5	24.42	0.00	2.16	2.11	0.00	0.05	0.00			0.000
				S	5	25.78	0.00	3.52	3.66	0.00	-0.13	0.00			0.000
MON	11.3	121	112	P	5	24.71	0.00	2.45	2.36	0.00	0.09	0.00			0.000
				S	5	26.11	0.00	3.85	4.08	0.00	-0.23	0.00			0.000
008	12.7	204	109	P	2	24.82	0.00	2.56	2.59	0.00	-0.03	0.88			0.610
				S	4	26.76	0.00	4.50	4.45	0.00	0.06	0.00			0.000
FOT	13.4	88	108	P	5	25.02	0.00	2.76	2.69	0.00	0.08	0.00			0.000
				S	5	27.02	0.00	4.76	4.61	0.00	0.15	0.00			0.000
007	13.6	148	108	P	3	24.91	0.00	2.65	2.72	0.00	-0.07	0.44			0.074
				S	5	26.92	0.00	4.66	4.68	0.00	-0.01	0.00			0.000
LOX	14.3	40	107	P	5	25.07	0.00	2.81	2.83	0.00	-0.02	0.00			0.000
				S	5	27.09	0.00	4.83	4.86	0.00	-0.03	0.00			0.000
001	17.8	3	103	P	2	25.66	0.00	3.40	3.38	0.00	0.02	0.88			0.290
				S	3	28.12	0.00	5.86	5.77	0.00	0.09	0.44			0.134
009	26.0	188	99	P	3	26.89	0.00	4.63	4.68	0.00	-0.05	0.44			0.155
				S	4	30.26	0.00	8.00	7.94	0.00	0.06	0.00			0.000
011	55.0	172	94	P	4	31.65	0.00	9.39	9.38	0.00	0.01	0.00			0.000
				S	5	38.43	0.00	16.17	15.80	0.00	0.37	0.00			0.000

TABLE C-5 -- EVENT: 7 FEB 86, 15:20

I	ORIGIN	LAT N	LON W	Z	NWR	RMS	DT	ADJUSTMENTS (KM) DLAT	DLON	DZ	RR
1	19.56	41 36.48	81 8.80	7.00	10	0.53	0.52	4.681	1.256	0.000	4.84
FOCAL DEPTH FREED											
2	20.08	41 39.01	81 9.71	7.00	10	0.13	0.13	-0.161	-0.484	-2.114	2.17
3	20.22	41 38.92	81 9.36	4.89	10	0.05	-0.03	0.103	0.087	-0.229	0.26
4	20.19	41 38.97	81 9.42	4.66	10	0.03	-0.01	-0.013	-0.016	0.000	0.02

YR	MO	DA	ORIGIN	LAT N	LON W	DEPTH	RMS	ERH	ERZ	GAP	XMAG	FMAG
86-	2-	7	1520 20.19	41 38.97	81 9.42	4.66	0.03	0.92	5.21	115		

RMSWT	DMIN	ITR	NEM	NWR	NWS	REMK
0.03	5.3	4	0	10	0	

STA	DIST	AZM	AN	P/S	W	SEC+CCOR	(TOBS	-TCAL	-DLY	=RES)	WT	XMG	FMG	R	INFO
CAL	4.2	9	129	P	4	21.51 0.00	1.32	1.26	0.00	0.07	0.00				0.000
				S	5	22.38 0.00	2.19	2.21	0.00	-0.02	0.00				0.000
HAM	5.3	166	122	P	1	21.56 0.00	1.37	1.41	0.00	-0.03	1.76				0.813
				S	5	22.46 0.00	2.27	2.47	0.00	-0.20	0.00				0.000
WSH	5.9	245	119	P	3	21.76 0.00	1.57	1.48	0.00	0.09	0.59				0.217
				S	5	22.82 0.00	2.63	2.60	0.00	0.04	0.00				0.000
ERJ	6.2	82	118	P	3	21.77 0.00	1.58	1.52	0.00	0.06	0.59				0.131
				S	5	22.71 0.00	2.52	2.66	0.00	-0.13	0.00				0.000
006	8.2	106	111	P		21.99 0.00	1.80	1.81	0.00	-0.01	2.35				0.768
				S	5	23.22 0.00	3.03	3.15	0.00	-0.12	0.00				0.000
002	8.9	0	109	P	1	22.09 0.00	1.90	1.92	0.00	-0.02	1.76				0.918
				S	5	23.39 0.00	3.20	3.33	0.00	-0.13	0.00				0.000
CUY	10.1	186	106	P	3	22.39 0.00	2.20	2.11	0.00	0.09	0.59				0.279
				S	5	23.89 0.00	3.70	3.65	0.00	0.05	0.00				0.000
MON	11.7	123	104	P	3	22.56 0.00	2.37	2.35	0.00	0.02	0.59				0.135
				S	5	24.09 0.00	3.90	4.06	0.00	-0.16	0.00				0.000
008	13.2	202	102	P	3	22.69 0.00	2.50	2.59	0.00	-0.09	0.59				0.492
				S	5	24.64 0.00	4.45	4.46	0.00	-0.01	0.00				0.000
FOT	13.4	90	102	P	3	22.83 0.00	2.64	2.64	0.00	0.00	0.59				0.128
				S	5	24.71 0.00	4.52	4.54	0.00	-0.02	0.00				0.000
LOX	14.0	42	101	P	3	22.85 0.00	2.66	2.73	0.00	-0.07	0.59				0.116
				S	5	24.92 0.00	4.73	4.68	0.00	0.05	0.00				0.000
001	17.3	4	99	S	5	25.80 0.00	5.61	5.55	0.00	0.06	0.00				0.000

TABLE C-6 -- EVENT: 10 FEB 86, 20: 6

I	ORIGIN	LAT N	LON W	Z	NWR	RMS	DT	ADJUSTMENTS (KM) DLAT	DLON	DZ	RR
1	12.86	41 36.48	81 8.80	7.00	13	0.54	0.57	4.753	1.010	0.000	4.85
FOCAL DEPTH FREED											
2	13.43	41 39.04	81 9.53	7.00	13	0.15	0.15	0.024	-0.355	-2.282	2.30
3	13.57	41 39.06	81 9.27	4.72	13	0.07	0.01	0.027	0.023	-0.945	0.94
4	13.59	41 39.07	81 9.29	3.77	13	0.04	0.00	0.000	0.012	-0.303	0.30
5	13.59	41 39.07	81 9.30	3.47	13	0.04	0.00	-0.002	0.019	-0.091	0.09
6	13.59	41 39.07	81 9.31	3.38	13	0.04	0.01	0.018	-0.037	-0.117	0.12

YR	MO	DA	ORIGIN	LAT N	LON W	DEPTH	RMS	ERH	ERZ	GAP	XMAG	FMAG
86-	2-	10	20 6 13.59	41 39.07	81 9.31	3.38	0.04	0.81	6.31	115		

RMSWT	DMIN	ITR	NFM	NWR	NWS	REMK
0.04	5.5	6	0	13	3	

STA	DIST	AZM	AN	P/S	W	SEC+CCOR	(TOBS	-TCAL	-DLY	=RES)	WT	XMG	FMG	R	INFO
CAL	4.0	8	116	P	5	14.89 0.00	1.30	1.11	0.00	0.19	0.00				0.000
				S	5	15.76 0.00	2.17	1.98	0.00	0.19	0.00				0.000
HAM	5.5	168	108	P	2	14.86 0.00	1.27	1.33	0.00	-0.06	1.18				0.552
				S	5	15.06 0.00	1.47	2.34	0.00	-0.87	0.00				0.000
ERJ	6.0	83	106	P	3	15.06 0.00	1.47	1.41	0.00	0.06	0.59				0.049
				S	5	16.24 0.00	2.65	2.49	0.00	0.16	0.00				0.000
WSH	6.1	244	105	P	3	15.16 0.00	1.57	1.43	0.00	0.14	0.59				0.279
				S	5	16.76 0.00	3.17	2.51	0.00	0.66	0.00				0.000
006	8.1	107	101	P		15.32 0.00	1.73	1.74	0.00	-0.01	2.36				0.556
				S	1	16.61 0.00	3.02	3.03	0.00	-0.01	1.77				0.788
002	8.7	359	100	P	1	15.40 0.00	1.81	1.83	0.00	-0.02	1.77				0.489
				S	3	16.75 0.00	3.16	3.19	0.00	-0.03	0.59				0.227
COT	9.3	149	99	P	3	15.54 0.00	1.95	1.94	0.00	0.01	0.59				0.106
				S	5	16.91 0.00	3.32	3.36	0.00	-0.04	0.00				0.000
CUY	10.3	187	98	P	3	15.72 0.00	2.13	2.10	0.00	0.03	0.59				0.214
				S	5	17.39 0.00	3.80	3.63	0.00	0.17	0.00				0.000
MON	11.6	124	97	P	3	15.91 0.00	2.32	2.30	0.00	0.01	0.59				0.115
FOT	13.3	91	96	P	3	16.19 0.00	2.60	2.58	0.00	0.02	0.59				0.115
				S	5	18.21 0.00	4.62	4.44	0.00	0.18	0.00				0.000
LOX	13.8	42	96	P	3	16.09 0.00	2.50	2.65	0.00	-0.16	0.59				0.090
				S	5	18.34 0.00	4.75	4.56	0.00	0.19	0.00				0.000
001	17.1	3	94	S	2	19.08 0.00	5.49	5.45	0.00	0.04	1.18				0.413

TABLE C-7 -- QUARRY BLAST: 5 FEB 86, 15:39

I	ORIGIN	LAT N	LON W	Z	NWR	RMS	DT	ADJUSTMENTS (KM) DLAT	DLON	DZ	RR
1	5.46	41 38.06	81 4.08	7.00	5	1.01	0.57	4.175	-4.587	0.000	6.20
FOCAL DEPTH FREED											
2	6.03	41 40.31	81 0.77	7.00	4	0.24	0.31	1.156	-0.601	-6.716	6.84
RMS INCREASE - MOVE HYPO 0.60 BACK											
3	6.34	41 40.94	81 0.33	0.28	5	0.86	-0.18	-0.694	0.361	4.030	4.10
AIRQUAKE PREVENTED											
4	6.15	41 40.56	81 0.59	4.31	5	0.21	0.07	0.020	0.099	-2.157	2.15
5	6.22	41 40.57	81 0.66	2.16	5	0.21	0.19	-2.847	0.341	0.000	2.86

YR	MO	DA	ORIGIN	LAT N	LON W	DEPTH	RMS	ERH	ERZ	GAP	XMAG	FMAG
86-	2-	5	1539	6.22 41 40.57	81 0.66	2.16	0.21	5.13	0.00	319		

RMSWT	DMIN	ITR	NFM	NWR	NWS	REMK
0.23	6.8	5	0	5	3	

STA	DIST	AZM	AN	P/S	W	SEC+CCOR	(TOBS	-TCAL	-DLY	=RES)	WT	XMG	FMG	R	INFO
006	6.8	220	90	P		7.46 0.00	1.24	1.50	0.00	-0.26	1.83				0.742
				S	2	8.36 0.00	2.14	2.64	0.00	-0.50	0.42				0.942
055	11.1	235	90	P		8.33 0.00	2.11	2.21	0.00	-0.10	1.83				0.679
				S	3	9.77 0.00	3.55	3.82	0.00	-0.27	0.46				0.981
003	13.2	261	90	S	3	10.38 0.00	4.16	4.39	0.00	-0.23	0.46				0.654

TABLE C-8 -- QUARRY BLAST: 5 FEB 86, 17:57

I	ORIGIN	LAT N	LON W	Z	NWR	RMS	DT	ADJUSTMENTS (KM) DLAT	DLON	DZ	RR
1	2.92	41 38.06	81 4.08	7.00	5	1.09	0.59	3.009	-4.607	0.000	5.50
FOCAL DEPTH FREED											
2	3.51	41 39.68	81 0.75	7.00	4	0.18	-0.15	1.738	-1.560	-2.838	3.67
3	3.36	41 40.62	80 59.63	4.16	4	0.14	0.00	0.089	-0.020	-3.055	3.05
RMS INCREASE - MOVE HYPO 0.60 BACK											
4	3.37	41 40.67	80 59.61	1.11	5	0.27	0.00	-0.053	0.012	1.833	1.83
5	3.37	41 40.64	80 59.62	2.94	5	0.11	-0.01	-0.969	-0.101	-0.164	0.98
6	3.35	41 40.12	80 59.55	2.78	5	0.03	0.03	-0.317	0.138	-0.055	0.35
7	3.39	41 39.95	80 59.65	2.72	5	0.03	0.01	-0.055	0.004	-0.010	0.05
8	3.39	41 39.92	80 59.65	2.71	5	0.03	0.00	-0.012	0.018	-0.002	0.02

YR	MO	DA	ORIGIN	LAT N	LON W	DEPTH	RMS	ERH	ERZ	GAP	XMAG	FMAG
86-	2-	5	1757	3.39 41 39.92	80 59.65	2.71	0.03	4.89	27.56	329		

RMSWT	DMIN	ITR	NFM	NWR	NWS	REMK
0.03	7.0	8	0	5	3	

STA	DIST	AZM	AN	P/S	W	SEC+CCOR	(TOBS	-TCAL	-DLY	=RES)	WT	XMG	FMG	R	INFO
006	7.0	236	96	P		4.92	0.00	1.53	1.55	0.00	-0.02	1.67			0.902
				S	3	5.98	0.00	2.59	2.72	0.00	-0.13	0.42			0.359
055	11.7	244	93	P		5.71	0.00	2.32	2.31	0.00	0.00	1.67			0.903
				S	2	7.42	0.00	4.03	3.99	0.00	0.03	0.83			0.834
003	14.4	267	92	S	3	8.04	0.00	4.65	4.74	0.00	-0.09	0.42			0.999